Master's thesis

NTNU
Norwegian University of Science and Technology
Faculty of Engineering
Department of Structural Engineering

Ane Bræin Skagestad & Ingvild Sørbel

# Evaluation of the Consistent Load Model for Norwegian Railway Bridges Subjected to Fatigue Considering Track Curvature and Non-Standard Influence Lines

Master's thesis in structural dynamics

June 2021

NTNU
Norwegian University of
Science and Technology

Ane Bræin Skagestad & Ingvild Sørbel

# Evaluation of the Consistent Load Model for Norwegian Railway Bridges Subjected to Fatigue Considering Track Curvature and Non-Standard Influence Lines

Master's thesis in structural dynamics
Supervisor: Associate Professor Gunnstein Thomas Frøseth
June 2021

Norwegian University of Science and Technology
Faculty of Engineering
Department of Structural Engineering

NTNU
Norwegian University of
Science and Technology

**Department of Structural Engineering**
Faculty of Engineering
**NTNU – Norwegian University of Science and Technology**

ACCESSIBILITY

OPEN

# MASTER THESIS 2021

| SUBJECT AREA: | DATE: | NO. OF PAGES: |
|---|---|---|
| Structural dynamics | 04.06.2021 | 12 + 81 |

TITLE:

## Evaluation of the Consistent Load Model for Norwegian Railway Bridges Subjected to Fatigue Considering Track Curvature and Non-Standard Influence Lines

Evaluering av den konsistente lastmodellen for norske jernbanebruer utsatt for utmatting med hensyn til sporkurvatur og ikke-standard influenslinjer

BY:

Ingvild Sørbel
Ane Bræin Skagestad

SUMMARY:
Approximately one-third of all bridges operating in the current Norwegian railway network are steel bridges built before 1960. After these bridges were built, the mechanism of fatigue has been found to be the leading cause of failure in steel structures. For a railway bridge, the main load is the trains. However, minimal data is available regarding historical traffic operating on the Norwegian bridges, making it difficult to determine the remaining fatigue life. In 2019 Frøseth & Rønnquist proposed a new load model for historical trains, referred to as the Consistent Load Model. The main criteria of the load model were that it should be simple, conservative and consistent.

The objective of this thesis is to evaluate whether the Consistent Load Model fulfills these criteria. Preliminary, this is done by performing fatigue life analyses of two railway bridges. These bridges were also assessed by Bane NOR in 2018, using a different load model. By comparing the results from the two analyses, the Consistent Load Model was found up to 50 times more conservative. These damage values are far beyond the critical level, indicating that the bridges should have collapsed. As the bridges have not collapsed, the load model can be considered conservative with unrealistically high damage values.

The results gave a larger variety of critical components than found by Bane NOR. Still, it does not prove that the Consistent Load Model fulfills the consistency criterion. For a calibration set of influence lines, the Consistent Load Model is designed to have consistencies of 40-50%. However, the influence lines of a bridge will have unlimited different shapes and lengths. The consistencies of the two bridges were therefore determined using most damaging train analyses. These analyses showed extremely poor consistencies. The reason was found to be the effect of centrifugal forces occurring from bridge curvature. Therefore, the new load model can only be considered consistent for a bridge without horizontal curvature. However, it was found that one can overcome this problem by using the most damaging speed for each stress point. The consistencies were then remarkably improved, while the load model still is kept simple and conservative.

RESPONSIBLE TEACHER: Associate Professor Gunnstein Thomas Frøseth

SUPERVISOR(S): Associate Professor Gunnstein Thomas Frøseth

CARRIED OUT AT: NTNU, Trondheim

**Institutt for konstruksjonsteknikk**
Fakultet for ingeniørvitenskap
**NTNU – Norges teknisk-naturvitenskapelige universitet**

TILGJENGELIGHET

ÅPEN

# MASTEROPPGAVE 2021

| FAGOMRÅDE: | DATO: | ANTALL SIDER: |
|---|---|---|
| Konstruksjonsdynamikk | 04.06.2021 | 12 + 81 |

TITTEL:

**Evaluering av den konsistente lastmodellen for norske jernbanebruer utsatt for utmatting med hensyn til sporkurvatur og ikke-standard influenslinjer**

Evaluation of the Consistent Load Model for Norwegian Railway Bridges Subjected to Fatigue Considering Track Curvature and Non-Standard Influence Lines

UTFØRT AV:

Ingvild Sørbel
Ane Bræin Skagestad

SAMMENDRAG:
Omtrent en tredjedel av dagens norske jernbanenettverk består av stålbruer bygget før 1960. Etter disse ble bygget, har utmatting vist seg å være den ledende årsaken til brudd i stålkonstruksjoner. For en jernbanebru gir togtrafikken den største belastningen. Det er imidlertid lite data tilgjengelig om historisk trafikk på norske bruer, noe som gjør det vanskelig å estimere gjenværende levetid for utmatting. I 2019 foreslo Frøseth & Rønnquist en ny lastmodell for historisk togtrafikk, her referert til som den konsistente lastmodellen. De tre hovedkriteriene for denne lastmodellen var at den skulle være enkel, konservativ og konsistent.

Målet med denne oppgaven er å evaluere om den konsistente lastmodellen oppfyller disse kriteriene. Dette gjøres i første omgang ved å utføre utmattingsanalyser for to jernbanebruer. Disse bruene ble også evaluert av Bane NOR i 2018 med en annen lastmodell. Ved å sammenligne resultatene for de to lastmodellene viste det seg at den konsistente lastmodellen er opptil 50 ganger mer konservativ enn den brukt av Bane NOR. Skadeverdiene er generelt langt over det kritiske nivået, noe som tilsier at bruene skulle ha kollapset. Ettersom dette ikke har skjedd, kan lastmodellen anses som konservativ med urealistiske høye skadeverdier.

Resultatene viste også at den konsistente lastmodellen finner større variasjon i kritiske konstruksjonsdeler. Dette beviser likevel ikke at modellen oppfyller konsistenskriteriet. For et kalibreringssett med standard influenslinjer er den konsistente lastmodellen utviklet med konsistenser på 40-50%. En bru vil imidlertid ha influenslinjer med store variasjoner, både i form og lengde. Ved hjelp av analyser som finner mest skadelig tog ble de virkelige konsistensene av bruene bestemt. Svært dårlig konsistent ble funnet for begge bruene. Årsaken viste seg å være effekten av sentrifugalkrefter som oppstår på grunn av sporkurvatur. Dermed kan den nye lastmodellen ikke betraktes som konsistent for en bru med horisontal krumning. Det ble imidlertid funnet at denne utfordringen kan løses ved å bruke den mest skadelige hastigheten for hvert spenningspunkt. Konsistensene forbedret seg da betraktelig, samtidig som lastmodellen forblir enkel og konservativ.

FAGLÆRER: Førsteamanuensis Gunnstein Thomas Frøseth
VEILEDER(E): Førsteamanuensis Gunnstein Thomas Frøseth
UFØRT VED: NTNU, Trondheim

# Preface

This master thesis is the final part of our Master's degrees at the Norwegian University of Science and Technology. The thesis is written for the Department of Structural Engineering in the period from January 2021 to June 2021.

We want to thank our supervisor Associate Professor Gunnstein T. Frøseth for his help and guidance through the thesis. His enthusiasm in the project has been very helpful. We would also like to thank Bane NOR for providing the material for the analyses of the bridges considered.

Ingvild Sørbel & Ane Bræin Skagestad

June 2021

# Abstract

Approximately one-third of all bridges operating in the current Norwegian railway infrastructure are steel bridges built before 1960. More than 80 % of all failure in steel structure is caused by fatigue. The fatigue mechanism was however not fully understood until the last half of the 20th century. Therefore, it is now essential to predict the state of older bridges regarding fatigue, such that collapse is avoided and the cost of maintenance and replacements is minimized.

To find the historic fatigue damage for a bridge component, the loading history has to be known. However, there is limited data available about the train traffic before the late 20th century. There is, nevertheless, some knowledge regarding the evolution of trains and in which periods they operated. Although the types of trains are known, there could be significant variations in, e.g., wagons, axles, passages and speeds.

Eurocode 1 provides a load model for trains to be used throughout history. The issue with this and other earlier established fatigue load models for railways is that they are not *consistent*, meaning that the load models may favor some bridge components. It will then be significant variations in damage introduced from a train in the load model relative to the train introducing the worst possible damage from one bridge component to another. In 2019 Frøseth & Rønnquist proposed a new load model, referred to as the *Consistent Load Model*, which takes this issue into account. The main criteria of the new load model were that it should be simple, conservative and consistent.

This thesis evaluates whether the Consistent Load Model fulfills the main criteria for bridges with curvature and components not included in the load model calibrations. In 2018 Bane NOR assessed 21 riveted steel bridges built before 1930. They performed fatigue life analyses using reference trains from Eurocode 1 and the Norwegian University of Science and Technology. These trains are together referred to as the *Conventional Load Model*. Two of these bridges, Svånå and Sokna Bridge, are in this thesis reassessed with the Consistent Load Model, using the results from Bane NOR as a comparison.

The Consistent Load Model is more conservative than the load model used in the previous assessment. The analysis with the Consistent Load Model gave fatigue damages up to 50 times higher for some cross-sections. These damage values are far beyond the critical level, indicating that the bridges should have collapsed. As the bridges have not collapsed, the load model can be considered conservative with unrealistically high damage values.

There was also a change in the ranking of most critical components. The Consistent Load Model found other and a greater variety of critical components than the Conventional load model. It does however not prove that the new load model fulfills the consistency criterion. For a calibration set of influence lines, the Consistent Load Model is designed to have consistencies of 40-50 %. The influence lines of a bridge will however have unlimited different shapes and lengths. The actual consistencies of Svånå and Sokna Bridge were therefore determined using *most damaging train* analyses. These analyses showed extremely poor consistencies. The consistency requirement can consequently not be considered fulfilled.

The reason for the poor consistencies was found to be the effect of the centrifugal force occurring from track curvature. Both Svånå and Sokna Bridge have horizontal curvature, introducing centrifugal forces depending on the speed of the passing train. How the centrifugal forces affect the influence lines varies greatly. The most distinct was found to be the cases where a high speed increases the peak of the influence line, and thereby the fatigue

damage. When the most damaging train is found at high speed, while much lower speeds are used in the load model, the fatigue damage introduced by the load model tends to be a million times smaller than for the most damaging train.

The consistencies were also calculated for two bridges with no curvature. The consistencies of these bridges were close to the desired levels found with the calibration set. This proves that the effect of the centrifugal force is causing the poor consistencies. The consistency requirement of the Consistent Load Model is therefore only fulfilled for a bridge not affected by centrifugal forces.

To increase the consistency for bridges with curvature, several alternatives have been tested. One alternative, where the speed for each passing train is chosen as the most damaging speed, showed a remarkable increase in consistency. The load model is then still kept simple and even more conservative than the original Consistent Load Model. However, it is important to acknowledge that the consistencies found are theoretical results. The ranking of the most exposed components may be different if the actual speed of the passing trains differs significantly from the most damaging one.

# Contents

# List of Symbols

| | |
|---|---|
| $\beta$ | Limit for maximum gradient |
| $\delta$ | Dirac-delta function |
| $\Delta\sigma_C$ | Detail category, reference value of the fatigue strength at $N_C = 2$ million cycles |
| $\Delta\sigma_D$ | Fatigue limit for constant amplitude stress ranges at $N_D = 5$ million cycles |
| $\Delta\sigma_L$ | Cut-off limit for stress ranges at $N_L = 10^8$ cycles |
| $\gamma_s$ | Density of steel |
| $\gamma_{Mf,p}$ | Partial safety factor for primary bearing |
| $\gamma_{Mf,s}$ | Partial safety factor for secondary bearing |
| $\kappa$ | Limit for maximum difference between fatigue damages |
| $\lambda$ | History length for Late Acceptance Hill-Climbing |
| $\mathbf{N}$ | Number of wagons allowed in a train set |
| $\mathscr{L}$ | Set of locomotives |
| $\mathscr{P}$ | Set of axle loads |
| $\mathscr{W}$ | Set of wagons |
| $\mathscr{W}_B$ | Set of bogie wagons |
| $\mathscr{W}_T$ | Set of two-axle wagons |
| $\nabla h$ | Gradient of a function h |
| $\nu$ | Poisson's ratio |
| $\Phi$ | Dynamic amplification factor |
| $\sigma$ | Stress in a cycle |
| $\Upsilon$ | Train set for most damaging train analyses |
| $\varphi$ | Ratio between damage from load model and damage from most damaging train |
| $\zeta$ | Consistency factor |
| $a$ | Traffic mix coefficient for the Consistent Load Model |
| $A_x$ | Cross-sectional area |
| $C$ | Fatigue resistance parameter scaling the relation between $N$ and $S$ |
| $D$ | Fatigue damage |
| $d\uparrow$ | Maximum fatigue damage |
| $D_1$ | Yearly fatigue damage |
| $D_{cr}$ | Critical fatigue damage |

| | |
|---|---|
| $D_h$ | Historical fatigue damage |
| $d_{SC}$ | Fatigue damage introduced by the Consistent Load Model |
| $E$ | Young's modulus |
| $f$ | Static load function |
| $f_r$ | Reduction factor for centrifugal force |
| $f_u$ | Tensile strength of steel |
| $f_y$ | Yielding strength of steel |
| $G$ | Shear modulus |
| $L$ | Total length of train |
| $l$ | Influence line function |
| $L_\phi$ | Determinant length |
| $L_{IL}$ | Length of influence line |
| $m$ | Fatigue resistance parameter representing the slope of the *log N* - *log S* curve |
| $M_y$ | Moment about y-axis |
| $M_z$ | Moment about z-axis |
| $N$ | Number of cycles until failure |
| $N_x$ | Axial force |
| $n_0$ | Number of train passages for a line in the railway network |
| $n_i$ | Number of cycles of one specific loading |
| $n_p$ | Number of axles in a train |
| $N_R$ | Design life expressed as number of cycles |
| $p_i$ | Axle load magnitude in a specific position |
| $Q$ | Total axle load |
| $q$ | Distributed axle load |
| $r$ | Radius of horizontal curvature for a bridge |
| $R_a$ | Vertical axle load |
| $R_h$ | Horizontal load from centrifugal force |
| $R_v$ | Vertical load from centrifugal force |
| $R_{il,i}$ | Value of an influence line for a specific point |
| $S$ | Stress range for cyclic loading |
| $s$ | Shift variable |

| | |
|---|---|
| $T_{RL}$ | Remaining fatigue life, number of years until fatigue failure |
| $Ti$ | Reference train number i |
| $v$ | Defined speed of a train |
| $v \uparrow$ | Maximum allowable speed for a train set |
| $v_L$ | Maximum speed of a locomotive |
| $W_y$ | Section modulus for bending about y-axis |
| $W_z$ | Section modulus for bending about z-axis |
| $z$ | Total response including dynamic amplification |
| $z_s$ | Static response |

# 1 Introduction

## 1.1 Background

In the 1840s, trade and transportation needs increased in Norway. Therefore, the interest was large for building a railway which would make these processes more effective. The construction of railways started in 1851, and three years later, the 68 km long *Hovedbanen* between Oslo and Eidsvoll was finished [1]. The Norwegian railway network continued to grow over the next century, reaching its peak length in 1962 of approximately 4500 km [2]. Today, the Norwegian railway network with regular traffic is about 3900 km long [3]. Much of the existing network has not been replaced since it was built. This is especially the case for bridges, as constructing new ones introduces significant investment costs and interrupts the railway operation. A large portion of the Norwegian railway bridges are therefore built more than 60 years ago [2].

The first railway bridges were mainly built using timber, as this was cheap and could be found locally. Although some techniques for making steel are said to have been from 500 BC, the process was slow and expensive for a long time. It was not until 1880 that the price of steel had a massive drop, making it competitive on the market [4]. In the mid 20th century, reinforced concrete also made its entrance to the construction industry and has been the dominating building material in the latest decades. However, most of the old bridges are in steel, with one-third of all bridges in the current Norwegian network being steel bridges built before 1960, as seen in Figure 1.1 [2].

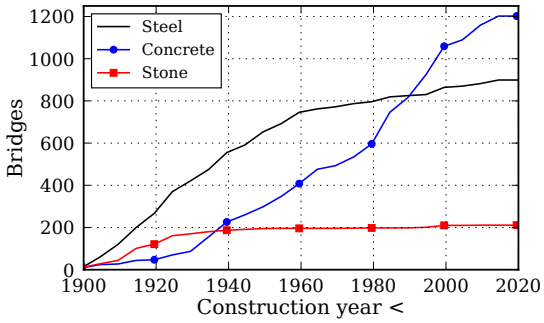


Figure 1.1: Cumulative distribution of construction year for bridges in the current Norwegian railway network differentiated for material [2][1].

Steel has many qualities making it superior for construction, as it is strong both in tension and compression and generally ductile. There are however multiple challenges connected to the old steel bridges. The loads which the bridges were originally designed for are not valid for the current situation, and as the structural engineering field has evolved, the knowledge of possible failure mechanisms has increased.

[1] Figure is taken from Frøseth [2] with permission from the author (February 2021).

## 1.2 Fatigue Life Analysis for Railway Bridges

In the 19th century industrial revolution, it was found that fracture could occur from cycling loading, although a constant load of the same magnitude would do no damage. It was however not understood why this happened or how it could be taken into account in the design process. It was not until the last half of the 20th century that the theories and knowledge of the fatigue mechanism had substantial improvements [5].

Fatigue is a weakening mechanism where cyclic loading initiate cracks in a material. As the crack extends a little for each cycle, it eventually reaches its critical length. When the reduced cross-section can not resist the applied load, fatigue failure occurs [6]. The fatigue loads leading to failure are lower than the static strength of the material. How many cycles the steel can withstand depends on ductility, strength, roughness and faults of the component [2].

It is considered that 80-90 % of all failures in steel structures are related to fatigue and fracture [7], often in combination with other phenomena such as sliding or physical contact, corrosion or elevated temperatures [8]. As many of the steel bridges in the Norwegian railway network were built before fatigue was fully understood, they are not explicitly designed to withstand this mechanism, possibly having disastrous consequences. However, replacing all old steel bridges would be too expensive, especially since it generally would require operation interruptions on the lines. It is therefore necessary to find the remaining fatigue life of the components of these bridges, such that resources for maintenance and replacements are used where it is needed.

To estimate the fatigue damage, $D$, it has to be known what cyclic loading a component is subjected to and how many cycles the component can withstand for the specific loading. Through decades of experiments and testing, the capacity of the different components are well known, described with SN-curves as presented in Subsection 2.1.3. The static response, e.g., the stress in a specific point at the bridge, is found by taking the convolution between the cyclic load, $f$, and the influence line of the specific point, $l$ [9] :

$$z_s(s) = (l * f)(s) \tag{1}$$

The influence line is a representation of the response at a certain location due to a moving unit load [9] and can be found theoretically. The big issue is however the load function, $f$.

## 1.3 Load Models for Railway Bridges

The design loads, including size, distribution and frequency, have changed a lot over the last century. The most significant contributor to fatigue damage in steel railway bridges is the trains, such that the load function is all trains that have ever operated on the bridge. There is however minimal data available about the trains from before the late 20th century [2]. Yet, it is known what types of trains operated in different time periods [10]. Although the trains are known, there could be considerable variations in, e.g., axle loads, number of wagons and number of passages.

Eurocode 1 proposes a load model for trains regarding historic fatigue based on different time periods [11]. The company responsible for the Norwegian national railway network, Bane NOR, assessed, in 2018, 21 riveted steel railway bridges built before 1930. For this fatigue life estimation, they used a combination of the load model from Eurocode 1 and additional trains suggested by the Norwegian University of Science and Technology, summing up to a load model denoted the *Conventional Load Model* in this thesis. It was then found that seven of these bridges have components exceeding their theoretical fatigue lifetime, while the remaining bridges still can operate safely for several more years [12].

The Conventional Load Model used by Bane NOR does have one prominent weakness. Depending on the influence line of the stress points on the bridge, the response from a specific train can vary greatly. For one point, maximum axle loads on all wagons will be most damaging, while another point may experience more damage from a train where some wagons are empty. The trains in the load model used in Bane NOR's assessment seem to be selected somewhat randomly and not with the intention of making consistent levels of introduced fatigue damage relative to the traffic inflicting most damage. Therefore, it is likely that some components are found to be more critical to fatigue than others, all though this may not be the case. Without this issue taken into account in the load model, it might also result in non-conservative damages for some stress points.

In 2019 Frøseth & Rønnquist published a suggestion for a new load model that takes this into account [13], referred to as the *Consistent Load Model* in this thesis. Their main focus was to find a simple, conservative and consistent model, meaning that the model should be easy to use, conservative for all points, and have the same relative damage in all elements. The latter requirement is important in fatigue assessments as it provides a correct ranking of the most exposed structural details of the bridge. The work of Frøseth & Rønnquist resulted in a model containing eight different trains defined either for passenger or freight trains, each applying for one specific time period.

## 1.4 Objectives

The main objective of this thesis is to evaluate the load model proposed by Frøseth & Rønnquist and whether or not it fulfills the criteria of being simple, conservative and consistent. Initially, this is done by performing fatigue calculations based on the Consistent Load Model, with the results from the Conventional Load Model as the basis of comparison. A fatigue life analysis with the Consistent Load Model is thus performed on two of the bridges already assessed by Bane NOR. Comparing the results and investigating the damage in different components can determine which load model is the most conservative and if the ranking of critical components changes. The two riveted steel bridges to be considered are Svånå Bridge and Sokna Bridge by Lundamo (further denoted Sokna Bridge), both being one-track bridges on the Norwegian railway *Dovrebanen*. Both bridges have horizontal curvature, with a radius of 1000 meters for Svånå Bridge and 500 meters for Sokna Bridge.

The fatigue analysis will provide some information about how the new, more consistent load model is compared to the old, more conventional one. However, it is difficult to say anything about true conservatism and consistency based on just fatigue life analyses. An additional analysis is therefore performed based on *most damaging train*. For each stress point and belonging influence line, the possible most damaging train is found for a specific time period for both passenger and freight trains. It is then determined how the damage from the Consistent Load Model compares to the true most damaging train. Based on the most damaging train analyses, it will be examined whether the new load model has any weaknesses and how these potential weaknesses can be treated.

# 2 Fatigue Damage for Railway Bridges

## 2.1 Fatigue

### 2.1.1 Basic Principles

Fatigue is a weakening mechanism where cracks initiate and grow in a material due to cyclic loading. When the crack has grown to a critical length, the reduced cross-section can not resist the applied load, and fatigue failure will occur [6]. The fatigue loads leading to failure are smaller than the static strength of the material. The fatigue mechanism can be divided into three phases; crack initiation, crack growth and ultimate failure. The characteristics of the different phases are highly dependent on whether the material behaves ductile or brittle. A brittle fracture occurs by rapid crack extension under elastic conditions. For ductile materials, the cyclic loading introduces plastic deformations and cleavages along certain planes in the material structure. Local stress concentrations will occur along these planes, which initiate small cracks and further propagate as the crack tip opens and closes until the cross-section can no longer withstand the load [14]. Steel structures may be subjected to both brittle and ductile fatigue depending on the conditions of the material with strength, roughness, faults and component design highly affecting the growth [2]. The treatment of the steel also influences the fatigue behavior. Welds are especially problematic as they generally introduce imperfections, high stress concentrations and residual stresses [15]. How the differences in material and design are treated will be presented in Subsection 2.1.3.

The fatigue endurance of a structural component is determined by Basquin's relation, given by

$$N(S) = CS^{-m} \tag{2}$$

where $N$ is the number of cycles until failure with a cycle stress of $S$. $C$ and $m$ are the fatigue resistant parameters, corresponding to a scaling of the relation and the slope of the *log N - log S* curve [2, 6]. The stress range, $S$, is defined as the difference between maximum and minimum stress in one cycle

$$S = \Delta\sigma = \sigma_{max} - \sigma_{min} \tag{3}$$

The fatigue damage, $D_i$, can be expressed as

$$D_i = \frac{n_i}{Ni} \tag{4}$$

where $n_i$ is the number of cycles the structural component is subjected to in the specific stress range and $N_i$ is the number of cycles the component can withstand for this stress.

The component may be subjected to varying stress histories during its lifetime and thereby different stress ranges. To account for the differences in stress range, the Palmgren-Miner linear damage hypothesis, often called the Miner's rule, may be applied [6]:

$$D = \frac{n_1}{N_1} + \frac{n_2}{N_2} + ... + \frac{n_i}{N_i} = \sum_{i=1}^{I} \frac{n_i}{N_i} \tag{5}$$

This can further be combined with Basquin's relation given in Eq. (2), yielding the following:

$$D = \frac{1}{C} \sum_{i=1}^{I} S_i^m \tag{6}$$

The remaining fatigue life of a bridge at a point in time is dependent on the already introduced historic fatigue damage and the fatigue damage from future cyclic stress. The remaining number of years, $T_{RL}$, for the fatigue service life can be calculated as

$$T_{RL} = \frac{D_{cr} - D_h}{D_1} \tag{7}$$

where $D_{cr}$ is the critical level of fatigue damage and $D_h$ is the historic fatigue damage from already experienced load cycles [2]. $D_1$ is the estimated yearly future damage.

### 2.1.2 Rainflow Counting Method

Most load histories introduce large varieties in stress cycles. Fatigue analysis requires that the loading sequence is decomposed into distinct cycles, $S_i$. For estimating the service life of bridges, the rainflow counting method is most commonly used [2]. The technique was first developed by Matsuishi-Endo in 1968 [16] and has its name after how raindrops fall from a typical Japanese roof. This may be represented by a flipped time-stress series as shown in Figure 2.1. From this, the number of cycles of each stress range can be determined [6]. The rainflow counting algorithm is thoroughly presented by C. Amzallag et al. [17].

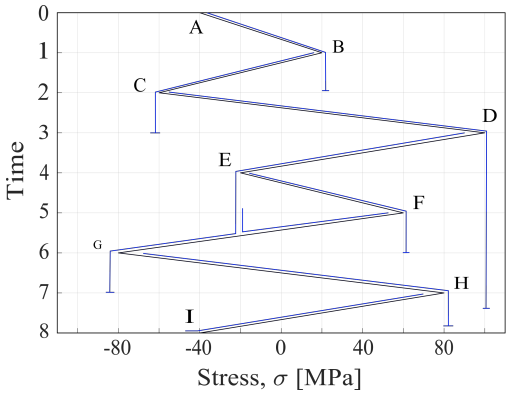


| Path | Cycles | Stress range |
|---|---|---|
| A-B | 0.5 | 60 MPa |
| B-C | 0.5 | 80 MPa |
| C-D | 0.5 | 160 MPa |
| D-G | 0.5 | 180 MPa |
| E-F | 1.0 | 80 MPa |
| G-H | 0.5 | 160 MPa |
| H-I | 0.5 | 120 MPa |

Figure 2.1: Principle of rainflow cycle counting.

### 2.1.3 SN-curves

SN-curves are logarithmic plots of how the stress range and number of cycles until failure corresponds. The curves for different materials and connections are determined empirically by multiple tests for constant stress ranges. Eurocode 3 defines a generalized curve that fits most steel structures, where $N_R$ is the number of cycles that can be withstood for a stress range $\Delta\sigma_R$ [18]. The curves are defined from Eq. (8) & (9) and illustrated in Figure 2.2.

$$\Delta\sigma_R^m \; N_R = \Delta\sigma_C^m \; 2 \cdot 10^6 \quad \text{with m} = 3 \text{ for } \quad N \leq 5 \cdot 10^6 \tag{8}$$

$$\Delta\sigma_R^m \; N_R = \Delta\sigma_D^m \; 5 \cdot 10^6 \quad \text{with m} = 5 \text{ for } \quad 5\dot{1}0^6 \leq N \leq 10^8 \tag{9}$$

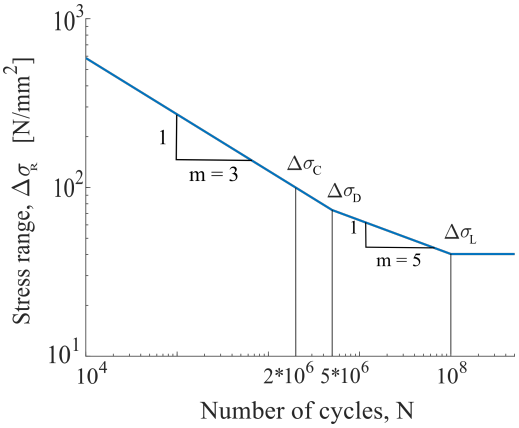


Figure 2.2: Typical SN-curve as defined in Eurocode 3.

$\Delta\sigma_C$ is the detail category, which is the reference value of the fatigue strength for 2 million cycles. The slope changes at 5 million cycles for the constant amplitude fatigue limit, $\Delta\sigma_D$. It is assumed that fatigue failure will not occur for low stress ranges, and the component can therefore withstand an unlimited number of cycles at stresses lower than this limit. The limit for fatigue failure is called the cut-off limit, $\Delta\sigma_L$. Both the constant amplitude fatigue limit and the cut-off limit are found from the detail category by

$$\Delta\sigma_D = 0.737\Delta\sigma_C, \qquad \Delta\sigma_L = 0.549\Delta\sigma_D$$

Eurocode 3 contains multiple tables defining the detail category for different steel components in a structure [18]. The tables include bolted and welded joints, in addition to plain members. Further on, the Eurocode applies the Miner's rule as presented in Eq. (5) with critical fatigue damage, $D_{cr}$, equal to 1.0. It also acknowledges rainflow cycle counting as a suitable method for extracting the load cycles.

The Eurocode does not include detail categories for riveted joints. In 2010 Taras & Greiner [19] suggested detail categories for riveted bridge components based on previous fatigue tests. A detail category of 71 MPa was then found to be conservative for all members. A secondary lower-bound option was also presented. Taras & Greiner found a linear curve with detail category 85 MPa and a slope of m = 5 to be appropriate for riveted joints.

## 2.2 Generation of Response in a Railway Bridge

Any variable loading applied to a railway bridge will induce stress cycles in the bridge material and possible challenges regarding fatigue. There are two sources of variable loads on a railway bridge, traffic loads and environmental loads. The traffic loads are generally higher in both intensity and frequency than the environmental loads. Heavy snow and wind only occur few times a year and can be considered small compared to the traffic loads. Consequently, in the estimation of the fatigue life of a railway bridge, only traffic loads have to be considered [2].

### 2.2.1 Static Loading

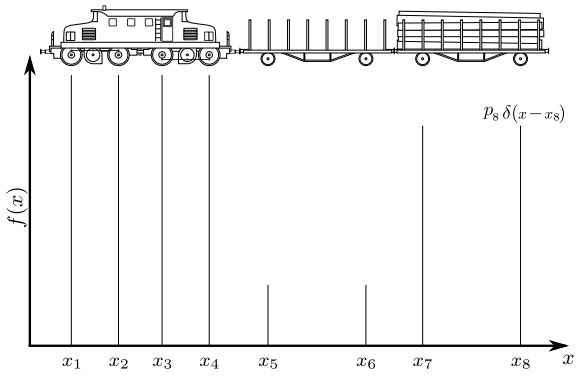


Figure 2.3: Load function of a train [2][1].

The static load function, $f$, of a train on a railway bridge is illustrated in Figure 2.3. This train has eight axles in position $x_i$ with a load magnitude of $p_i$. To define the static loading at an arbitrary point, $x$, the Dirac-delta function, $\delta$, has to be introduced [9]. The Dirac-delta function is a generalized function that enables representations of singularities and point loads in mathematical and structural problems [20]. The function is defined zero except for one point, $x_0$, by:

$$\delta(x - x_0) = 0 \quad \text{for all} \quad x \neq x_0 \tag{10}$$

and

$$\int_{-\infty}^{\infty} \delta(x - x_0)\, dx = 1 \tag{11}$$

Representing each axle by the load magnitude and the Dirac-delta function, the static load function can be defined as

$$f(x) = \sum_{i=1}^{n_p} p_i \delta(x - x_i) \tag{12}$$

where $n_p$ is the number of axles in a train [9].

### 2.2.2 Influence Lines

An influence line (IL) represents the response at a certain location in a structural member due to a moving unit load [9]. The influence line can represent any measurable quantity (moment, deflection, axial stress etc.) as a function of the position of the applied load. An illustration of the influence line for the moment in the midspan of a simply supported beam is shown in Figure 2.4. Assuming a linear structure, where the principle of superposition holds, it has been shown that it is possible to generate the response to an arbitrary load using the influence line [9]. Defining the arbitrary load as the load function in Eq. (12), the static response, $z_s$ is obtained by the convolution of the influence line, $l$, and the load function, $f$, as

$$z_s(s) = (l * f)(s) = \sum_{i=1}^{n_p} p_i l(s - x_i) \tag{13}$$

The shift variable, $s$, denotes the distance the load has moved along the path of the influence line [2].

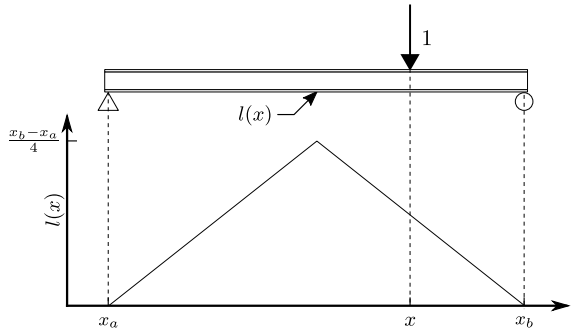


Figure 2.4: Illustration of an influence line. Moment in the mid-span of a simply supported beam with the x-coordinate as the position of the moving unit load [2][1].

### 2.2.3 Dynamic Amplification Factor

The complete response in a structure subjected to cyclic loading consists of both a static and dynamic response. In fatigue analysis, it has been shown that a complete response generated by a static solution and a dynamic amplification factor (DAF) yields similar results as a complete dynamic analysis. This conclusion applies only if the speed of the train and the mass ratio between train and bridge do not impose resonance in the structure [21]. However, such conditions are usually only seen for speeds higher than 200 km/h [22]. An approach with a static solution obtained by influence lines and a dynamic amplification factor is therefore generally considered sufficient to predict the response history of existing railway bridges in fatigue assessments [2, 23].

The dynamic amplification factor, $\Phi$, is defined somewhat differently in different codes. Eurocode 1 (EC1) includes different definitions depending on how well the track is maintained and which calculations are to be done. For fatigue assessments of loading due to trains, the reduced amplification factor in Eq. (14) is to be used [11].

$$\Phi = 1 + \phi = 1 + \frac{1}{2}(\phi' + \frac{1}{2}\phi'') \tag{14}$$

Here

$$\phi' = \frac{K}{1 - K + K^4} \tag{15}$$

where

$$K = \begin{cases} \frac{v}{160}, & L_\phi \leq 20m \\ \frac{v}{47.16 L_\phi^{0.408}}, & L_\phi > 20m \end{cases} \tag{16}$$

and

$$\phi'' = 0.56 e^{-\frac{L_\phi^2}{100}} \tag{17}$$

where $v$ is the vehicle speed and $L_\phi$ is the determinant length. The determinant length is determined according to Table 6.2 in Eurocode 1 [11].

The total response, *z(s)*, is then obtained by the static response from Eq. (13) multiplied with the dynamic amplification factor in Eq. (14) [21]:

$$z(s) = z_s(s) \cdot \Phi \tag{18}$$

# 3 Loading from Trains

## 3.1 A Brief Introduction to the Norwegian Railway History

Historically, four types of tractive vehicles have been present in the Norwegian railway network, where the distribution is shown in Figure 3.1. Steam locomotives were the only type present until 1923 when electric locomotives were introduced [10]. Diesel locomotives were put into service in the 1950s, about the same time the decline in the use of steam locomotives began. Around 1930, multiple units (MU) were introduced. These trains do not have a dedicated locomotive, but multiple wagons joined together where one or more of the wagons are equipped with a motor [24]. MUs provide approximately 40 % of today's total running train distance.

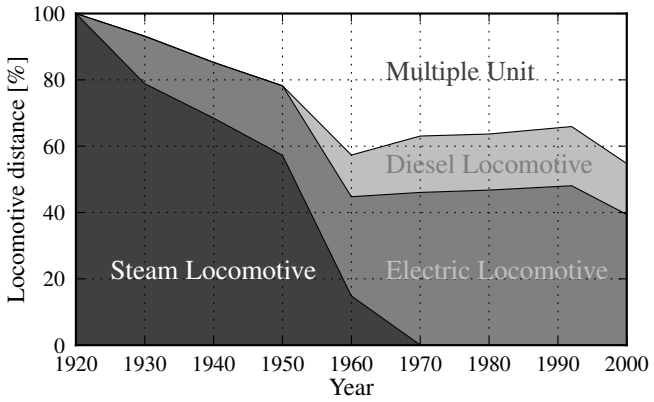


Figure 3.1: Distribution of tractive vehicles in Norway, as percentages of total running distance of trains [10][2].

It is not only the use of tractive vehicles that have changed during the railways' history. Both axle load, train speed and number of wagons have generally increased, as a result of trade and population growth together with technical advances. Figure 3.2 shows the evolution of maximum axle loads for locomotives, freight wagons and passenger wagons. For locomotives, the axle load has increased from approximately 11 tonnes to 21 tonnes. The gray markers represent narrow-gauge locomotives, i.e., locomotives with a narrower track than standard dimensions [10]. As seen in the figure, freight wagons have a higher maximal axle load than passenger wagons.

It is also worth mentioning that the axle load of an empty freight wagon can be assumed 25 to 50 % of the maximum axle load, dependent on the type of freight. The axle load of a passenger wagon depends on the number of passengers. It has been shown that subtracting 2.5 tonnes per axle from the maximum axle loads yields reasonable estimates of an empty passenger wagon [10].

[2]Figure is taken from Frøseth & Rønnquist [10], with permission from the authors and the publisher Taylor & Francis (April 2021).

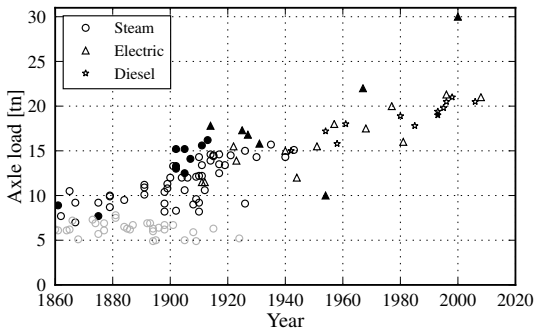


(a) Locomotives

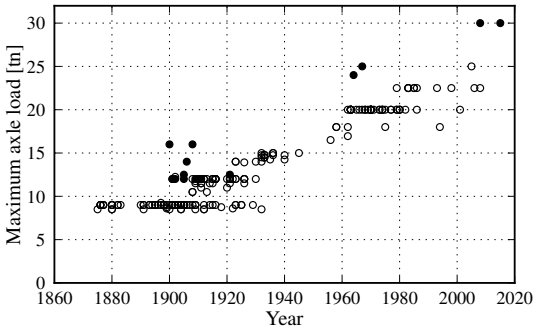


(b) Freight wagons

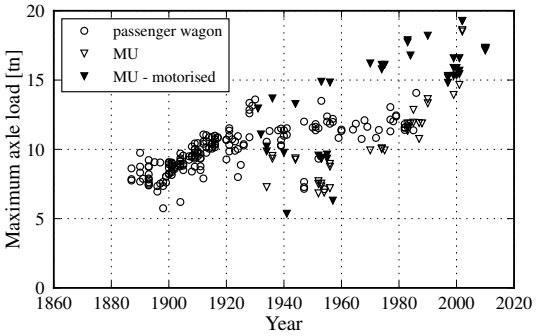


(c) Passenger wagons

Figure 3.2: Evolution of maximal axle load [10][2].

The fastest steam locomotive in the Norwegian railway network was introduced in 1913 with a maximum nominal speed of 90 km/h. Electric-powered trains were introduced a few years later, and reached a speed of 100 km/h around 1940. The maximum speed continued to increase after 1950, reaching 200 km/h in modern electric locomotives [10]. However, the maximum locomotive speed is not the only factor of permitted train speed. There are also speed restrictions on the infrastructure to ensure safe and economical operations [25]. Table 3.1 shows the development of maximum speed on the infrastructure imposed by such restrictions. Due to a higher axle load for freight trains, the speed limits are noteworthy lower than for the passenger trains.

Table 3.1: Historic maximum speed on the infrastructure, speed given in km/h [10].

| Type of train | 1950 | 1970 | 1990 | 2000 | 2016 |
|---|---|---|---|---|---|
| Passenger | 90 | 120 | 130 | 160 | 210 |
| Freight | 65 | 80 | 80 | 80 | 100 |

In addition to passenger and freight trains, some trains can be categorized as mixed trains with both passenger and freight wagons. Mixed trains have generally been used on lines with low traffic volume, or in the initial years after a new line opening [10]. Mixed trains were in service until 1968 [26], but the use was limited. Already in 1936, mixed trains accounted for only 6 % of the total running train distance. Most of the traffic on the Norwegian railway network can therefore be considered as either passenger-only or freight-only trains [10].

The number of axles and wagons in a train has also changed during the history. With data on both train running distance and axle running distance available, it is possible to estimate the historical average number of axles in each train. Such estimates shows that freight trains have had a significantly higher average number of axles than passenger trains throughout the history. This is related to a higher number of wagons in freight trains. While the number of freight wagons has been 20-25 through most of the history, it has been 5-8 for passenger trains. In multiple units, the number of wagons has increased from one wagon in 1930 to three wagons in 1990. MUs have also had a lower number of axles in each train compared to regular passenger trains [10].

The number of axles on a train is also dependent on the wagon design and geometry. A wagon is described by the distance between buffer and wheelset center, $a$, the center-center distance between two wheelsets, $b$, and the distance between wheels, $c$, in addition to the wagon length. The most common wagons are the two-axle wagons, the four-axle bogie wagons and the six-axle Jacobs bogie wagons, all shown in Figure 3.3. While the two-axle wagon and the bogie wagon have been in service since the beginning of the railway history, Jacobs bogie wagons were not introduced before 1993. The distribution between the three wagon types has varied for freight trains, with a current distribution of approximately 40 % two-axle wagons, 20 % bogie wagons and 40 % Jacobs bogie wagons. The design of passenger trains has, on the other hand, largely remained the same, with the bogie wagon as the most common type. Jacobs bogie wagons are however found in the newest multiple unit trains. The length of each wagon has generally increased during the history for both freight and passenger wagons [10].

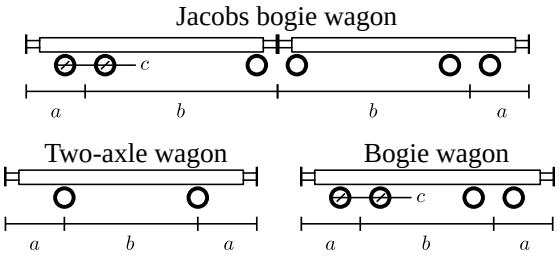


Figure 3.3: Geometry of wagons [10][2].

## 3.2 Load Models for Trains with Respect to Fatigue

A load model represents the load a structural component is subjected to at any instant of time as a function of magnitude and frequency [9]. Life estimation of railway bridges depends on the stress cycles in the material, represented by the load model. An accurate load model for trains is therefore essential in assessments of remaining fatigue life. A fatigue load model consists of a reference load and a set of calibration factors. According to Frøseth [2] there are two different types of load models presented in the literature. The first has a collection of standard trains as the reference load, with calibration factors that allow different compositions of these standard trains. Contrariwise, the second type has the reference load as one single load case with calibrations factors that account for differences in traffic and structural parameters.

Regardless of the type of load model, the primary intention is to introduce as similar fatigue damages to the components as the actual traffic loads. To make the model as equivalent as possible, calibration factors are adjusted by relevant data on the traffic situation. However, the traffic on the railway network is not homogeneous, and the load model must be adjusted for every investigated structure [2]. This fact requires available data on the historical traffic.

A major challenge in fatigue life estimations is the lack of such data. Measurements of historical traffic loads are generally not available. There is also a lack of data from other sources that could have been used to determine realizations or probabilistic descriptions of the load situation. Therefore, there are generally not sufficient data available to calibrate a load model, and the exact past traffic conditions can consequently not be thoroughly represented [10]. With only limited data available, several load cases may correspond to a given set of data. Each case introduces different fatigue damages in the structure, and to ensure a safe fatigue estimation the most damaging load case must be considered [2].

Therefore, it is necessary to establish load models that can represent all traffic cases. There are three desirable requirements of a load model [13]:

- Simple
- Conservative
- Consistent

The criterion of being simple refers to the usage of the load model. A complex load model is challenging to implement and the possibility of making errors increases. A simple load model, with few reference loads and attached factors, is therefore advantageous [13].

A conservative load model is a model that induces the same or more damage to the structure compared to the true traffic. This requirement will ensure that the true remaining life of the investigated component is at least as long as the calculated reaming fatigue life. Fulfilling this criterion ensures that the bridge is safe to operate within the estimated fatigue life [13]. Even though there is a lack of data on historical traffic, there are good descriptions of the locomotives and wagons that existed during different time periods. This makes it possible to determine the composition of locomotive and wagons that caused the most fatigue damage in a specific period. Assuming that all trains passed the component with this train composition, a conservative prediction of the traffic is made.

A load model should however not be too conservative. If the fatigue life of a bridge is estimated significantly shorter than the true life, there will be unnecessary use of resources and investments. Structural components may be replaced long before needed, or even worse, a safe and sufficient bridge might be demolished. It is also important that the same level of conservatism is introduced in each structural component. If the load model is more conservative for some components than others, the ranking of most critical cross-sections may have faults. Inspections are often performed based on analyses. If the fatigue analysis indicates one specific component as critical, this component will likely be inspected more thoroughly than other sections. This introduces the last criterion of consistency [13].

Figure 3.4 illustrates this issue. For different IL lengths, the fatigue damage is normalized against the damage introduced by the most damaging train and plotted for two different hypothetical components of the same structure. If the structural properties of the two components and the stress which they are subjected to are roughly equal, the fatigue damage introduced should be equal as well. This is not seen in the figure, where component 1 is more conservative than component 2. For a length of 7 meters, the analysis will conclude that component 2 only has 20 % of the damage compared to component 1. A railway load model for fatigue is considered consistent if all structural components have the same level of introduced fatigue damage relative to the fatigue damage from the most damaging train. The level of consistency can be expressed by the consistency factor, $\zeta$, defined as the ratio between the minimum and maximum normalized fatigue damage in all components of the structure [13]. The consistency factor is further defined in Subsection 3.3.2.

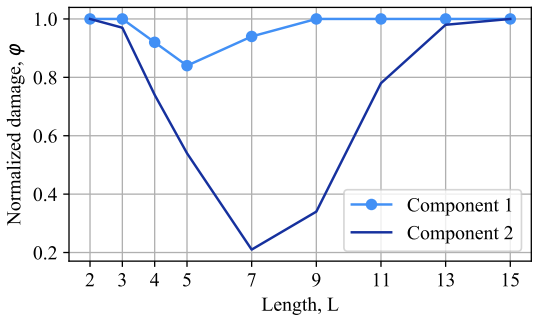


Figure 3.4: Normalized fatigue damage introduced in two structural components for an arbitrary load.

Several load models are suggested for fatigue life estimations in the literature, with two of them presented in the following subsections. The first is the load model used by Bane NOR [27], the Conventional Load Model, while the second is the load model proposed by Frøseth & Rønnquist [13], the Consistent Load Model. Both load models are thoroughly described, as the fatigue calculations in this thesis are based on the Consistent Load Model with the Conventional Load Model as the basis of comparison.

### 3.2.1 Load Model 1: The Conventional Load Model

Bane NOR has proposed a load model suitable for fatigue damage assessments [27]. The model uses a combination of reference trains from Eurocode 1 [11] and customized trains suggested by NTNU. The reference trains in Figure 3.5 are used to represent the freight traffic after 1985 and freight traffic in the future. Freight traffic before 1985 is represented

by the reference trains in Figure 3.6. Passenger traffic, both before and after 1985, are represented by the reference trains in Figure 3.7. In the EC1 trains, $Q$ is the total axle load and $q$ the axle load distributed over the total length of train, $L$. $V$ in the figure is the speed of the reference train. Letters in the train loop refer to the locomotive (L) or type of wagon (A, B or C). For both EC1 trains and NTNU trains, axle loads are shown above the trains while axle pitches are showed below. The axle loads are defined in newtons or tonnes, and the axle pitches in meters.

As seen in the figures, the traffic load is divided into five periods of time; pre-1900, 1900-1930, 1930-1960, 1960-1985 and post-1985. Since Figure 3.5 contains multiple reference trains for one time period, a distribution according to Table D.1 in EC1 [11] is used. The final distribution is presented in Table 3.2.

Table 3.2: Distribution of reference trains from EC1 [11].

| Reference train | Distribution [%] |
|---|---|
| 5 | 21.2 |
| 6 | 36.4 |
| 7 | 24.2 |
| 8 | 18.2 |

The presented reference trains are however not used directly in the load model. They are instead used with an adjusted number of wagons, determined by Bane NOR. The adjustments are fulfilled when the weight of each train is approximately 225 tonnes for passenger trains and 750 tonnes for freight trains, but no smaller than these values [27].

The speed of each reference train is also defined somewhat differently in the load model. For the reference trains applying for periods before 1985, the speed is determined by the speeds in Figures 3.6 & 3.7 and the current speed over the investigated bridge by

$$v = \text{speed in reference train} \leq \text{current speed} \tag{19}$$

where the current speed is found from national databases. Traffic after 1985 is, on the other hand, only described by a speed equal to the current speed over the investigated bridge.

Results from fatigue assessment by Bane NOR state that there may be some issues with the Conventional Load Model, as the same structural components tend to be indicated critical in most of the bridges studied [12]. The reason may be an inconsistent load model that induces higher relative fatigue damage in some of the components. As described in Section 2.2, fatigue damage is highly affected by the influence line. Some of the components will therefore experience highest fatigue damage when a train passes with maximum axle load, while others have the highest damage from trains where some wagons are empty. The reference trains in the Conventional Load Model seem to be selected somewhat randomly and not with the intention of making consistent levels of introduced fatigue damage in all structural components. There might therefore be errors when ranking the most exposed details and thus challenges in the inspections.

**Type 5** Locomotive-hauled freight train

$\Sigma Q = 21600\text{kN}$ $V = 80\text{km/h}$ $L = 270{,}30\text{m}$ $q = 80{,}0\text{kN/m'}$

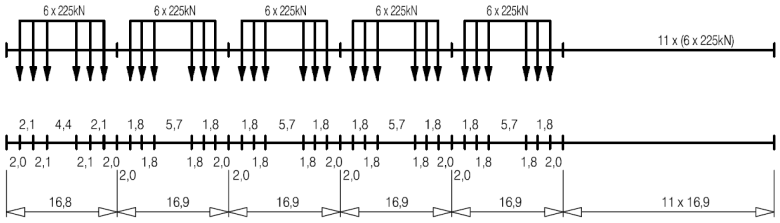


**Type 6** Locomotive-hauled freight train

$\Sigma Q = 14310\text{kN}$ $V = 100\text{km/h}$ $L = 333{,}10\text{m}$ $q = 43{,}0\text{kN/m'}$

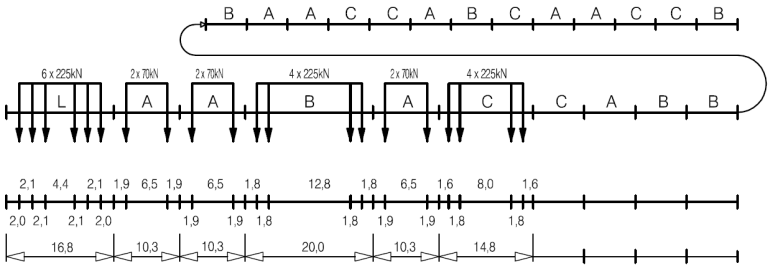


**Type 7** Locomotive-hauled freight train

$\Sigma Q = 10350\text{kN}$ $V = 120\text{km/h}$ $L = 196{,}50\text{m}$ $q = 52{,}7\text{kN/m'}$

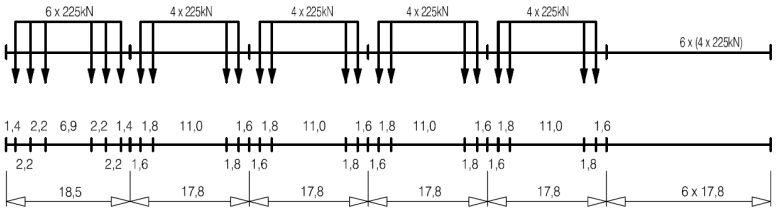


**Type 8** Locomotive-hauled freight train

$\Sigma Q = 10350\text{kN}$ $V = 100\text{km/h}$ $L = 212{,}50\text{m}$ $q = 48{,}7\text{kN/m'}$

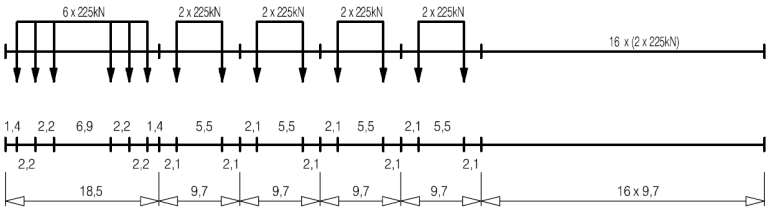


Figure 3.5: Reference trains for freight traffic, given by EC1 [11][3].

[3]Type 5 - Type 8 section D.3 (1) in NS-EN 1991-2:2003+NA:2010: Action on Structures - Part 2: Traffic loads on bridges copied by Ingvild Sørbel and Ane Bræin Skagestad for use in the thesis "Evaluation of the Consistent Load Model for Norwegian Railway Bridges Subjected to Fatigue Considering Track Curvature and Non-Standard Influence Lines" with permission from Standard Online AS 09.03.2021. Standard Online is not responsible for any errors in the reproduced material. See www.standard.no.

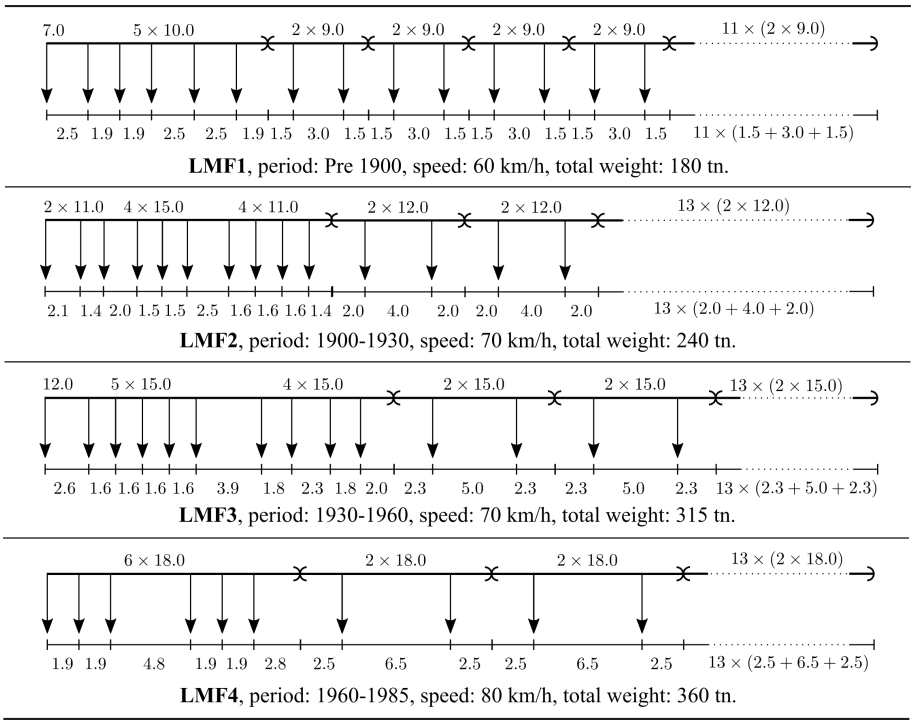


Figure 3.6: Reference trains for freight traffic as suggested by NTNU [27]. Figure is used with permission from NTNU (March 2021).

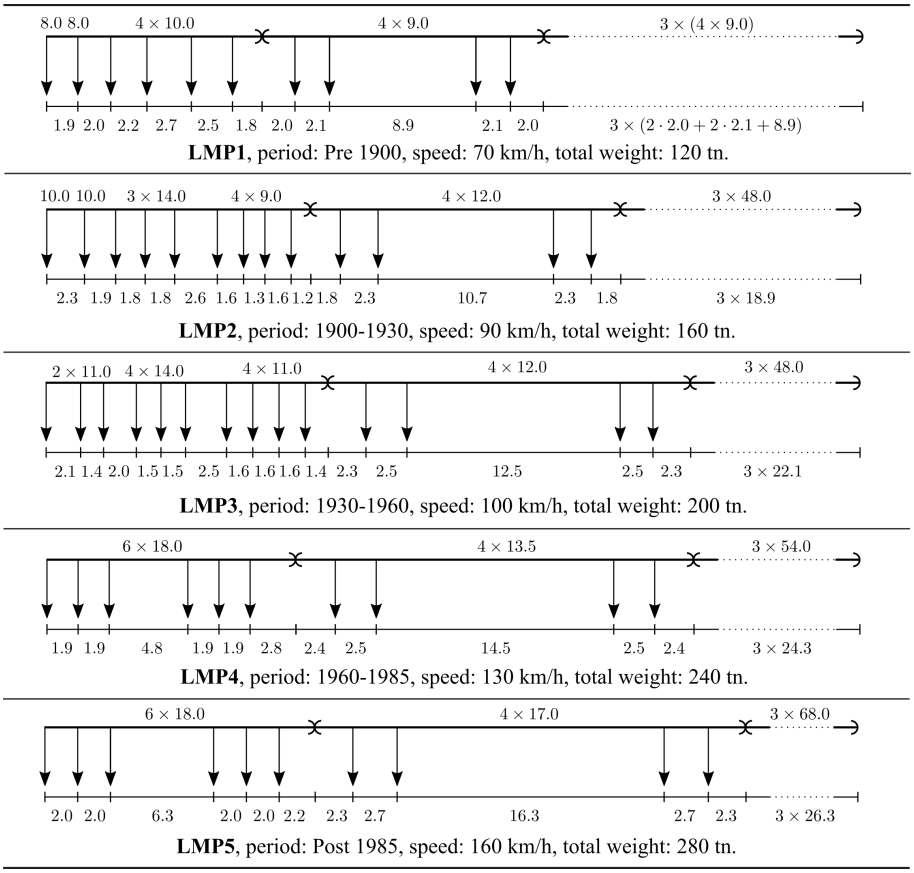


Figure 3.7: Reference trains for passenger traffic as suggested by NTNU [27]. Figure is used with permission from NTNU (March 2021).

### 3.2.2 Load Model 2: The Consistent Load Model

A more consistent load model for fatigue life estimations is proposed by Frøseth & Rønnquist [13]. This model is designed to introduce 1-2 times higher fatigue damage than the possible most damaging train composition passing the bridge. The Consistent Load Model is developed for bridges in the Norwegian railway network and consists of eight reference trains. Four trains apply for passenger traffic and four trains apply for freight traffic. Each reference train represents traffic from a historical period, where the periods 1900-1930, 1930-1960, 1960-1985 and 1985-today are studied. Traffic before 1900 is not considered due to small fatigue damage contributions compared to modern traffic.

All reference trains are presented in Figures 3.8 & 3.9. Each reference train consists of a locomotive (L) and base wagons (A,B,C,D). The numbers above the locomotives and wagons denote the axle load, while the numbers below denote the axle pitch, given in respectively tonnes and meters. The loop in each reference train indicates the composition of locomotives and wagon, where some of the wagons have a belonging number. This is a load modifier, meaning that the axle load from the specific base wagon should be modified with this number. Each reference train has a belonging traffic mix coefficient, $a_i$. The traffic mix coefficient is used to determine the total numbers of passages $n_i$ by reference train $T_i$, in the relation

$$n_i = a_i * n_0 \tag{20}$$

where $n_0$ is the total number of train passages for a line in the railway network during a particular time period. The total fatigue damage introduced by the load model for one train passage can then be written as

$$D = a_i * d_{SC}(T_i) \tag{21}$$

where $d_{SC}(T_i)$ is the fatigue damage introduced in structural component $SC$ by train $T_i$. Unlike the Conventional Load Model, the speed is only determined by the speed in Figures 3.8 & 3.9, not the current speed over the investigated bridge.

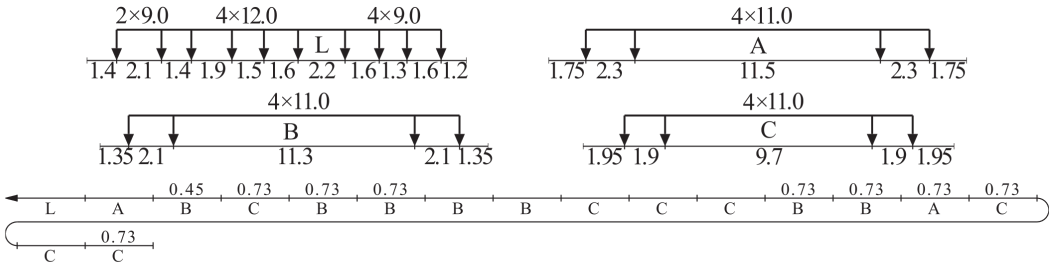


**Train 1**, period: 1900–1930, speed: 34 km/ h, total length: 306.2 m, total weight: 686.8 tn. $a_1 = 5.7$

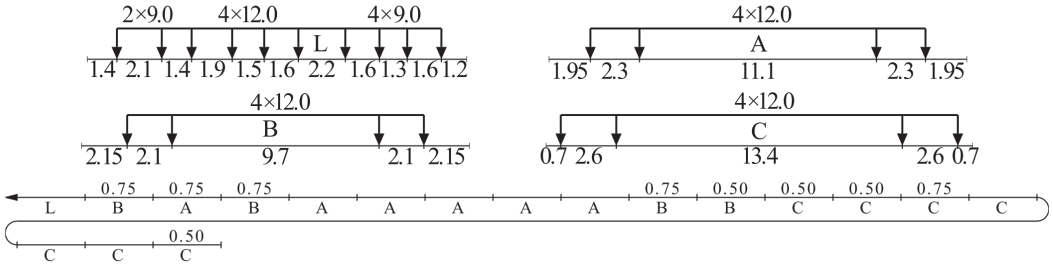


**Train 2**, period: 1930–1960, speed: 63 km/ h, total length: 348.2 m, total weight: 762.0 tn. $a_2 = 5.4$

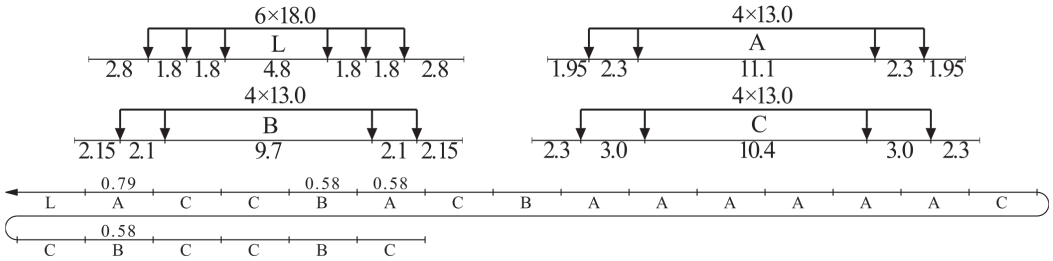


**Train 3**, period: 1960–1985, speed: 71 km/ h, total length: 415.2 m, total weight: 1071.6 tn. $a_3 = 2.4$

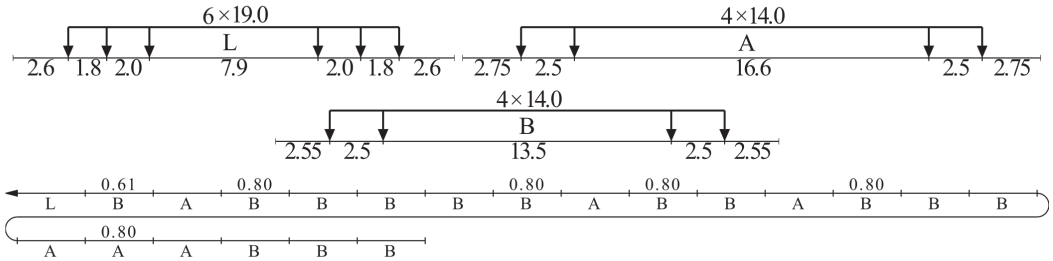


**Train 4**, period: 1985–, speed: 144 km/ h, total length: 513.7 m, total weight: 1156.2 tn. $a_4 = 2.8$

Train composition given by the loop, the identifier at the bottom and the load modifier at the top.

Figure 3.8: Reference trains for passenger traffic [2][1].

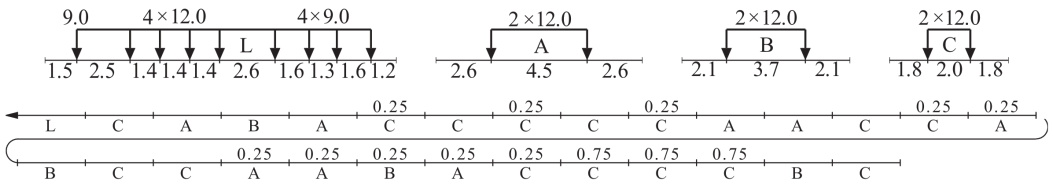


**Train 5**, period: 1900–1930, speed: 5 km/ h, total length: 209.7 m, total weight: 543.0 tn. $a_5 = 10.7$

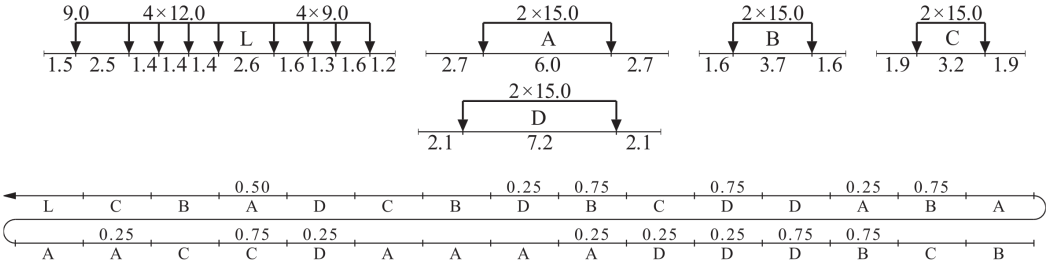


**Train 6**, period: 1930–1960, speed: 12 km/ h, total length: 293.7 m, total weight: 745.5 tn. $a_6 = 9.4$

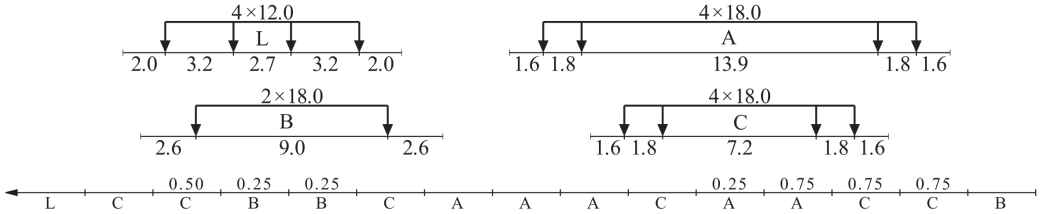


**Train 7**, period: 1960–1985, speed: 24 km/ h, total length: 243.2 m, total weight: 750.0 tn. $a_7 = 20.2$

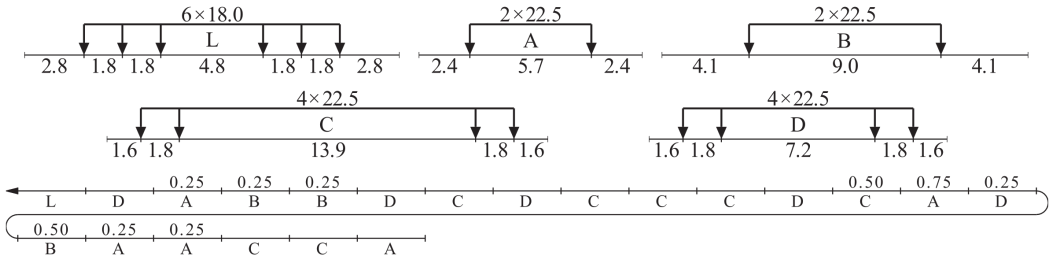


**Train 8**, period: 1985–, speed: 5 km/ h, total length: 336.6 m, total weight: 1233.0 tn. $a_8 = 15.0$

Train composition given by the loop, the identifier at the bottom and the load modifier at the top.

Figure 3.9: Reference trains for freight traffic [2][1].

| IL | Shape | Base system | Description |
|---|---|---|---|
| 1 |  | – | Total load effect |
| 2 |  | | $M_{AB}$ |
| 3 |  | 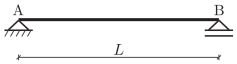  | $V_{AB}$ |
| 4 |  | | $M_{AB}$ |
| 5,5r |  | 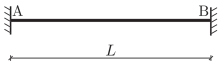  | $M_A$ , $M_B$ |
| 6,6r |  | | $M_{AB}$ , $M_{BC}$ |
| 7 |  | 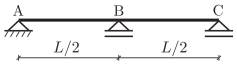  | $M_B$ |
| 8 |  | | $M_{BC}$ |
| 9,9r |  | 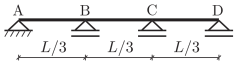  | $M_B$ , $M_C$ |
| 10,10r |  | | $M_{AB}$ , $M_{CD}$ |

Figure 3.10: Calibrated influence lines in the Consistent Load Model [2][1].

The Consistent Load Model is calibrated on the standard influence lines in Figure 3.10, parameterized by a length, $L_{IL}$. A structural component is then defined by one of these influence lines with a length selected form $L_{IL} = \{2.0, 3.0, 4.0, 5.0, 7.0, 9.0, 11.0, 15.0, 17.0, 23.0, 29.0, 37.0, 53.0, 101.0\}$. Components with short IL lengths are more sensitive to load positioning than components with longer lengths [13], which explains why the set of $L_{IL}$ contains a higher density of small lengths than the longer ones. As seen in Figure 3.10, some of the influence lines are asymmetric with two belonging numbers; IL and ILr. ILr represents the same influence line as IL, only reversed to the right side.

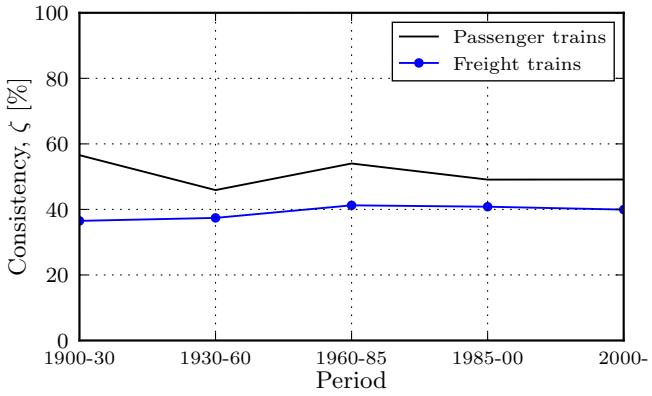


Figure 3.11: Consistency for passenger and freight trains in the Consistent Load Model [2][1].

Figure 3.11 illustrates the level of consistency in the proposed load model. The consistency is slightly better for passenger traffic, with approximately 50 % for passenger trains and 40 % for freight trains. The consistencies described apply however only to structural components with influence lines and lengths from the calibration set. Frøseth & Rønnquist discuss several reasons and consequences for the suboptimal level of consistency. They conclude that the structural component indicated critical to fatigue damage by the load model may be reassessed with a methodology that finds the most damaging train for each structural element, in order to make an entirely correct ranking of the most exposed details [28]. Further information on this methodology and the consistency is described in the following section.

## 3.3 Consistency based on Most Damaging Train (MDT)

The reference trains in the Consistent Load Model are suggested based on a methodology of finding the train that introduces the worst fatigue damage in different structural elements based on their influence line [13]. Due to high computational demands, such analyses can not be done for every component of an entire bridge on a daily basis. However, finding the most damaging train can, as mentioned, be used to investigate the consistency and ensure a correct ranking of the most exposed details. Finding the most damaging train is an optimization problem where the exact solution is found by checking the fatigue damage introduced by different trains in a defined train set. Theoretically, this can be done by checking all possible sets of trains, but due to computational demands approximate methods must be adopted [28].

### 3.3.1 Hill-Climbing and Late Acceptance Hill-Climbing

There are several strategies to obtain the solution to an optimization problem. A local search is one strategy. In a local search, a local neighborhood around every element in the solution space is used to reach the final solution. Each step slightly modifies the current solution, by for instance a swapping or a deleting of items [29]. Thus, the solution is improved by searching close to the current best-known solution. Local search algorithms start from an arbitrary solution and iterates by rejecting or accepting solution candidates until a final stopping condition occurs [30].

Hill-Climbing (HC) is one of the simplest local search strategies [30], where the final solution is obtained at the maximum or minimum in a graphical representation of the solution space. At these points, all neighbors lead in the wrong direction, and the search for the final solution must consequently be fulfilled. Local search heuristics work best in a coherent solution space, where a better solution is expected to lead in the right direction of the final solution [29]. However, there is a possible issue with the HC heuristic if the solution space contains local maxima. In this case, HC finds an optimum depending on the starting point, but most likely not the true global maxima [28]. This phenomenon is illustrated in Figure 3.12. If the starting point is close to the local maximum, the algorithm leads the solution towards this point. When the local maximum is reached, no better solution is found and the stopping condition occurs, even though the global maximum is not found.

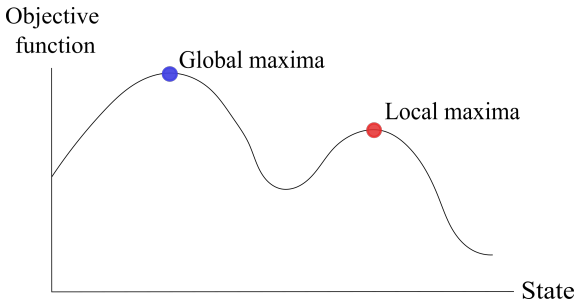


Figure 3.12: Principle of hill climbing.

The Late Acceptance Hill-Climbing (LAHC) is another local search algorithm, able to escape local optimums [30]. Unlike the HC heuristic, LAHC accepts non-improving moves depending on the recent moves in the solution history. While the solution candidate in HC is compared with the current solution, LAHC compares the solution candidate with the solution a given number of iterations ago. The history length, $\lambda$, is the only customized parameter in the LAHC algorithm and determines the number of non-improving moves accepted. A LAHC heuristic with $\lambda = 1$ corresponds simply to the standard HC heuristic [28].

### 3.3.2 The Consistency Factor

HC and LAHC can both be used to find the most damaging train for all structural components [28]. The maximum fatigue damage, $d\uparrow$, induced in a component is then found by the most damaging train for this particular component and its belonging influence line, according to Eq. (13) & (18). The maximum fatigue damage can further be used in the evaluation of the consistency. With the level of fatigue damage induced in component $SC$ as in Eq. (21), the definition of the consistency factor yields

$$\zeta(T_1, ..., T_n, a_1 ..., a_n) = \frac{min(\frac{\sum_{i=1}^{n} a_i d_{SC}(T_i)}{d_{SC}\uparrow})}{max(\frac{\sum_{i=1}^{n} a_i d_{SC}(T_i)}{d_{SC}\uparrow})} \tag{22}$$

which is equal to one for an entirely consistent load model [13].

# 4 Methodology

This thesis is based on the calculations of the fatigue life of two different bridges, Svånå Bridge and Sokna Bridge. Even though the truss systems differ, as Svånå Bridge has most of its truss underneath the train tracks (Figure 4.2) and Sokna Bridge has its truss on the upper side of the tracks (Figure 4.4), the principle used for estimating the remaining fatigue life is the same. Therefore, the method presented in this section applies to both bridges considered.

The remaining fatigue life of these bridges was in 2018 assessed by Bane NOR [31, 32]. Their results are therefore used as a basis for comparison. The main objective of this thesis is to distinguish how the results from the Consistent Load Model for trains differ from what has previously been used. Assumptions and simplifications are therefore kept the same as in the calculation done by Bane NOR.

## 4.1 Initial Calculations

### 4.1.1 Material Properties

The material properties used for the fatigue life estimation are based on the Norwegian Handbook for Classification of Bridges, R412 [33]. All relevant properties are presented in Table 4.1.

Table 4.1: Steel properties used for fatigue life estimation.

| Steel property | Magnitude |
|---|---|
| Density | $\gamma_s = 77\ kN/m^3$ |
| Yielding strength | $f_y = 220\ N/mm^2$ |
| Tensile strength | $f_u = 350\ N/mm^2$ |
| Young's Modulus | $E = 2.1 * 10^5\ N/mm^2$ |
| Shear Modulus | $G = 0.8 * 10^5\ N/mm^2$ |
| Poisson's Ratio | $\nu = 0.3$ |

The partial safety factors depend on the consequence of failure. According to NS-EN 1993-1-9 [18] the factor of the primary bearing, $\gamma_{Mf,p}$, is set to 1.35 while the factor of the secondary bearing, $\gamma_{Mf,s} = 1.15$. See Subsection 4.1.2 for the differentiation between primary and secondary bearing.

### 4.1.2 Bridge Models

Nodes, elements and classification of Svånå and Sokna Bridge are provided by Bane NOR [31,32], and form the basis of the fatigue life calculations. Both Svånå and Sokna are riveted steel bridges, built before 1920. The bridge components are differentiated into primary and secondary bearing, depending on how the loads are transferred through the structure. Generally, the primary system transfers the loads throughout the structure until it reaches the supports. The secondary bearing's main purpose is to transfer additional loads, i.e., the train load, to the primary system. To illustrate the differentiation of primary and secondary bearing, an element model of Sokna Bridge has been replicated and presented in Figure 4.1 as an example.

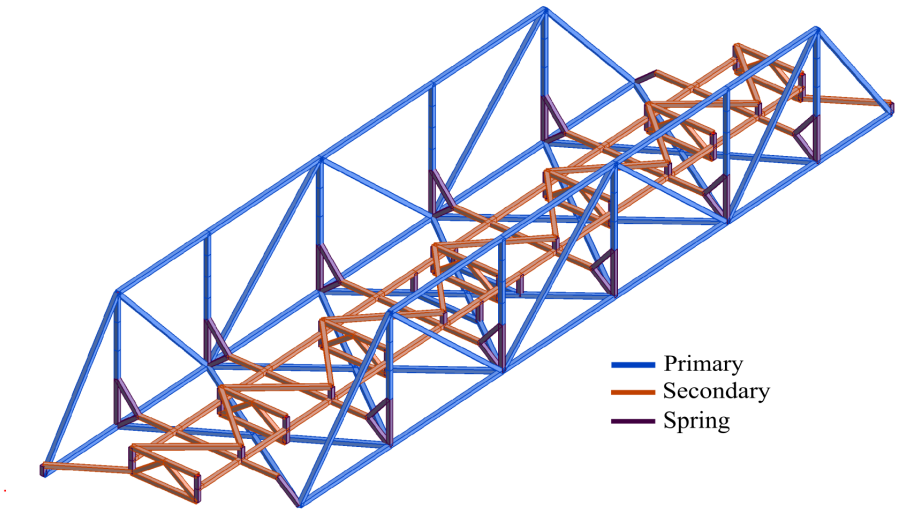


Figure 4.1: Structure categories for Sokna Bridge.

#### Svånå Bridge

Svånå Bridge is a part of the Norwegian railroad Dovrebanen, on the route between Hjerkinn and Oppdal. It was built in 1918 and has a span of 21 meters. Svånå is a truss bridge with the truss constructed beneath the train track. The bridge has a horizontal curvature with a radius of 1000 meters.

The cross-sections are combinations of rectangular plates and L-profiles. The element model of the bridge contains the two main trusses, two stringers and seven cross girders. It also has wind, wobble and break bracing.

Some simplifications and assumptions have been made by Bane NOR. In 1935 the bridge was locally reinforced around one of the supports. Some additional rivet plates were also added. It is assumed that these reinforcements do not affect the behavior of the structure and are therefore disregarded. It is further assumed that the center of gravity for each bridge element coincides with the grid lines of the bridge. For larger eccentricities, rigid coupling springs are used. It is also assumed that some smaller bars do not contribute to the cross-sectional area or the second area of moment, but do contribute to torsion.

An equivalent plate thickness is therefore calculated for these bars. The cross girders are modeled with crossing diagonals in order to obtain the correct stiffness.

Figure 4.2 shows the placement and classification of the different structural elements for Svånå Bridge, as given by Bane NOR. For details about the cross-sections and element numbering and more thorough explanations of the assumptions and simplifications, see the report on Svånå Bridge from Bane NOR [31].

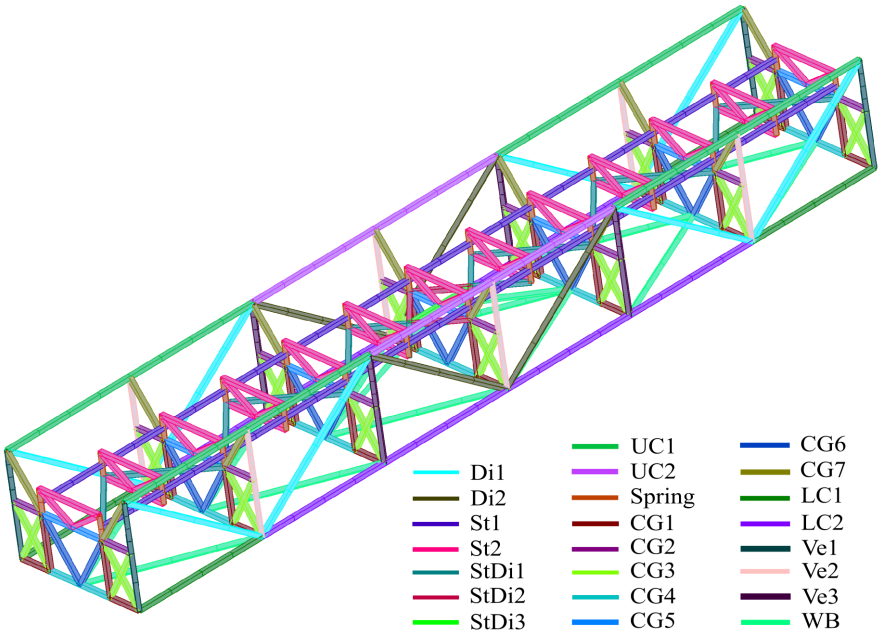


Figure 4.2: Replica of element model of Svånå Bridge showing cross-sections classes.

### Sokna Bridge

Sokna Bridge is also a part of Dovrebanen, on the route between Støren and Trondheim. The bridge was built in 1917 and consists of three equal truss bridges as shown in Figure 4.3. Each bridge has a span of 20 meters, with the truss constructed above the train track. Sokna Bridge has a horizontal curvature with a radius of 500 meters.

The element model contains the two trusses on each side of the track, wind bracing at the lower chord, stringers, cross-girders, wobble bracing and stiffeners between the stringers. The cross-sections consists of combinations of rectangular plates and isosceles L-profiles.

Some simplifications and assumptions by Bane NOR have also been done for Sokna Bridge. The bridge was reinforced in 1942, and these reinforcements are assumed to apply for the entire lifetime of the bridge. The node between the cross-girder and vertical in the truss is further assumed rigid. It is also assumed that the center of gravity in each bridge element coincides with the grid lines of the bridge. For larger eccentricities, rigid coupling springs are used. It is also assumed a constant eccentricity between the center of the bridge and the center of the rails, determined as the eccentricity at the midspan of the bridge.

Figure 4.3: Picture of Sokna Bridge.

The element model of Sokna Bridge is visualized in Figure 4.4. Note that the model only shows one of the three equal spans. For more details on modeling and calculations, see Bane NORs report on Sokna Bridge by Lundamo [32].

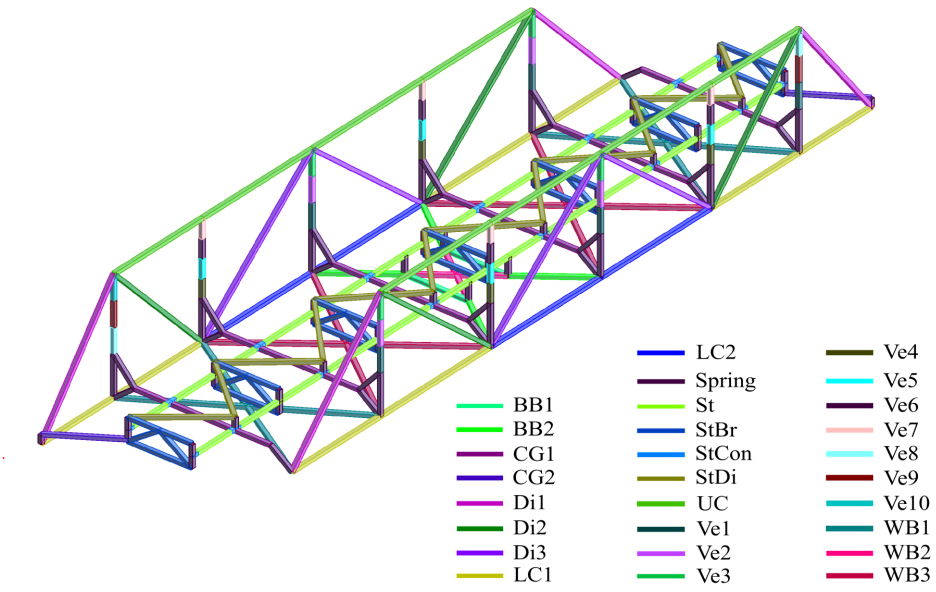


Figure 4.4: Replica of element model of Sokna Bridge showing cross-sections classes.

### 4.1.3 Finding the Response

To find the response as explained in Subsection 2.2.2, the influence lines of the bridges have to be determined. These are found using a unit load over the two train tracks of each bridge. As both Svånå and Sokna Bridge have horizontal curvature, centrifugal forces are introduced in addition to the axle load of the train, as illustrated in Figure 4.5. The trainload is split into three parts to get the correct effect of the centrifugal force in the determination of the influence line [27]:

- Vertical axle load, $R_a$
- Vertical forces introduced by the centrifugal force, $R_v$
- Horizontal load from the centrifugal force, $R_h$

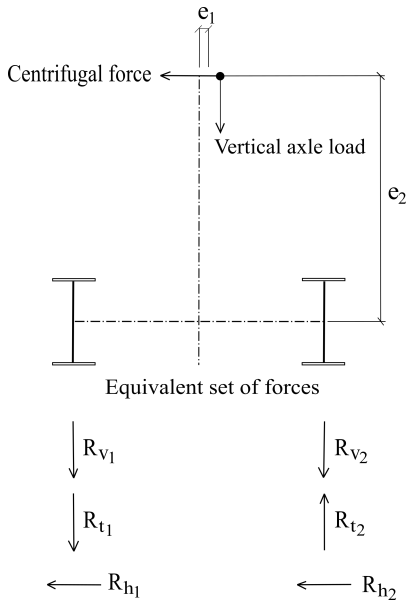


Figure 4.5: Contributions from train loading.

These three influence lines are provided by Bane NOR for each defined stress point in the element model. The influence lines are provided for each category of axial force, moment about y-axis and moment about z-axis [31, 32]. In order to obtain the correct scaling of $R_v$ and $R_h$ due to the centrifugal force, the following is applied [11, 27]:

$$Q_{tk,i} = \frac{v^2}{127r}(f_r \cdot R_{il,i}) \tag{23}$$

where $v$ is the train speed, $r$ is the radius of the curvature and $R_{il,i}$ is either the value of $R_v$ or $R_h$ for the stress point considered. The reduction factor, $f_r$, is neglected both by Bane NOR and in the analysis with the Consistent Load Model.

The permanent loads on the train tracks are also provided. However, the analysis does not consider whether the component is under tension or compression. As the permanent loads do not change the magnitude of the stress ranges, they do not impact the results for fatigue damage. Permanent loads are consequently not considered in the analysis with the Consistent Load Model.

The response is further found by taking the convolution of the influence lines and the loading from the considered train, $f$, as explained in Section 2.2. The load function is defined by the reference trains in Figures 3.8 & 3.9, and provided in Python codes by Frøseth [34]. The dynamic amplification factor from Eq. (14) is included for the vertical loads, while 1.0 is used for the horizontal load caused by the centrifugal force [27]. The determinant length needed as input for the DAF is also provided by Bane NOR. The response from the three influence lines is then found by the following:

$$z = f * [(R_a + Q_{tk,v}) \cdot \Phi + Q_{tk,h}] \tag{24}$$

The response is found for the axial load, $N_x$, the moment about the y-axis, $M_y$, and the moment about the z-axis, $M_z$. The three responses are combined into one single stress history, $\sigma$, by dividing each response by the corresponding cross-sectional parameter, respectively $A_x$, $W_y$ and $W_z$, before adding them together.

## 4.2 Fatigue Life Estimation

To find the fatigue damage, the stress history has to be translated to stress ranges. Here, the rainflow cycle counting function, which executes the principle described in Subsection 2.1.2, is used. The fatigue damage for the specific train is further found by applying Miner's rule, as in Eq. (5).

SN-curves are used to obtain the number of cycles a component can withstand for a specific stress range. Since both Svånå and Sokna Bridge are steel bridges with riveted components, a trilinear SN-curve with detail category 71 MPa is primarily used. After the fatigue damage is calculated, the elements with $D_h$ higher than the critical level of 1.0 are changed to a linear curve with detail category 85 MPa, and slope $m = 5$, as this also was found to be conservative by Taras & Greiner [19]. The partial safety factors are introduced by dividing the detail category by the value corresponding to the primary or secondary bearing. Figure 4.6 shows the four curves used in the fatigue life analyses.

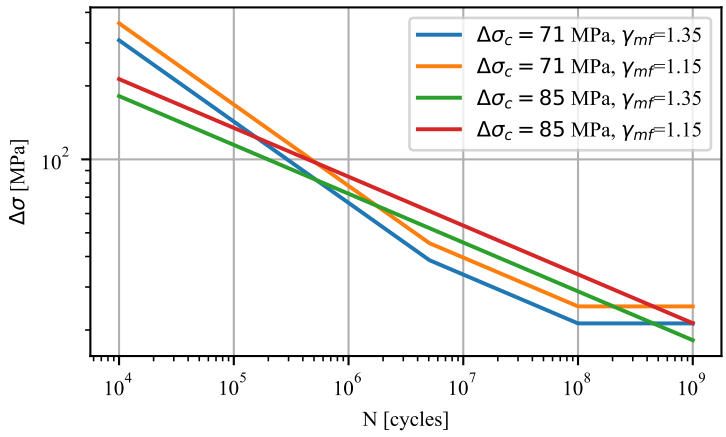


Figure 4.6: The four different SN-curves used in the fatigue life analysis.

The fatigue damage found by applying Miner's rule, $d_{Ti}$, corresponds to the damage from one passing of one of the reference trains from the Consistent Load Model. Depending on the direction, positive or negative influence lines are used in the convolution when calculating the response. It is further assumed that half of the trains pass in one direction and the other half in the opposite direction. Therefore, the fatigue damage for one train is calculated as the average of the damage found using the structural element's positive and negative influence lines. The total fatigue damage for the particular train is found by the following:

$$D_{Ti} = a_i \cdot \frac{d_{Ti,pos} + d_{Ti,neg}}{2} \cdot n_i \tag{25}$$

where $a_i$ is the traffic mix coefficient for the reference train $i$, and $n_i$ is the total number of passages for the specific train type and period.

Historically, there have been very few counts of passages on the Norwegian railroad, making the data available limited. An assumption of the number of trains passing on each track every year has therefore been made. Bane NOR used the passages in 2011, 2014 and 2015 as the basis for their calculations. The maximum yearly passages from those three years were used for all years in the historical fatigue calculations. The yearly passages used for Svåna and Sokna Bridge are presented in Table 4.2 [27].

Table 4.2: Yearly number of train passages as a maximum of 2011, 2014 and 2015.

| Bridge | Route | Yearly Passenger Trains | Yearly Freight Trains |
|---|---|---|---|
| Svånå | Hjerkinn - Oppdal | 2850 | 4480 |
| Sokna | Støren - Trondheim | 5367 | 4480 |

The total number of passages is found by multiplying the yearly passages by the number of years the reference train is valid. The historic damage is found from the construction year of the bridge until 2018. 2018 is considered instead of 2021, as this was the year the basis of comparison was performed. A linear yearly increase in passages of 5 % for passenger trains and 2 % for freight trains is further assumed [27]. The total number of passages used for each reference train is presented in Table 4.3. $T4_{1year}$ and $T8_{1year}$ denote the first year after the historic fatigue calculations are made. See Subsection 3.2.2 for details about the loading from reference trains T1 - T8.

Table 4.3: Passages for each reference train in the fatigue analysis, using the same yearly number of passages as determined by Bane NOR.

| Train | Period | Type | $n_i$, Svånå | $n_i$, Sokna |
|---|---|---|---|---|
| T1 | Year built-1930 | Passenger | 34 200 | 69 771 |
| T2 | 1930-1960 | Passenger | 85 500 | 161 010 |
| T3 | 1960-1985 | Passenger | 71 250 | 134 175 |
| T4 | 1985 $\rightarrow$ | Passenger | 94 050 | 177 111 |
| T5 | Year Built-1930 | Freight | 53 760 | 58 240 |
| T6 | 1930-1960 | Freight | 134 400 | 134 400 |
| T7 | 1960-1985 | Freight | 112 000 | 112 000 |
| T8 | 1985 $\rightarrow$ | Freight | 147 840 | 147 840 |
| $T4_{1year}$ | Future | Passenger | 2 850 | 5 367 |
| $T8_{1year}$ | Future | Freight | 4 480 | 4 480 |

The calculation in Eq. (25) is performed for trains T1 - T8. The total historic damage for each structural element is found as the sum of the fatigue damage from each train by

$$D_h = D_{T1} + D_{T2} + D_{T3} + ... + D_{T8} \tag{26}$$

The critical level of fatigue damage, $D_{cr}$, is considered as 1.0 [18], meaning that the components with damage smaller than 1.0 still have remaining theoretical fatigue life, $T_{RL}$. As it is assumed an increase in passages of 5 % for passenger trains and 2 % for freight trains in the future, Eq. (7) has to be rewritten. The remaining fatigue life is then determined by applying Newton's Method [35] on the following equation:

$$T_{RL} = \frac{1 - D_h}{D_{1,T4} * 1.05^{T_{RL}} + D_{1,T8} * 1.02^{T_{RL}}} \tag{27}$$

where $D_{1,T4}$ and $D_{1,T8}$ is the damage introduced by T4 and T8 in one year.

Frøseth & Rønnquist estimated historical yearly train passages by studying old timetables. These estimates [13] are reproduced and presented in Appendix A. Even though their findings are assumed more realistic than using the same number of passages for all years, the numbers presented in Table 4.3 are used in the main fatigue analysis. Keeping all other factors than the actual load model constant makes it easier to distinguish how the change in load model affects the results.

However, the number of passages obtained by Frøseth & Rønnquist is used in a supplementary analysis to study how the difference in passages affects the results. The total number of passages for each period and train type, as presented in Table 4.4, is found by interpolating the yearly passages from Figure A.1.

Table 4.4: Passages for each reference train in the fatigue analysis, using passages interpolated from timetables.

| Train | Period | Type | $n_i$, Svånå | $n_i$, Sokna |
|---|---|---|---|---|
| T1 | Year built-1930 | Passenger | 19 272 | 89 936 |
| T2 | 1930-1960 | Passenger | 71 723 | 260 340 |
| T3 | 1960-1985 | Passenger | 74 095 | 499 220 |
| T4 | 1985 → | Passenger | 129 940 | 601 060 |
| T5 | Year Built-1930 | Freight | 41 792 | 65 445 |
| T6 | 1930-1960 | Freight | 95 448 | 171 915 |
| T7 | 1960-1985 | Freight | 100 560 | 118 810 |
| T8 | 1985 → | Freight | 174 900 | 191 500 |
| $T4_{1year}$ | Future | Passenger | 3 650 | 22 630 |
| $T8_{1year}$ | Future | Freight | 5 110 | 6 925 |

# 5 Results from the Fatigue Analyses

## 5.1 Svånå Bridge

### 5.1.1 Critical Components

Table 5.1 presents the most damaged element in each section class found from the analysis with the Consistent Load Model. For the cross-section classes not presented in the table, all stress points had fatigue damage, $D_h$, smaller than 0.3. Table 5.2 is a collection of the results from the calculations done by Bane NOR [31]. It also shows the most damaged point for each cross-section class. Note that only the results for points with remaining fatigue life smaller than 50 years were available.

Table 5.1: Svånå Bridge - Most critical point for each section class found with the Consistent Load Model.

| Element | $T_{RL}$ [yrs] | $D_h$ | $\Delta\sigma_C$ [MPa] | Section | Category |
|---|---|---|---|---|---|
| 24041 | 0.0 | 11.4196 | 85 | Di2 | primary |
| 13061 | 0.0 | 10.5817 | 85 | Ve3 | primary |
| 42021 | 0.0 | 6.7964 | 85 | St1 | secondary |
| 32031 | 0.0 | 1.8779 | 85 | CG4 | secondary |
| 24061 | 0.0 | 1.7364 | 85 | Di1 | primary |
| 11044 | 0.0 | 1.5725 | 85 | LC2 | primary |
| 22041 | 0.0 | 1.2095 | 85 | UC2 | primary |
| 44251 | 0.0 | 1.1624 | 85 | St2 | secondary |
| 31061 | 0.3 | 0.9915 | 71 | CG5 | secondary |
| 35101 | 1.4 | 0.9681 | 71 | CG1 | secondary |
| 22013 | 4.2 | 0.9065 | 71 | UC1 | primary |
| 23021 | 7.9 | 0.8272 | 71 | Ve1 | primary |
| 36151 | 36.1 | 0.3108 | 71 | CG3 | secondary |

Table 5.2: Svånå Bridge - Most critical point for each section class found with the Conventional Load Model [31].

| Element | $T_{RL}$ [yrs] | $D_h$ | $\Delta\sigma_C$ [MPa] | Section | Category |
|---|---|---|---|---|---|
| 13061 | 0.0 | 1.3646 | 85 | Ve3 | primary |
| 41121 | 2.3 | 0.9470 | 71 | St1 | secondary |
| 14041 | 6.7 | 0.8468 | 71 | Di2 | primary |
| 11044 | 26.4 | 0.6373 | 71 | LC2 | primary |
| 36021 | 26.7 | 0.5485 | 71 | CG4 | secondary |
| 14014 | 36.9 | 0.5461 | 71 | Di1 | primary |

The Consistent Load Model results in more severe fatigue damage, with the highest being 11.4. As the damage values from the Consistent Load Model are significantly higher, eight cross-section classes are found critical, compared to only one (Ve3) with the Consistent Load Model. Ve3 is also found critical in the new analysis, but is now passed in ranking by the diagonals (Di2). Although the ranking has changed, the six cross-section types most damaged are the same for both load models.

### 5.1.2 Damage Distribution

In Table 5.3, the most damaged point from Table 5.1 is considered. For this specific point, freight trains cause the greatest fatigue damage, as it is found that almost 98 % of the total damage is done by freight trains. For the passenger trains, the distribution of damage is fairly similar for all periods. Freight trains have, on the other hand, 99 % of the damage done after 1960. Table 5.3 also shows that T8 for 1985 until 2018 provides the most significant damage.

Table 5.3: Svånå Bridge - Distribution of damage from each reference train for the most critical point at element 24041.

| Train | $D_{tot}$ | [%] | [%] |
|---|---|---|---|
| T1 | 0.0224 | 0.20 | |
| T2 | 0.1056 | 0.92 | |
| T3 | 0.0406 | 0.36 | Passenger |
| T4 | 0.0659 | 0.58 | 2.06 |
| T5 | 0.0305 | 0.27 | |
| T6 | 0.0745 | 0.65 | |
| T7 | 2.6636 | 23.32 | Freight |
| T8 | 8.4165 | 73.70 | 97.94 |
| Sum | 11.4196 | 100 | 100 |

Figure 5.1 takes a closer look at the four most critical cross-section types. It shows a fairly similar distribution of damage for the different reference trains, as presented in Table 5.3. The only deviation is that the relative damage from passenger trains is slightly higher for cross-section type Ve3 (Element 13061) and CG4 (Element 32031).

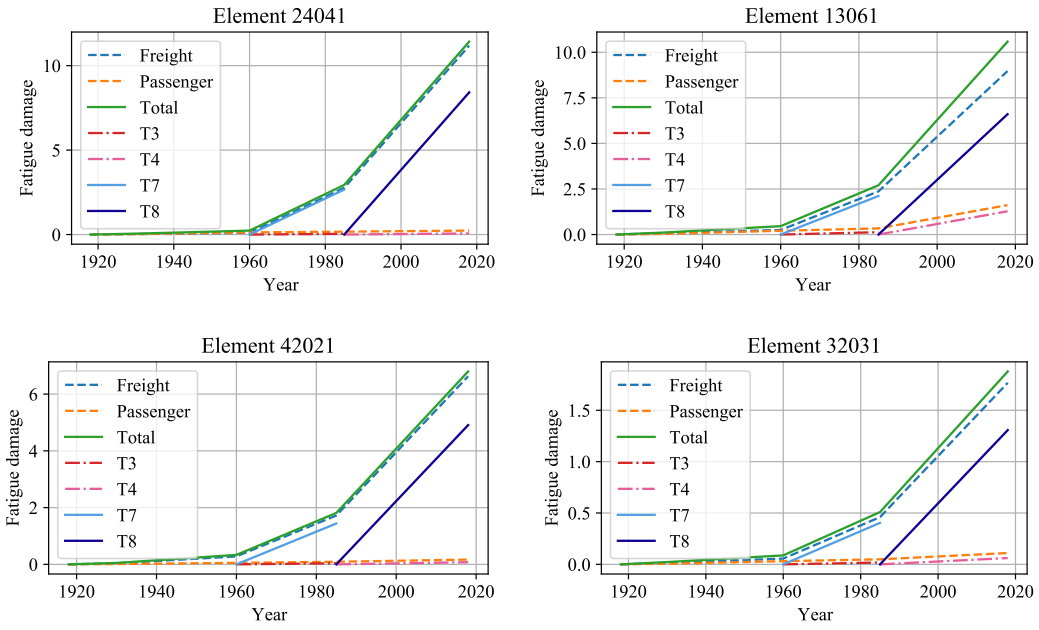


Figure 5.1: Svånå Bridge - Damage by train for most critical elements in most critical cross-section types.

### 5.1.3 Detail Category

Preliminary, the calculation was run with all points having a detail category of 71 MPa and a trilinear curve from Eurocode 3. Based on these results, all elements with historical damage higher than 1.0 were changed to a detail category of 85 MPa and a linear curve, as explained in Section 4.2. Although 85 MPa is also seen as lower-bound, it significantly impacted the estimated historical damage. Table 5.4 compares the most damaged cross-sections before and after the SN-curve was changed. The fatigue damage of the most critical points is then halved or reduced even more. The change in curve also affects the ranking.

Table 5.4: Svånå Bridge - Change in fatigue damage when detail category is changed for critical components.

| Section type | $\Delta\sigma_C = 71$ MPa | $\Delta\sigma_C = 85$ MPa |
|---|---|---|
| Ve3 | $D_h = 26.29$ | $D_h = 10.58$ |
| St1 | $D_h = 23.25$ | $D_h = 6.80$ |
| Di2 | $D_h = 22.82$ | $D_h = 11.42$ |
| CG4 | $D_h = 7.85$ | $D_h = 1.88$ |

### 5.1.4 Number of Passages

The same fatigue calculations were also performed using the number of passages as defined in Table 4.4. The difference in passages between Bane NOR's constant passages and Frøseth & Rønnquist's timetable is also shown in Figure 5.2. Table 5.5 presents the results found for the timetable analysis. Compared to the fatigue damage obtained with constant yearly passages, it is slightly higher. What is found to be the most critical cross-section type does however remain unchanged.

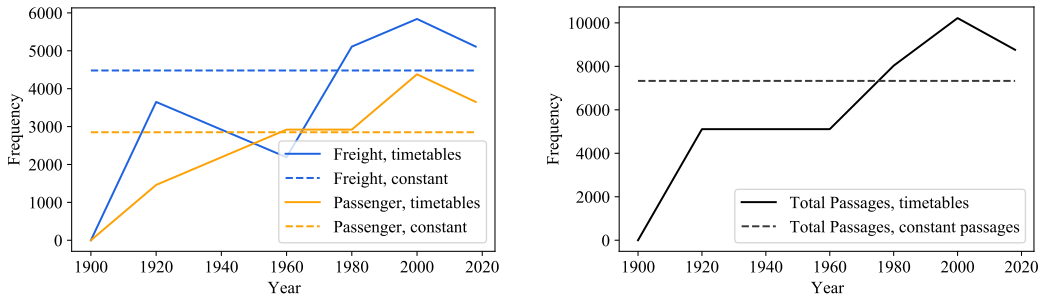


Figure 5.2: Svånå Bridge - Passages defined as constant each year versus passages from timetable.

Table 5.5: Svånå Bridge - Most critical point for each section class found with the Consistent Load Model and number of passages from timetable.

| Element | $T_{RL}$ [yrs] | $D_h$ | $\Delta\sigma_C$ [MPa] | Section | Category |
|---|---|---|---|---|---|
| 24041 | 0.0 | 12.6596 | 85 | Di2 | primary |
| 13061 | 0.0 | 11.9552 | 85 | Ve3 | primary |
| 42021 | 0.0 | 7.4878 | 85 | St1 | secondary |
| 32031 | 0.0 | 2.0780 | 85 | CG4 | secondary |
| 24061 | 0.0 | 1.8769 | 85 | Di1 | primary |
| 11044 | 0.0 | 1.7267 | 85 | LC2 | primary |
| 44251 | 0.0 | 1.5101 | 85 | St2 | secondary |
| 22041 | 0.0 | 1.2979 | 85 | UC2 | primary |
| 22013 | 0.1 | 0.9976 | 71 | UC1 | primary |
| 35061 | 1.4 | 0.9669 | 71 | CG5 | secondary |
| 35091 | 2.1 | 0.9496 | 71 | CG1 | secondary |
| 23021 | 4.0 | 0.9083 | 71 | Ve1 | primary |
| 36151 | 31.7 | 0.3674 | 71 | CG3 | secondary |
| 23111 | 32.6 | 0.3487 | 71 | Ve2 | primary |

## 5.2 Sokna Bridge

### 5.2.1 Critical Components

Table 5.6 presents the most damaged element in each section class found with the Consistent Load Model. For the cross-section classes not presented in the table, all details had fatigue damage smaller than 0.7. Table 5.7 is a collection of the results from the calculations performed by Bane NOR [32]. It also shows the most damaged point in each cross-section class. Note that only the results for stress points with remaining fatigue life smaller than 100 years were available.

Table 5.6: Sokna Bridge - Most critical point for each section class found with the Consistent Load Model.

| Element | $T_{RL}$ [yrs] | $D_h$ | $\Delta\sigma_C$ [MPa] | Section | Category |
|---|---|---|---|---|---|
| 41102 | 0.0 | 14.6949 | 85 | St | secondary |
| 61141 | 0.0 | 10.9867 | 85 | StBr | secondary |
| 41081 | 0.0 | 8.1810 | 85 | StCon | secondary |
| 13024 | 0.0 | 3.5119 | 85 | Di2 | primary |
| 63121 | 0.0 | 2.3978 | 85 | StDi | secondary |
| 72061 | 0.0 | 2.1154 | 85 | WB2 | primary |
| 11044 | 0.0 | 1.8982 | 85 | LC2 | primary |
| 11061 | 0.0 | 1.7912 | 85 | LC1 | primary |
| 31034 | 0.0 | 1.3785 | 85 | CG1 | secondary |
| 16034 | 0.0 | 1.2428 | 85 | Ve1 | primary |
| 16024 | 0.0 | 1.0074 | 85 | Ve2 | primary |
| 12033 | 0.7 | 0.9838 | 71 | UC | primary |
| 72021 | 2.5 | 0.9268 | 71 | WB1 | primary |
| 71052 | 5.5 | 0.8779 | 71 | BB2 | primary |
| 72031 | 7.1 | 0.8364 | 71 | WB3 | primary |
| 13044 | 7.3 | 0.8307 | 85 | Di3 | primary |
| 16014 | 9.0 | 0.7791 | 85 | Ve3 | primary |
| 65022 | 6.8 | 0.7759 | 71 | CG2 | secondary |

Table 5.7: Sokna Bridge - Most critical point for each section class found with the Conventional Load Model [32].

| Element | $T_{RL}$ [yrs] | $D_h$ | $\Delta\sigma_C$ [MPa] | Section | Category |
|---|---|---|---|---|---|
| 13024 | 32.8 | 0.5617 | 71 | Di2 | primary |
| 11044 | 46.1 | 0.5223 | 71 | LC2 | primary |
| 16034 | 52.1 | 0.3313 | 71 | Ve1 | primary |
| 41151 | 54.4 | 0.3385 | 85 | St | secondary |
| 41031 | 55.3 | 0.3540 | 71 | StCon | secondary |
| 11014 | 55.8 | 0.4330 | 71 | LC1 | primary |
| 16024 | 63.2 | 0.2748 | 71 | Ve2 | primary |
| 16014 | 85.5 | 0.1989 | 71 | Ve3 | primary |
| 71074 | 95.4 | 0.1966 | 71 | WB2 | primary |

The Consistent Load Model results in more extensive fatigue damage for Sokna Bridge, with the highest being 14.7. Different parts of the stringers (St) were found to be the most critical parts, along with some of the diagonals (Di2) and the wind bracing (WB2). Eleven different cross-section types were critical for fatigue damage with the Consistent Load Model, while the Conventional Load Model resulted in all components still having remaining fatigue life. There are also considerable differences in which cross-sections were found to be most exposed.

### 5.2.2 Damage Distribution

Tables 5.8 & 5.9 describes the contribution to fatigue damage from each train for the most critical point at the stringer and at the diagonal, respectively. While Svånå Bridge had a clear tendency for freight trains contributing the most, this varies more for Sokna Bridge. The stringer had almost 88 % of its fatigue damage from passenger trains, where the highest contribution is from T4. For the diagonal, freight trains are the most damaging.

Table 5.8: Sokna Bridge - Distribution of damage from each reference train for the most critical point at element 41102.

| Train | $D_{tot}$ | [%] | [%] |
|---|---|---|---|
| T1 | 0.0085 | 0.06 | |
| T2 | 0.0787 | 0.53 | |
| T3 | 0.1529 | 1.04 | Passenger |
| T4 | 12.6549 | 86.12 | 87.75 |
| T5 | 0.0061 | 0.04 | |
| T6 | 0.0380 | 0.26 | |
| T7 | 0.4731 | 3.22 | Freight |
| T8 | 1.2827 | 8.73 | 12.25 |
| Sum | 14.6949 | 100 | 100 |

Table 5.9: Sokna Bridge - Distribution of damage from each reference train for the most critical point at element 13024.

| Train | $D_{tot}$ | [%] | [%] |
|---|---|---|---|
| T1 | 0.0262 | 0.75 | |
| T2 | 0.1058 | 3.01 | |
| T3 | 0.0792 | 2.25 | Passenger |
| T4 | 0.6126 | 17.44 | 23.45 |
| T5 | 0.0304 | 0.87 | |
| T6 | 0.0694 | 1.98 | |
| T7 | 0.6258 | 17.82 | Freight |
| T8 | 1.9626 | 55.88 | 76.55 |
| Sum | 3.5119 | 100 | 100 |

As for Svånå Bridge, Sokna Bridge also has most of its contribution from the more recent periods. The period after 1960 accounts for approximately 95 % of the total damage in Elements 41102 & 13024. This can also be seen in Figure 5.3, where all the most damaged parts of the bridge have the highest contribution from the most recent periods.

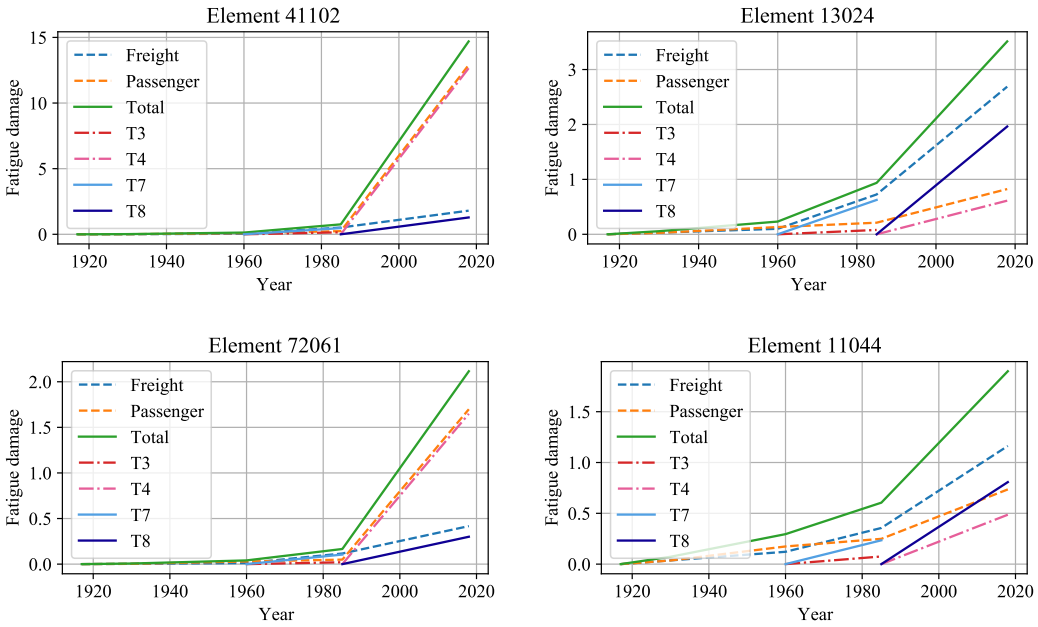


Figure 5.3: Sokna Bridge - Damage by train for most critical elements in most critical cross-section types.

### 5.2.3 Detail Category

Table 5.10 shows how the historical fatigue damage changed for Sokna Bridge when the SN-curves were altered from a trilinear 71 MPa curve to a linear 85 MPa curve.

Table 5.10: Sokna Bridge - Change in fatigue damage when detail category is changed for critical components.

| Section type | $\Delta\sigma_C = 71$ MPa | $\Delta\sigma_C = 85$ MPa |
|---|---|---|
| St | $D_h = 31.54$ | $D_h = 14.70$ |
| StCon | $D_h = 20.46$ | $D_h = 8.18$ |
| StBr | $D_h = 12.60$ | $D_h = 10.99$ |
| Di2 | $D_h = 11.98$ | $D_h = 3.51$ |

All section types have reduced fatigue damage with the linear curve. The most significant reduction is found for St, StCon and Di2.

### 5.2.4 Number of Passages

The fatigue life calculations were repeated using the number of passages defined in Table 4.4. The difference in the number of passages is also shown in Figure 5.4. It is then clear that the passages found from timetables are much higher than the passages used by Bane NOR after approximately 1920. This affects the results, presented in Table 5.11, where the damage of the stringer is more than three times higher in this supplementary analysis. All components have more serious fatigue damage when the number of passages from timetables is used. While only 11 cross-section types were critical regarding fatigue

damage for the assumed constant passages, 18 were found critical in this analysis. Although the ten most critical components are the same in the two analyses, there are some slight changes in ranking.

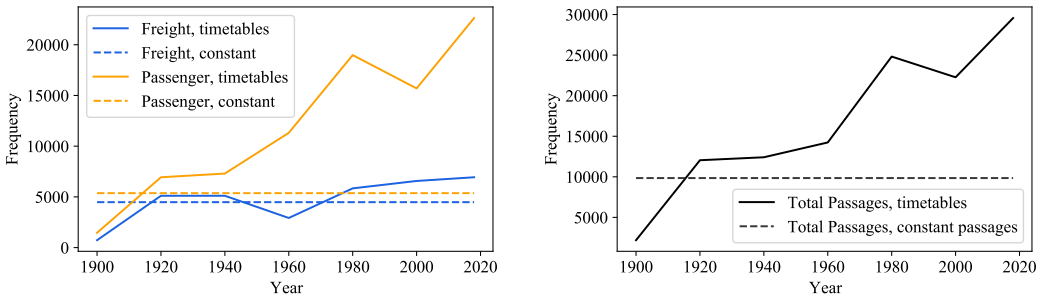


Figure 5.4: Sokna Bridge - Passages defined as constant each year versus passages from timetable.

Table 5.11: Sokna Bridge - Most critical point for each section class found with the Consistent Load Model and number of passages from timetable.

| Element | $T_{RL}$ [yrs] | $D_h$ | $\Delta\sigma_C$ [MPa] | Section | Category |
|---|---|---|---|---|---|
| 41103 | 0.0 | 45.7588 | 85 | St | secondary |
| 61141 | 0.0 | 37.2774 | 85 | StBr | secondary |
| 41081 | 0.0 | 27.4652 | 85 | StCon | secondary |
| 63121 | 0.0 | 8.1348 | 85 | StDi | secondary |
| 72061 | 0.0 | 6.2178 | 85 | WB2 | primary |
| 13024 | 0.0 | 5.8483 | 85 | Di2 | primary |
| 11061 | 0.0 | 4.4670 | 85 | LC1 | primary |
| 11044 | 0.0 | 3.5873 | 85 | LC2 | primary |
| 31034 | 0.0 | 2.6751 | 85 | CG1 | secondary |
| 16034 | 0.0 | 2.2815 | 85 | Ve1 | primary |
| 81011 | 0.0 | 1.9984 | 85 | BB1 | primary |
| 16024 | 0.0 | 1.9072 | 85 | Ve2 | primary |
| 72081 | 0.0 | 1.8145 | 85 | BB2 | primary |
| 65021 | 0.0 | 1.5632 | 85 | CG2 | secondary |
| 16014 | 0.0 | 1.5278 | 85 | Ve3 | primary |
| 13044 | 0.0 | 1.3330 | 85 | Di3 | primary |
| 71041 | 0.0 | 1.3282 | 85 | WB3 | primary |
| 72021 | 0.0 | 1.2845 | 85 | WB1 | primary |
| 18034 | 1.2 | 0.9600 | 71 | Ve8 | primary |
| 13011 | 2.2 | 0.9414 | 71 | Di1 | primary |
| 22014 | 2.3 | 0.9373 | 71 | UC | primary |
| 18024 | 7.7 | 0.7389 | 71 | Ve9 | primary |

# 6 Discussion of the Fatigue Analysis

The main focus of this discussion is how the new Consistent Load Model differs from the previously used Conventional Load Model. It is also considered how the fatigue life analysis is performed and whether this may affect the results.

## 6.1 Conservatism

It is generally found much greater historical fatigue damage, $D_h$, with the Consistent Load Model. For Svånå Bridge, the most significant deviation between the Consistent and Conventional Load Model is more than 1200 %. This tendency is even higher for Sokna Bridge, with a difference of 4240 % for the stringers. The most common deviation for all components is in the range of 200 - 600 %.

The Consistent Load Model suggested by Frøseth & Rønnquist is definitely more conservative than the Conventional Load Model used by Bane NOR. The main idea of the Consistent Load Model is that the composition of trains and traffic mix coefficients should result in damages that are 1-2 times higher than the damage from the possible most damaging train for all components of the bridge. The deviation between the two load models is much higher than 100 - 200 %, even for the cross-section types found to be most critical by Bane NOR. It is then likely that the reference trains used in the Conventional Load Model are not the most damaging train for any bridge component.

Both bridges were found with very high fatigue damage with the Consistent Load Model, suggesting that the bridges needed reparation or replacement many years ago. As the analyses are based on the year 2018, and the bridges still are operating three years later, these damage levels are not realistic. The Consistent Load Model is based on the theoretical most damaging trains. However, it is not likely that all trains passing are the most damaging ones. It is also possible that the theoretical most damaging train does not exist in the actual traffic. Therefore, all older steel railway bridges would, most likely, be found to have historic damage higher than the critical with this level of conservatism. As a load model should be conservative, it is reasonable that collapse is indicated before the actual lifetime is reached. However, the damage level of the Consistent Load Model seems too conservative, and the loads should therefore be somehow reduced. A reduction factor could, for example, be estimated by measuring the actual damage from the trains operating today and comparing this to the damages from the Consistent Load Model.

There are also other factors than the load model resulting in conservative fatigue damage levels. The SN-curves used in the analyses are assumed conservative for riveted steel bridges. Partial safety factors are included as well, making the curves even more conservative. The SN-curves are of immense importance to the fatigue damage levels. A slight change in detail category may significantly decrease the number of cycles that the structural component can withstand. This is especially the case for a trilinear curve where the slope changes along the curve.

Using the trilinear curve with a detail category of 71 MPa seems to be more conservative. All the most damaged points had their fatigue damage reduced when changed to the linear 85 MPa curve, as shown in Tables 5.4 & 5.10. This may however not always be the case. The trilinear 71 MPa curve is less conservative for high stress ranges, as shown in Figure 4.6. The bracing of the stringer (StBr) for Sokna Bridge had less reduction when changing

the curve than the rest of the components. It is then likely that this part experiences higher stress ranges than the other critical components. One should therefore be careful with assuming that the trilinear 71 MPa curve always is more conservative.

Adjustments of the SN-curve are made both in the analysis with the Consistent Load Model and by Bane NOR. As the same adjustment is made, the deviation between the two assessments should not be affected. Still, it might give slight differences in ranking of critical components, further discussed in Section 6.2. Bane NOR has also checked that the force in the rivets with changed SN-curve does not exceed the rivets' shear capacity. All rivets checked by Bane NOR were found with forces well below the shear capacity [31, 32]. Thus, an assumption done for the analysis with the Consistent Load Model is that none of the rivets have reached their shear capacity. If this is not the case, the deviation between the two analyses would be even more distinct as the fatigue damage is larger with the trilinear curve.

## 6.2 Critical Components

The primary purpose of the Consistent Load Model is that all structural components should have the same relative damage with respect to the most damaging train. When trains with maximum axle load are used, some elements will be pretty damaged, while it introduces almost no damage for others. Suppose inspections of the bridges are being done based on these results. In that case, it may lead to the inspectors overlooking parts of the bridge that might be critical to fatigue damage, but that has not shown up as crucial in the calculations. This is the issue that Frøseth & Rønnquist are trying to avoid with their new load model.

For Svånå Bridge, Bane NOR found the verticals as the only components with fatigue damage greater than 1.0. With the Consistent Load Model, a total of eight section types were found to be critical. As the new model is more conservative, the damage should be greater. What is more important is that the ranking of the most critical element type has changed. The analysis performed in this thesis found that the diagonals are most critical. The Consistent Load Model also finds the verticals having severe damage, although less critical than the diagonals.

The change in the ranking of most critical components is not as obvious for Sokna Bridge, as no components were found with fatigue damage higher than the critical level with the Conventional Load Model. From Table 5.7 it can, however, be seen that the diagonals and lower chord were found with greater damage than the remaining element types. Different parts of the stringer were found to be most critical with the Consistent Load Model. It is possible that the stringer (St) also had a high damage value with the Conventional Load Model, as this is the only cross-section class that was changed to a linear 85 MPa curve. However, the remaining parts of the stringer, StCon and StBr, were by Bane NOR found with remaining fatigue life of respectively more than 50 and 100 years, such that the change in SN-curve does not apply for these components. Changing the detail category also resulted in a slight change in ranking for the Consistent Load Model. Di3 and Ve3 were calculated with a detail category of 85 MPa. This means that they initially, in the analysis with 71 MPa, were assessed with damages above the critical level of 1.0. When the detail category was changed, they were ranked less critical than some of the other cross-section classes with damage just below 1.0.

With the Conventional Load Model, the primary bearing was most critical for both Svånå and Sokna Bridge. For Svånå Bridge, this is still the case with the Consistent Load Model, but the stringer, a part of the secondary bearing, is also found to have fatigue damage well above the critical level. For Sokna Bridge, the stringer is now clearly the most vital part of the structure, making the secondary bearing of higher importance than the primary.

The previously stated implies that the Consistent Load Model finds a larger variety of cross-section classes as critical. The vertical components of Svånå Bridge were the only components found to have exceeded their fatigue life by Bane NOR. The fact that these and other members were found critical with the Consistent Load Model substantiates that the Consistent Load Model finds a wider specter of cross-section classes, and might therefore be more consistent than the Conventional Load Model. However, this finding does not guarantee that the new load model truly satisfies the consistency criterion. Further evaluation of the consistency is put under the loop in Chapter 7.

## 6.3 Damage Distribution

As already stated in Subsections 5.1.2 & 5.2.2, the most recent periods provide the most fatigue damage. The historic fatigue damage after 1960 provides 93, 98 and 99 % of the total damage for the section points presented in Tables 5.3, 5.8 & 5.9. The trains representing the traffic from 1985 until 2018, T4 and T8, are the most significant contributors to the historical damage. The main reason is that the trains have evolved to having higher axle loads and more wagons over the last hundred years, as presented about the evolution of trains in Section 3.1. These factors largely affect the stress ranges introduced on the steel structure.

The total damage from a reference train is dependent on the years defined for each train. This especially applies to T1 and T5. These reference trains are only defined from when the bridge was built until 1930, resulting in only 12 and 13 years. Therefore, the relative damage from one passing of these trains is slightly higher than the percentages presented in Tables 5.3, 5.8 & 5.9. If the fatigue damage for each train is seen as yearly damage, the later periods would still contribute more to the total damage. Table 6.1 shows an example of this for Sokna Bridge.

Table 6.1: Yearly damage from each reference train for element 13025 for Sokna Bridge.

| Train | Period | Years | D | $D_{year}$ | [%] |
|---|---|---|---|---|---|
| T1 | 1917-1930 | 13 | 0.0262 | 0.0020 | 1.73 |
| T2 | 1930-1960 | 30 | 0.1058 | 0.0035 | 3.03 |
| T3 | 1960-1985 | 25 | 0.0792 | 0.0032 | 2.72 |
| T4 | 1985-2018 | 33 | 0.6126 | 0.0186 | 15.94 |
| T5 | 1917-1930 | 13 | 0.0304 | 0.0023 | 2.01 |
| T6 | 1930-1960 | 30 | 0.0694 | 0.0023 | 1.99 |
| T7 | 1960-1985 | 25 | 0.5258 | 0.0250 | 21.50 |
| T8 | 1985-2018 | 33 | 1.9626 | 0.0595 | 51.08 |

To make the new load model even more simple, one possibility could be only to consider reference trains T3, T4, T7 and T8. Since the model generally is conservative, the damage prior to 1960 could either be neglected or added as 5-10 % of the damage found after 1960. As this is stated only by considering the eight stress points in Figures 5.1 & 5.3, it would need some further examination to be concluded.

Freight trains are usually assumed to be the most damaging. Even though they generally operate at lower speeds than passenger trains, the freight trains have higher axle loads and more wagons which introduces higher stress ranges. The tendency is clear for the points considered for Svånå Bridge in Figure 5.1. However, this is not the case for Sokna Bridge, as shown in Figure 5.3. Two of the points considered have more damage from passenger trains, and the percentage of damage from passenger trains is generally more prominent than what is seen for Svånå Bridge.

Sokna Bridge is likely to have more damage from passenger trains as more passenger trains are passing than freight trains. Svånå, on the other hand, has more passages of freight trains. This can be seen from Table 4.2. Another factor that may introduce more significant fatigue damage from passenger trains is that the speed of these trains in the Consistent Load Model is a lot higher than for the freight trains. Higher speed also introduces higher centrifugal forces on the structural elements. This might be more distinct for Sokna Bridge as the radius of the horizontal curvature is 500 meters versus 1000 meters for Svånå.

Figure 6.1 compares the influence line and stress ranges obtained for T4 and T8 for the most damaged point at Sokna Bridge. From the influence lines, it is seen that the peak is remarkably higher for the speed from T4 than the speed from T8. It can then be concluded that this point of the stringer is highly affected by centrifugal forces. The bottom figure shows the stress ranges that are obtained for the two trains. It is then likely that the passenger train, T4, introduces higher fatigue damage, as there are both more cycles and higher ranges.

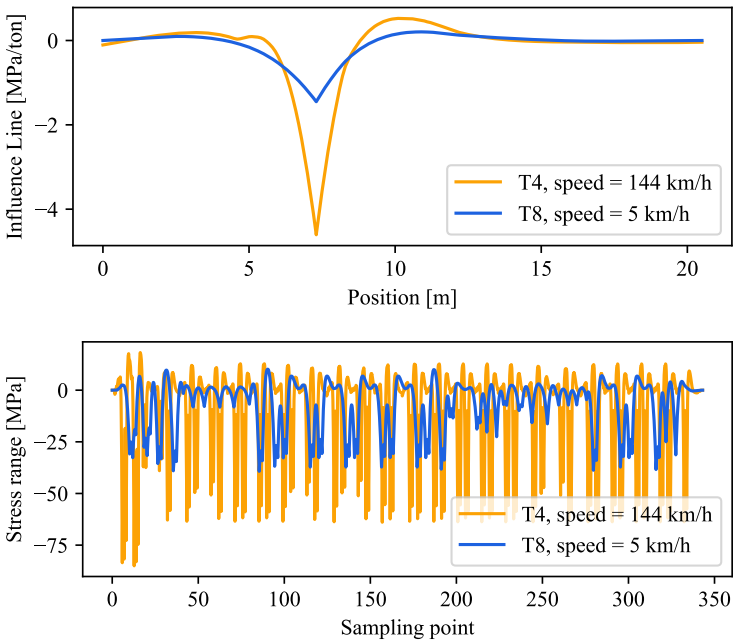


Figure 6.1: The effect of different train speeds on an influence line with large contributions from centrifugal forces.

As an example of the opposite case, when the freight train T8 provides the most considerable fatigue damage, element 13024 from Sokna Bridge is considered. From Figure 6.2, it is seen that the change in the influence line is not as distinct. The centrifugal force is therefore not as important. It is not easy to tell which train introduces the most fatigue damage as the stress ranges are approximately the same. The figure represents one passage of T4/T8, and it may seem like T4 is more damaging as it has more cycles and 887 more yearly passages than T8. This is however not the case when the traffic mix coefficient is introduced. T4 only has $a = 2.8$ against T8 with a coefficient of 15.0. The traffic mix coefficient is included in the Consistent Load Model to account for differences in traffic and structural parameters and is of great importance to the fatigue damage.

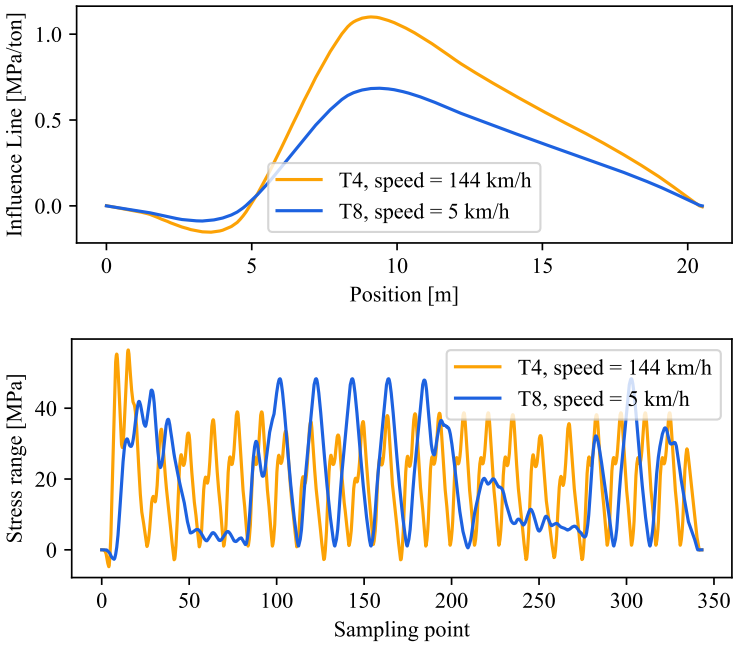


Figure 6.2: The effect of different train speeds on an influence line with smaller contributions from centrifugal forces.

## 6.4 Differences in Speed

One of the most significant differences between the Conventional Load Model and the Consistent Load Model is the permitted speed in each reference train. The speeds are higher for the Conventional Load Model and determined by both the allowable speed in the reference trains and the current speed over the investigated bridge. In contrast, the Consistent Load Model only is determined by relatively low speeds in the reference trains. The velocities in the Conventional Load Model are generally more realistic and most likely closer to the actual speeds the trains have passed with throughout history. However, there could be significant variations, e.g., for bridges close to stations or where the curvature would require lower speeds.

The lowest speeds are found for the freight trains, where for example T8 has a speed of 5 km/h in the Consistent Load Model. The reason is not that the passing trains are assumed to have such low speeds. Instead, the speed is adjusted to obtain the desired level of consistency. The speed of T8 with the Conventional Load Model is, on the other hand, determined by the current speed over the bridge and is likely much higher than 5 km/h.

As already shown in Section 6.3, many influence lines are dependent on speed through the centrifugal forces. The lower speeds in the Consistent Load Model cause lower centrifugal forces than the speeds in the Conventional Load Model, where the Conventional Load Model most likely has the most realistic ones. However, it is not sure that the highest centrifugal force causes the worst damage, as the load models are dependent on other parameters like wagon design and axle loads. Fatigue damage is also reliant on differences in stress, not only the maximum level. The results from the fatigue analysis also confirm this. The Consistent Load Model provides worse damage than the Conventional Load Model even though it has lower speeds and introduces lower centrifugal forces.

## 6.5 Number of Passages

It is also taken a closer look at how the number of passages throughout history affects fatigue damage. A supplementary analysis, using the passages as defined in Table 4.4, was then performed. The results for the two bridges are presented in Subsections 5.1.4 & 5.2.4.

For Svånå Bridge, the most critical components experience an increase in damage of approximately 10 % when the passages from the timetables are considered. Figure 5.2 shows that these passages are fewer than what has been used in the primary analysis until approximately 1980 before they increases to a level above the constant level of passages. Since most of the fatigue damage is by trains from the most recent periods, the increase in damage is a likely observation.

The stringer components of Sokna Bridge have an increase of 240 %. Figure 5.3 shows that the stringer (Element 41102) has almost all its damage from the period after 1985. Figure 5.4 shows that the passages found from timetables are higher than the constant level passages through the whole lifetime of the bridge, with the difference increasing with time. As the number of passages in 2018 is around three times higher for the timetables, it also makes sense that the damage for this component is three times higher. The increase of the remaining section types varies wildly, depending on how much of the damage is from the most recent period. The cross-section classes generally have an increase of around 80 % for Sokna Bridge.

It would be reasonable to assume that the number of passages from timetables is more historically correct than the assumption of constant yearly passages, as the timetables are based on historical data. They also show that it has been both an increase and decrease in passages over the last 100 years. The constant yearly passages should be more reliable around 2010-2015, as they are taken as the maximum count of passages from 2011, 2014 and 2015. However, the passages from the timetables are significantly higher both for Svånå and Sokna Bridge around these years.

One possibility is that the counting system has been out of service for some periods. However, it is not likely that this has happened for all three counted years without being discovered. Another more likely explanation is that the local trains have not been included in the counts by Bane NOR. Local trains are smaller, with smaller axle loads and fewer wagons. Therefore, these trains might have been assumed not to contribute as much to the total fatigue damage. As the specific cause for differences in passages is not known, this is only an assumption. To obtain the correct damage, it might be wise in future fatigue analyses to use the passages found from timetables for historical data and the passages from counts for the years available.

# 7 Further Exploration of Consistency

Even though the 14 influence lines in Figure 3.10 can represent many different structural components, a much greater set of influence lines is represented in a real railway bridge. Furthermore, the length parameter may also take other values than given in the set of $L_{IL}$. It is impossible to include all possible influence lines and lengths when developing a load model. The calibration set is therefore incomplete compared to an actual set of structural components [13]. Since the consistency level of 40 % to 50 % in the Consistent Load Model only apply to the calibration set, it is interesting to investigate the level of consistency for all influence lines and lengths. Such a consistency exploration will then evaluate how well the Consistent Load Model is suited for fatigue calculations of railway bridges.

## 7.1 Methods

### 7.1.1 Correlation Between Influence Lines

As a preliminary exploration, the correlations between the standard influence lines from Figure 3.10 and the actual influence lines of both Svånå and Sokna Bridge were studied. The standard influence lines with lengths in the set of $L_{IL}$ were generated and compared with the ILs of the bridges. The correlation was then found using cross-correlation [36]. In order to compare the damage from a specific train for the standard influence lines and the ILs of the bridge, all lines were scaled, with the highest point being 1.0. The ratio between damage from the influence line of the bridge and the standard influence line with the highest correlation, was then found for all stress points on the bridges.

The correlation was found reasonably good, with an average of over 90 % for both bridges. However, the fatigue damage ratio did vary greatly, and no connection between correlation and damage ratio was found. One reason might be the shape of the peaks. A sharp peak will generally result in greater fatigue damage as it produces higher stresses. If one line has a rounded peak and the compared line has a sharp peak, the cross-correlation will be close to 1.0 as long as the remaining parts of the line correspond. Since a sharp peak might provide both a high correlation and low damage ratio, it was concluded that this check was not suited to investigate the consistency.

### 7.1.2 Check with Most Damaging Train

In further investigation of the consistency, the most damaging train for all stress points defined at the two bridges was studied. Late Acceptance Hill-Climbing, explained in Subsection 3.3.1, was used for the optimization problem. The objective function to be maximized was the fatigue damage, $D$, and the state was a predefined set of trains.

The work of Frøseth & Rønnquist [13,28] was used as the basis for the MDT analyses. For each time period, a unique set of locomotives and wagons were defined corresponding to possible passenger or freight trains from this period. For each reference train T1-T8, the most damaging train was found for all stress points for the corresponding period and type of train.

LAHC is a time-consuming algorithm, especially since thousands of stress points were to be checked for its most damaging train. Some restrictions were therefore made to make it possible to perform the analyses within a limited time. T4 and T8 cover two of the defined periods, 1985 - 2000 and 2000 - →. It was found that these periods provided close to the same damage and were consequently merged. Therefore, the most damaging train for T4 and T8 was only taken as the most damaging train from 2000 - →.

It should also be noted that when finding the most damaging train, all possible trains from Frøseth & Rønnquist [13] were not considered. Both locomotives and wagons were reduced to make the optimization problem less demanding. The reduced train set used in the MDT optimization is presented in Appendix B. It is chosen as those locomotives and wagons that are most different from each other, such that the deviation from the most damaging train in the reduced set to the complete set should be minimal. Even with this reduced set, the MDT analysis turned out to spend several weeks on the most demanding periods and type of trains. A complete train set, including all possible locomotives and wagons, would be too challenging concerning computational efficiency.

The intention was to increase the success rate of finding the global maximum within an acceptable time frame. Frøseth & Rønnquist found the success rate of finding the most damaging train for some of the influence lines in the calibration set. These success rates [28] are shown in Figure 7.1. It can be seen that a history length of 2000 has to be used to achieve a success rate close to 100 % for all IL lengths. However, they also show that a history length of 100 provides the highest increase in success rate for most influence lines. The history length used in the MDT analysis was therefore chosen as $\lambda = 100$.

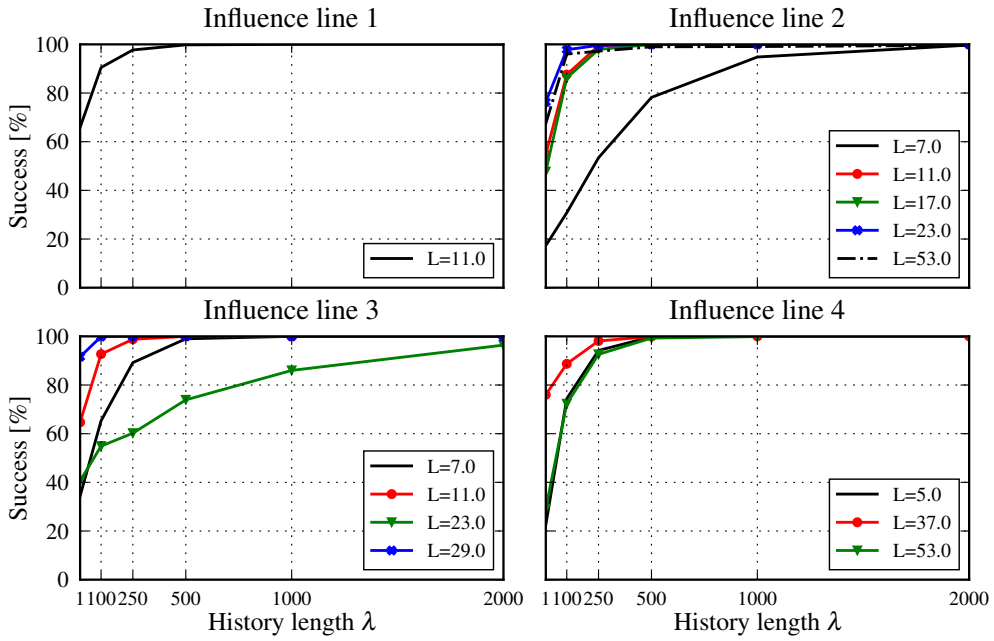


Figure 7.1: Success rate of finding the most damaging train for different history lengths. IL 1-4 correspond to IL 1-4 in the calibration set from the Consistent Load Model [2][1].

By running through the optimization algorithm multiple times for some of the stress points, it was found that the difference between the fatigue damage for the iteration with the smallest and highest damage was less than 1 %. However, since only some of the points were checked, the optimization was run twice in every stress point to minimize the risk of picking out a local maximum. The most damaging train was then taken as the train giving the greatest damage out of these two iterations.

The damage from one passing of each reference train was then compared to the most damaging train for the corresponding time period and type of train. The ratio of each stress point for reference train $i$, $\varphi_i$, was then found by

$$\varphi_i = \frac{D_{Ti}}{D_{MDTi}} \tag{28}$$

All ratios for the specific reference train, $Ti$, were collected in a vector containing the ratios of all stress points of the bridge, $\Phi_i$. The consistency for each train was then found from this vector by

$$\zeta_i = \frac{min(\Phi_i)}{max(\Phi_i)} \tag{29}$$

A preliminary check with MDT showed that some of the ratios between the fatigue damage from the load model and the most damaging train were remarkably high, resulting in poor overall consistency. It was then discovered that the damage from the most damaging train gave unlikely low values compared with the load model and consequently a high ratio, $\varphi_i$.

The contribution from the centrifugal forces was also here found to be the cause. Figure 7.2 shows an example of how an influence line with no centrifugal force differs from an influence line with the centrifugal force for a train speed of 144 km/h. In this case, a high speed evens out the original influence line, resulting in a low damage value. A lower speed would therefore give greater fatigue damage for this particular element.

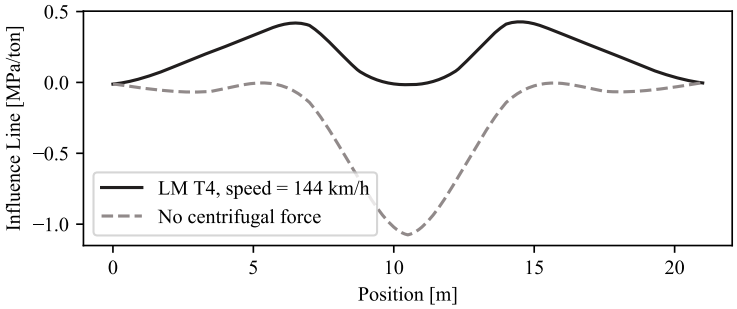


Figure 7.2: Influence line where no centrifugal force is most critical.

In the original MDT algorithm used in the development of the Consistent Load Model, the speed of the trains was only taken into account in the calculation of the dynamic amplification factor [13]. The speed was determined by the following:

$$v = min(v_L,\ v\uparrow) \tag{30}$$

where $v_L$ is the maximum speed of the locomotive and $v\uparrow$ is the maximum allowable speed for each period and type of train. These maximum speeds are given in Appendix B.

Since both Svånå and Sokna Bridge have horizontal curvature and consequently centrifugal forces dependent on speed, the speed must also be considered in the calculations of the influence lines. The train set in the optimization algorithm was therefore extended to include different scaling of the speed. Each train then got three additional speeds, as in Eq. (31), such that the influence lines were updated for each velocity.

$$V = \{0.25 \times v,\ 0.50 \times v,\ 0.75 \times v,\ v\} \tag{31}$$

The fact that the influence lines are dependent on speed does raise a possible issue with the reduced train set. The locomotives have different permitted velocities, where the reduced train set does not contain all the highest speeds. If all locomotives were considered, the permitted speed of the line would determine the maximum speed for most of the freight traffic. In some of the reduced train sets, none of the locomotives have permitted speed higher than the maximum allowable speed. A similar issue may occur if the fatigue damage is worse at low speeds and such locomotives are not taken into account in the train set. Since almost all periods consist of several locomotives with different speeds, and the damage is calculated as 25, 50 and 75 % of the maximum speed, this effect will most likely be negligible. However, it is essential to acknowledge that this is a possible source of error and that the same maximum speeds should be used in any comparison with the MDT analysis.

Including additional velocities resulted in higher MDT damage values for those elements initially indicated very low. More realistic ratios between damage from the Consistent Load Model and most damaging train were then found. However, there was still a low overall consistency, as some elements had low ratio values, i.e., the most damaging train induced remarkably greater fatigue damage than the load model. The MDT analysis results are presented in Subsection 7.2.1.

## 7.2 Evaluation of Consistency

### 7.2.1 Results of Most Damaging Train Analyses

The damage ratio, $\varphi$, and consistency, $\zeta$ are found for all stress points in both Svånå and Sokna Bridge, where Table 7.1 shows the collected results for all points corresponding to the different trains in the Consistent Load Model. All damage ratios from the check with the most damaging train are visualized in Figure 7.3.

Table 7.1: Damage ratio and consistency in the different time periods.

| | Svånå Bridge | | | | Sokna Bridge | | | |
|---|---|---|---|---|---|---|---|---|
| Train | Average $\varphi$ | Max $\varphi$ | Min $\varphi$ | $\zeta$ [%] | Average $\varphi$ | Max $\varphi$ | Min $\varphi$ | $\zeta$ [%] |
| T1 | 1.4491 | 2.5397 | 0.0012 | 4.9e-2 | 1.3578 | 2.5450 | 0.0010 | 3.9 e-2 |
| T2 | 1.5324 | 2.6264 | 0.0016 | 5.9e-2 | 1.4789 | 2.6091 | 0.0859 | 3.3 |
| T3 | 1.1245 | 2.3559 | 0.0001 | 2.8e-3 | 0.7666 | 2.3139 | 0.0013 | 5.8 e-2 |
| T4 | 2.2049 | 4.2385 | 0.0482 | 1.1 | 2.2575 | 4.5476 | 0.0086 | 0.2 |
| T5 | 2.2799 | 4.3692 | 9.13e-7 | 2.1e-5 | 2.0621 | 4.1724 | 3.51e-6 | 8.4e-5 |
| T6 | 2.0758 | 6.6720 | 1.47e-7 | 2.2e-6 | 1.7169 | 4.5100 | 5.12e-7 | 1.1e-5 |
| T7 | 1.9791 | 4.0630 | 1.82e-5 | 4.5e-4 | 1.7423 | 4.0880 | 2.83e-5 | 6.9e-4 |
| T8 | 1.6169 | 5.5511 | 3.45e-9 | 6.2e-8 | 1.3476 | 4.3317 | 5.99e-9 | 1.4e-7 |

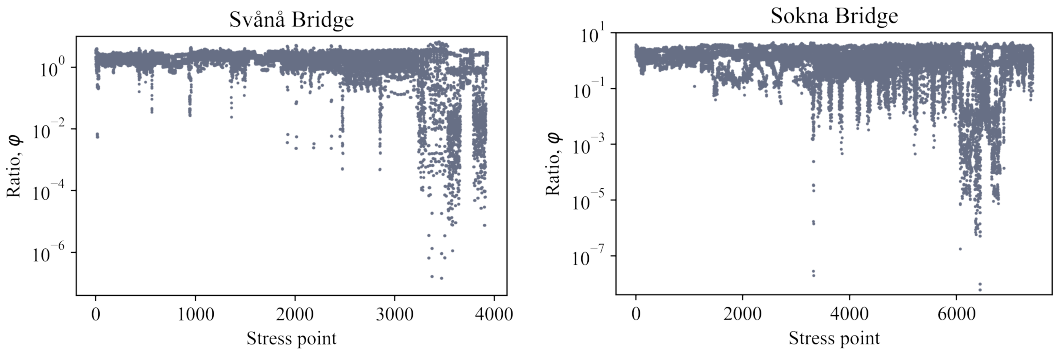


Figure 7.3: All damage ratios for Svånå and Sokna Bridge.

All reference trains have poor consistency, far from the desired level of 50 % for passenger trains and 40 % for freight trains. Svånå and Sokna Bridge show especially low consistencies for freight trains. Both bridges considered, the highest consistency is found for T4. T2 for Sokna Bridge shows a better consistency than the other trains, but the same train is lower for Svånå Bridge. Therefore, it is difficult to determine whether T2 is better than the others or if the values are random.

T3 for Sokna Bridge is the only train with a lower average $\varphi$ than 1.0. It means that reference train T3 generally is introducing lower damages than the most damaging trains. If the most damaging train is one of the actual trains passing, there might be an issue with the conservatism. A ratio below 1.0 is not necessarily a problem since the majority of the trains most likely have passed with lower damage than MDT, but since data is missing, one can not be sure. However, it is essential that all trains introduce damage similar to the damage from MDT with regards to consistency.

### 7.2.2 Causes of Poor Consistency

The low consistencies found for the two bridges are far from the desired level for the Consistent Load Model. Once again, the differences in speeds were found to be the cause. For some stress points, the centrifugal force has close to no attribution to the influence line. One example of this is shown in Figure 7.4. For these cases, the ratio between the fatigue damage from the Consistent Load Model and the most damaging train, $\varphi$, was generally between 1 and 2, which is the desired result.

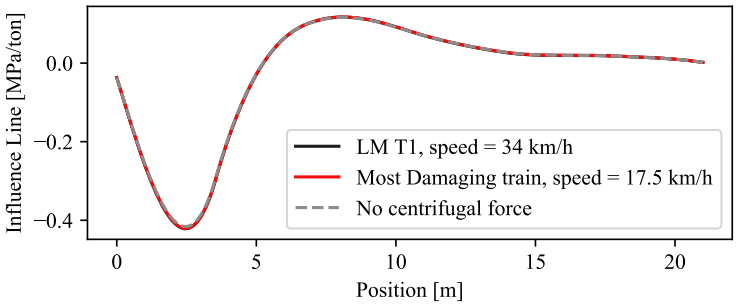


Figure 7.4: The influence line of a stress point not affected by the centrifugal force.

Some ratios are also higher than 2. One possible reason is that only four different speeds are included in the MDT algorithm. The most damaging speed may lay somewhere between these four speeds, such that the true most damaging train is not found. This will generally result in ratios slightly higher than the true ratios, as already explained as a possible issue with the reduced train set in Subsection 7.1.2.

The lower ratios are however the biggest challenge. A large number of influence lines are most critical at high speeds. Especially the freight trains are assigned low speeds in the load model, resulting in fatigue damage up to 10 million times smaller than the damage from MDT. This might also explain why the freight trains had especially low consistencies. Figure 7.5 shows an example of how an influence line with a low damage ratio is affected by different train speeds. How the fatigue damage varies for this line is shown in Figure 7.6. This particular relation between speed and damage is typical for many stress points, but could take any shape, as many influence lines are critical at lower speeds.

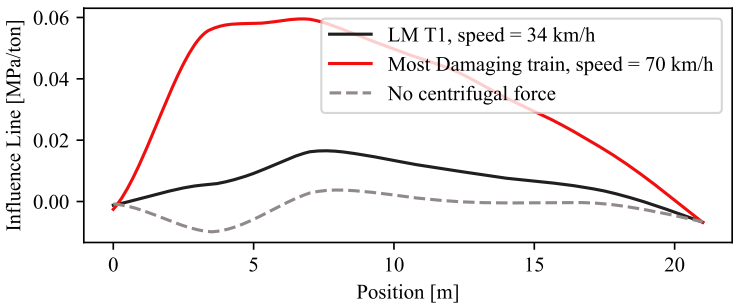


Figure 7.5: The effect of different train speeds on an influence line with low ratio.

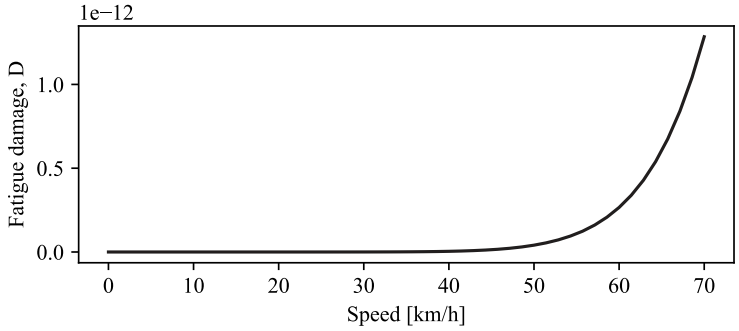


Figure 7.6: Relation between fatigue damage and speed for an influence line with low ratio.

### 7.2.3 Differences in Cross-Section Classes

The consistency within the different cross-section classes is also explored. The results are attached in Appendix C. Sokna Bridge has in general lower consistency in each class compared to Svånå Bridge, with an average of 4.2 % for Sokna and 12.5 % for Svånå. One reason may be differences in radius of curvature. Sokna has a smaller radius than Svånå, and consequently a sharper turn, which introduces higher horizontal forces on the elements. Since the horizontal forces are highly dependent on speed, and the speed in the reference trains and MDT often are quite different, it is explicable that the fatigue damage and the ratios are in a broader range for Sokna than for Svånå. Sokna also has almost twice the number of stress points defined, giving more possibilities for abnormalities.

The stringers and stringer-connected elements are found among those components with the lowest consistency in both bridges. These are shown as the elements starting with *St* in Figures 4.2 & 4.4. These elements are all a part of the secondary bearing system, which absorbs the axle loads directly and transfers them to the primary system. The stringers are mainly resisting the forces by bending about both the strong and weak axis. The main contribution to the moment about the weak axis is the horizontal forces occurring from the centrifugal force. The speed is therefore very decisive for the stringers. The influence line, and thus fatigue damage, will then vary significantly with speed, resulting in low consistency when the MDT and load model speeds are not the same.

The wind bracing (WB) also shows a very low consistency for Svånå Bridge. These elements transfer mainly horizontal forces and are therefore sensitive for changes in centrifugal force due to speed. Like the stringers, this may explain low consistency values. The wind bracing in Sokna Bridge has however somewhat better consistency than those in Svånå. A different bearing system in the two bridges may be the explanation. While the wind bracing is a part of the secondary system for Svåna, it is a part of the primary in Sokna. The bracing has different geometry, being crossed in Sokna and V-shaped in Svånå. The forces are then transferred differently, and the impact of speed seems reduced when the wind bracing is shaped as for Sokna Bridge.

### 7.2.4 Lower Damage Values

Some elements have extremely low fatigue damage, both by the reference trains in the Consistent Load Model and the most damaging train. Such low values are very sensitive to changes and provide unwanted damage ratios, which result in a low overall consistency. Since these values also contribute minimally to the total fatigue damage, it may be reasonable to disregard these ratios in the evaluation of the complete consistency.

The greatest fatigue damage in each stress point for each train was generally found in the magnitude of $10^{-6}$ to $10^{-7}$. Fatigue damage smaller than 0.1 % of the greatest damage is considered insignificant of the total fatigue damage. All stress points with an MDT damage smaller than $10^{-10}$ were therefore disregarded.

Table 7.2: Damage ratio and consistency for all stress points with MDT damage higher than $10^{-10}$.

| | Svånå Bridge | | | | Sokna Bridge | | | |
|---|---|---|---|---|---|---|---|---|
| Train | Mean $\varphi$ | Max $\varphi$ | Min $\varphi$ | $\zeta$ [%] | Mean $\varphi$ | Max $\varphi$ | Min $\varphi$ | $\zeta$ [%] |
| T1 | 1.6802 | 2.5397 | 0.4851 | 19.1 | 1.4680 | 2.4624 | 0.0019 | 7.9 e-2 |
| T2 | 1.7339 | 2.6264 | 0.7167 | 27.3 | 1.5058 | 2.6091 | 0.1361 | 5.2 |
| T3 | 1.2088 | 2.3559 | 0.0001 | 1.2 | 0.7461 | 2.3139 | 0.0013 | 5.8 e-2 |
| T4 | 2.2283 | 4.2385 | 0.0482 | 1.1 | 2.2738 | 4.5476 | 0.0086 | 0.2 |
| T5 | 2.4220 | 3.3830 | 0.9308 | 27.5 | 2.3386 | 3.9825 | 0.0745 | 1.9 |
| T6 | 2.2093 | 4.4167 | 0.4219 | 10.2 | 1.8912 | 4.5100 | 5.12 e-7 | 1.1 e-5 |
| T7 | 2.1659 | 4.0119 | 0.0006 | 1.5 e-2 | 1.7898 | 4.0879 | 2.83 e-5 | 6.9 e-4 |
| T8 | 1.6272 | 4.1522 | 1.14 e-6 | 2.8 e-5 | 1.3557 | 4.3239 | 5.99 e-9 | 1.4 e-7 |

Table 7.2 presents some key values of the damage ratios for Svånå and Sokna Bridge when the stress points with low fatigue damage are removed. Compared to Table 7.1, the consistency has increased for some trains, especially for Svånå Bridge. The average ratios do not change significantly and are both increasing and decreasing for different periods and trains, suggesting that the points with low fatigue damage may lay both in the high and low spectra of ratios.

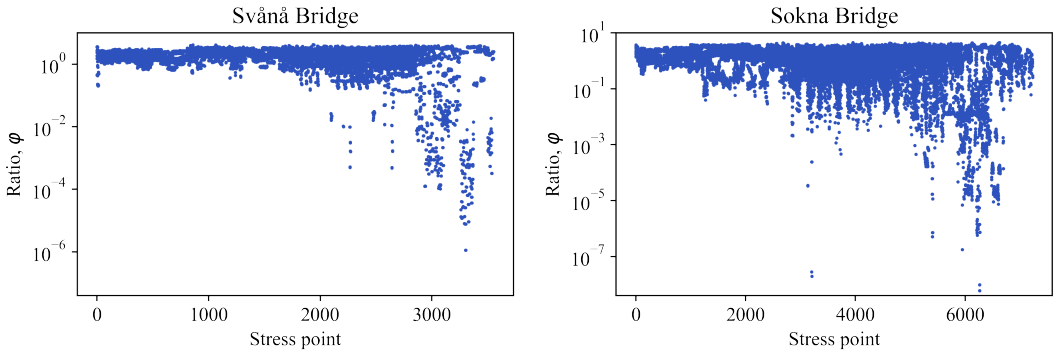


Figure 7.7: All ratios for Svånå and Sokna Bridge when stress points with low damage are removed.

Although some of the trains now have acceptable consistency, some do not change at all. Most of the values are still far from what is desired for the Consistent Load Model. The ratios for the stress points with fatigue damage higher than $10^{-10}$ are plotted for both bridges in Figure 7.7. When compared to all ratios for the two bridges in Figure 7.3, it can be seen that they still cover almost the whole range. This is especially the case for Sokna Bridge. Sokna has, as already mentioned, a smaller radius of curvature which introduce larger centrifugal forces. Therefore, the effect is more extensive for Sokna, such that more points, also the ones with high fatigue damage, are greatly influenced by the train speed.

### 7.2.5 Consistency for Bridges with No Horizontal Curvature

The effect of centrifugal force as presented in Subsection 7.2.2 seems to be the leading cause of the poor consistency. The tracks of some of the bridges assessed by Bane NOR do not have any horizontal curvature. An MDT analysis was performed on two of these bridges to test the Consistent Load Model when centrifugal forces have no contribution. The method used for the MDT analyses was the same as presented in Subsection 7.1.2.

#### Møstadbekken Bridge

One of the bridges chosen was a simple beam bridge, Møstadbekken Bridge. The element model of this bridge is very straightforward, with only two parallel beams and a total of 128 defined stress points [37]. Figure 7.8 shows a replica of the model used by Bane NOR.

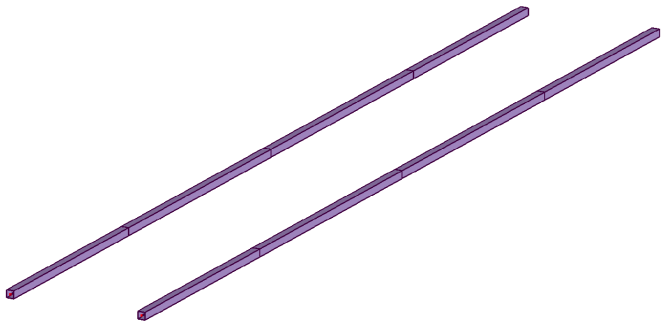

Figure 7.8: Replica of element model of Møstadbekken Bridge.

The most damaging train was found for all influence lines of this bridge, such that all ratios, $\varphi$, and consistencies, $\zeta$, could be found. The consistencies of the beam bridge are presented in Table 7.3. The ratios are in the conservative range, with the smallest ratio being 1.336 for T8 and the highest being 2.833 for T5.

Table 7.3: Consistencies for Møstadbekken Bridge.

| Train | Consistency, $\zeta$ [%] |
|---|---|
| T1 | 74.3 |
| T2 | 65.1 |
| T3 | 83.8 |
| T4 | 66.3 |
| T5 | 86.8 |
| T6 | 62.1 |
| T7 | 63.9 |
| T8 | 67.6 |

The results are actually better than the desired level of consistency for the calibration set in the Consistent Load Model. As the bridge has similar structural components and few stress points, this is a likely observation. Two typical IL shapes are found for Møstadbekken Bridge, both shown in Figure 7.9.

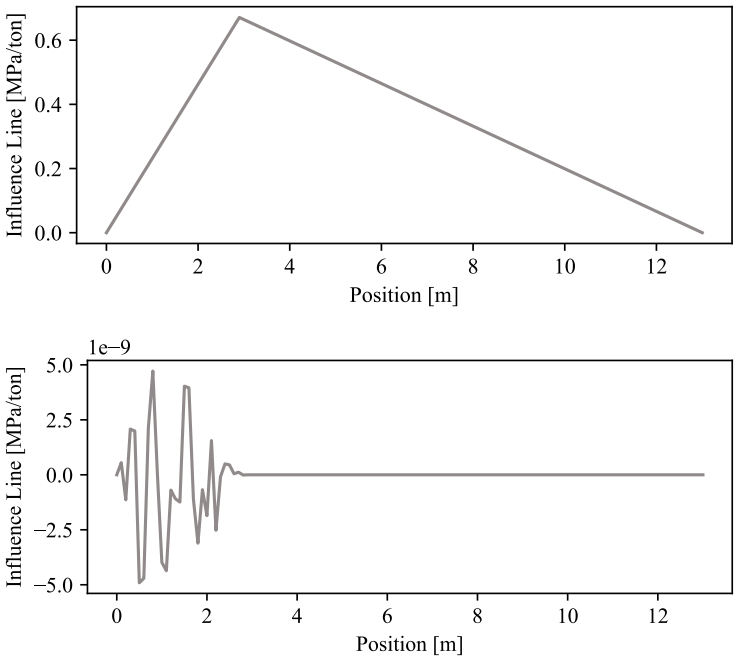


Figure 7.9: The most common shapes of the influence lines of Møstadbekken Bridge.

Note that the magnitude differs significantly, where the lower influence line presented is essentially zero. These lines result in fatigue damages in the magnitude of approximately $10^{-48}$. The ratios are however still at the desired level, resulting in superior consistencies.

### Driva Bridge

As the previous bridge only considered a limited variety in influence lines, a second bridge without horizontal curvature was assessed. The bridge chosen was Driva Bridge. A replica of the model used by Bane NOR [38] is shown in Figure 7.10. The MDT analyses for Driva Bridge were performed using a history length of 50 and only running the calculation one time. This modification was made to reduce the computational time.

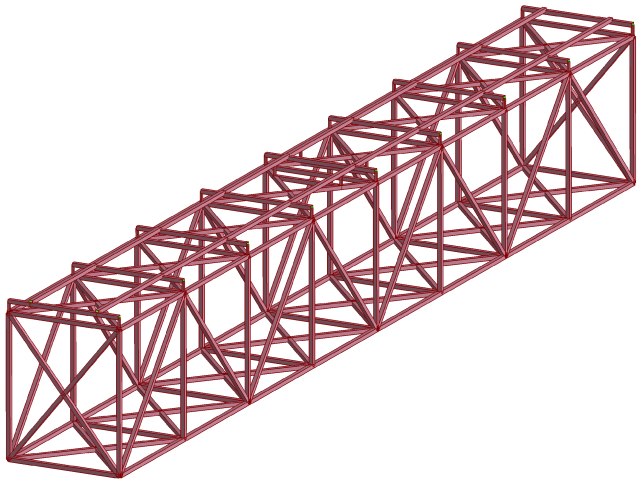

Figure 7.10: Replica of element model of Driva Bridge.

By finding the most damaging train and ratios, the consistencies presented in Table 7.4 were found. The consistencies for T5 and T6 are approximately half of what is desired for freight trains in the Consistent Load Model. For the remaining trains, the consistencies are close to those observed for the influence lines in the calibration set. By checking multiple stress points, it was found that the influence lines of Driva Bridge differ a lot and may take on any shape. Therefore, it is likely that the consistencies are lower for Driva than both for the calibration set and Møstadbekken Bridge.

Table 7.4: Minimum damage ratio and consistency for Driva Bridge.

| Train | Min $\varphi$ | Consistency, $\zeta$ [%] |
|---|---|---|
| T1 | 1.1891 | 52.7 |
| T2 | 1.1645 | 41.8 |
| T3 | 0.8993 | 48.6 |
| T4 | 1.6819 | 52.7 |
| T5 | 0.7488 | 23.6 |
| T6 | 0.7394 | 19.1 |
| T7 | 1.4530 | 47.3 |
| T8 | 0.9194 | 32.0 |

There is a possible issue with the conservatism for some of the reference trains. It can be seen from Table 7.4 that T3, T5, T6 and T8 have some ratios below the critical level of 1.0. It is however found that many of these ratios are connected to minor damages. As in Subsection 7.2.4, the smaller damage values are removed to determine if these ratios can be disregarded. The minimum ratios and consistencies found for damage points with MDT damage greater than $10^{-10}$ are presented in Table 7.5.

Table 7.5: Minimum damage ratio and consistency for all stress points with MDT damage higher than $10^{-10}$ for Driva Bridge.

| Train | Min $\varphi$ | Consistency, $\zeta$ [%] |
|---|---|---|
| T1 | 1.1976 | 53.1 |
| T2 | 1.1756 | 42.2 |
| T3 | 0.8993 | 48.6 |
| T4 | 1.6924 | 53.1 |
| T5 | 1.0589 | 35.2 |
| T6 | 1.0495 | 32.3 |
| T7 | 1.4530 | 48.7 |
| T8 | 0.9194 | 33.6 |

When only the higher damage values are considered, T3 and T8 are the only reference trains with a ratio below 1.0. These reference trains, therefore, do not fulfill the desired level of conservatism for all stress points. How one might treat this issue is discussed in Subsection 7.3.3. However, the remaining trains all have damages relative to the most damaging train above the desired level. As the stress points with lower damage values are less critical, the conservatism requirement may be considered fulfilled for these reference trains.

Removing the smallest damage values has also increased most of the consistencies. The most significant increases are found for the freight trains, such that all consistencies are beyond 32 %. The results indicate that the Consistent Load Model provides adequate consistencies for a bridge not affected by centrifugal forces. The consistency also appears to be satisfactory for non-standard influence lines in general.

The number of non-standard influence lines appears to be the determining factor, where the consistency decreases with a structure's complexity. For bridges equally or less complex than Driva Bridge and without horizontal curvature, the consistency criterion may however be considered fulfilled. These results also confirm that centrifugal force is the main challenge for Svånå and Sokna Bridge. Therefore, the focus continues to be on how one can eliminate the negative impact of centrifugal force.

## 7.3 Possible Solutions

To solve the consistency issue caused by the influence of centrifugal force, some possible solutions have been tested. Note that some of the presented alternatives are not recommended, rather included to show the thought process and some occurring challenges.

### 7.3.1 Alternative 1: MDT for Stress Points with High Influence from Speed Using Gradient

The first idea was to measure how much the influence line and fatigue damage change with speed. For the stress points where speed significantly impacts the fatigue damage, the most damaging train has to be found. Multiple speeds were then defined from 0 km/h to the maximum speed of the period and type of train considered, according to Eq. (30). The maximum speeds for the reduced train set are presented in Table 7.6.

Table 7.6: Maximum speed in km/h found for each train in the Consistent Load Model.

| Train | Max speed [km/h] |
|---|---|
| T1 | 70 |
| T2 | 70 |
| T3 | 120 |
| T4 | 143 |
| T5 | 45 |
| T6 | 65 |
| T7 | 80 |
| T8 | 90 |

For each speed, the influence line was updated, and the fatigue damage was calculated. The gradient was used as the primary measurement for how much the influence line is affected by speed. In general, the gradient of a function $h(x)$ is defined as in Eq. (32).

$$\nabla h = (\frac{\delta h}{\delta x_1}, ..., \frac{\delta h}{\delta x_n}) \tag{32}$$

In this case, the gradient is dependent on the fatigue damage, $D$, and the speed, $v$:

$$\nabla D_i = \frac{D(v_i) - D(v_{i-1})}{\Delta v} \tag{33}$$

The magnitude of the fatigue damage varies for each point. The gradient therefore has to be normalized such that a common limit, $\beta$, can be chosen for all points. The average damage for the point is consequently used. The criterion for when the most damaging train has to be found was defined as follows:

$$\frac{max(|\nabla D|)}{D_{average}} > \beta \tag{34}$$

$|\nabla D|$ is the vector containing the absolute value of all gradients, as the fatigue damage of the influence lines both can be increasing and decreasing with higher speeds.

The gradient alone was not sufficient to find all critical points. For some of the stress points, the difference in fatigue damage from a high and low speed was considerable, although the gradient was low. These influence lines experienced an even gradient throughout the whole speed spectra. Therefore, a second criterion had to be introduced:

$$\frac{D_{v=0}}{D_{v=max(v)}} \quad V \quad \frac{D_{v=max(v)}}{D_{v=0}} > \kappa \tag{35}$$

The limits, $\beta$ and $\kappa$, were chosen such that all points with MDT damage greater than $10^{-10}$ and ratio, $\varphi$, smaller than 0.5, were returned.

This method was tested for reference trains T1-T4 for Svånå Bridge. Table 7.7 shows the limits found for the four different trains tested. It also presents the number of stress points found with a damage ratio below 0.5 and fatigue damage higher than $10^{-10}$, and the number of points with a ratio smaller than 1.0. The two last columns show how many points with a ratio beneath 1.0 were returned as needing MDT analysis (true positives) and the number of points with a ratio higher than 1.0 that this method returned as critical (false positives).

Table 7.7: $\beta$ and $\kappa$ found for Svånå Bridge and returned number of stress points.

| Train | $\beta$ | $\kappa$ | $\varphi < 0.5$ & D $> 10^{-10}$ | $\varphi < 1$ | True positives | False positives |
|---|---|---|---|---|---|---|
| T1 | $\infty$ | 7.10 | 4 | 783 | 416 | 44 |
| T2 | $\infty$ | $\infty$ | 0 | 609 | 0 | 0 |
| T3 | 0.0749 | $\infty$ | 557 | 1634 | 951 | 0 |
| T4 | $\infty$ | 2.94 | 125 | 466 | 175 | 2225 |

It can be seen from Table 7.7 that this alternative provides a large number of false positives. It returns that all influence lines dependent on speed must be checked for the most damaging train, whether a low or high speed is the most damaging. T1 has a fairly low speed of 34 km/h for the Consistent Load Model. The points returned as false positives for this train are critical at low speeds. It is therefore just a coincidence that this reference train has a low speed. T2 and T3 in the Consistent Load Model have neither exceptionally high nor low speeds, such that the deviation is not as significant, and no false positives are found. The problem of false positives is especially considerable for T4 with a speed of 144 km/h. The check then returns 2225 false positives. These stress points have the largest damage from high speeds. As the train runs at a high speed, the ratio is good, although the stress points are highly dependent on the speed.

The limit for which points are to be returned as critical could be lowered. One example could be that all points with a ratio smaller than 0.1 are to be returned. Lowering the limit would decrease the number of points having to be checked. This solution would however be less conservative for some points and provide unsatisfactory consistency.

Svånå Bridge is defined with a total of 3932 stress points. For T4 alone, this alternative finds that 2400 points have to be checked for MDT with the limits presented above. MDT analysis is a time-consuming and advanced operation, and the simplicity requirement of the Consistent Load Model does not apply if this alternative is used. Alternative 1 was therefore not further tested. Instead, other alternative methods were explored.

### 7.3.2 Alternative 2: Maximum Speed and MDT for Stress Points with Highest Fatigue Damage for Low Speeds

From Table 7.7, it was seen that most stress points are critical at high speeds, as T4 provided the highest number of false positives. The second alternative solution includes changing the speed of the trains in the Consistent Load Model to the highest allowed speed for the period. Only the stress points with a lower critical speed than the maximum speed must then be checked for MDT.

Similar to the first alternative, multiple speeds were defined between 0 km/h and the maximum speed for each train. The fatigue damage for trains T1-T8 was found for all speeds and all stress points. The criterion for which points have to be checked for MDT was then defined as follows:

$$\frac{max(D)}{D_{v=max(v)}} > \kappa \tag{36}$$

$\kappa$ was set to 2.0, meaning that all stress points with critical fatigue damage higher than two times the damage for the highest speed have to be checked for most damaging train. The number of stress points returned to be checked for each train is presented in Table 7.8.

Table 7.8: Number of stress points having to be checked for MDT with Alternative 2.

| Train | Svånå Bridge | Sokna Bridge |
|---|---|---|
| Total stress points | 3932 | 7424 |
| T1 | 244 | 438 |
| T2 | 242 | 403 |
| T3 | 213 | 1643 |
| T4 | 292 | 1631 |
| T5 | 196 | 105 |
| T6 | 292 | 504 |
| T7 | 208 | 517 |
| T8 | 209 | 625 |

The number of stress points having to be checked for most damaging train is significantly reduced. For T4 for Svånå Bridge, it has changed from 2400 to 292, making this method less time-consuming than Alternative 1. For Svånå Bridge, approximately 6 % of the stress points have to be checked for MDT. However, more variation is found for Sokna, where it ranges from 1-22 %.

To determine the change in consistency, T4 has been used. T4 is the only reference train with speed in the Consistent Load Model similar to what is suggested in this alternative. How the minimum ratios and consistency changed for Svånå and Sokna Bridge can be seen in Table 7.9. The smallest ratio, $\varphi$, is now 0.74 for both bridges. This results in consistencies of 17.4 % and 16.2 %, which is a lot closer to the desired level. Figure 7.11 shows logarithmic scatter plots of the ratios for T4 before and after Alternative 2 is performed. It is then seen that all the lowest ratios are removed.

Table 7.9: Change in consistency for T4 for Svånå and Sokna Bridge with Alternative 2.

| | Svånå Bridge | Sokna Bridge |
|---|---|---|
| $\varphi_{min,before\ check}$ | 0.0482 | 0.0086 |
| $\varphi_{min,after\ check}$ | 0.7369 | 0.7387 |
| $\zeta_{before\ check}$ | 1.1 % | 0.2 % |
| $\zeta_{after\ check}$ | 17.4 % | 16.2 % |

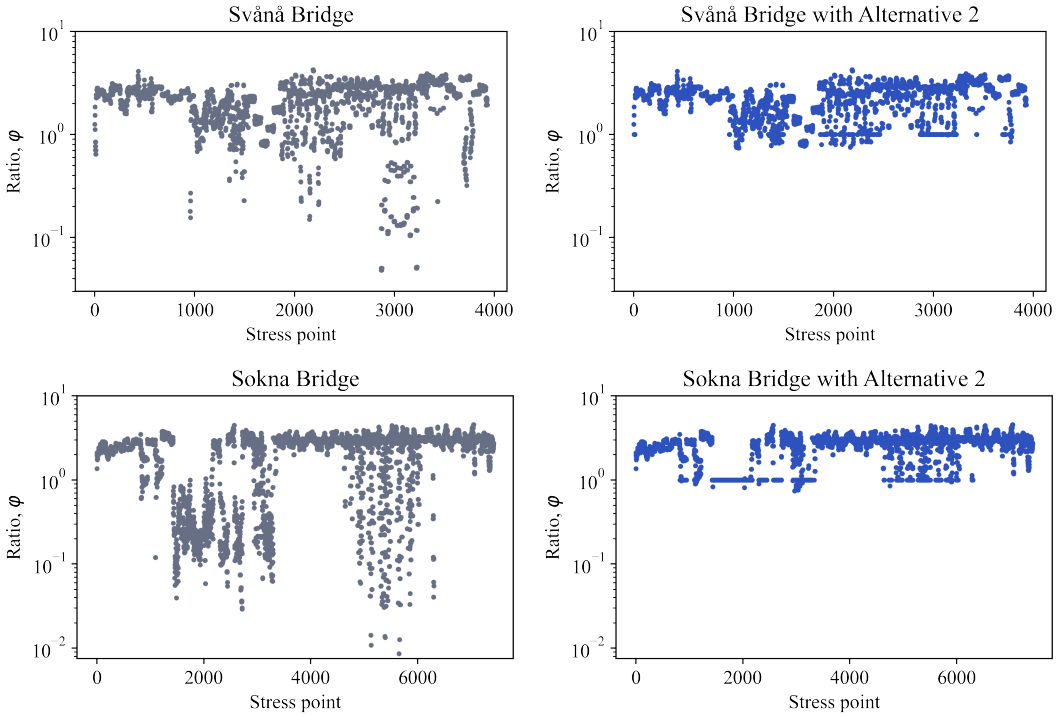


Figure 7.11: Change in ratios for T4 for Svånå and Sokna Bridge with Alternative 2.

Although this alternative increases the consistency of the model while performing an MDT analysis on fewer points than the previous alternative, it still requires the user of the model to master the MDT optimization algorithm. As mentioned, this is a more advanced and time-consuming analysis, taking away the simplicity criterion in the Consistent Load Model.

### 7.3.3 Alternative 3: Finding the Most Damaging Speed

It is desirable to keep the load model simple, such that all engineers can easily adopt it. As the previously proposed alternatives both had difficulties on this criteria, a more simple option without using an MDT analysis is considered.

The speeds for each reference train in the Consistent Load Model were chosen because they showed a tendency of higher consistency for the calibrated influence lines. It was however not considered that the influence lines of bridges with horizontal curvature are highly dependent on the speed of the train passing.

One possible option is to change the speeds in the reference trains to the mean value of the speed for all passing trains in each period. This would give a more correct influence line for bridges with horizontal curvature, and therefore more realistic fatigue damage. However, the consistency of the model would not improve that much, as the true most damaging train most likely would have a lower or higher speed. Another challenge is the lack of data on passing trains. The maximum speed of the locomotives in each period is known, but not the actual speed when the train passed the bridge. There could also be significant variations from one bridge to another. The accurate mean value of the speed is therefore difficult to determine. Since the consistency of the model most likely is not notably improved, this is a problematic solution.

Another option is to check the fatigue damage with different speeds, and choose the speed causing the worst damage for each influence line. A vector, $\mathbf{v}$, is established from a minimum speed of 5 km/h to the maximum speed of the period and type of train considered, according to

$$\mathbf{v} = \{5,\ max(v_L, v \uparrow)\} \tag{37}$$

See Frøseth & Rønnquist [13] for the complete data on the maximum speed for each period and train type. The fatigue damage from reference train $Ti$ is then calculated with the Consistent Load Model for speed number $n$ in the speed vector by

$$D_n = a_i * d_{SC}(T_{i,v_n}) \tag{38}$$

This calculation is performed for all speeds and collected into a vector, $\mathbf{D}$. The final fatigue damage in each element is then taken as the one causing the greatest damage:

$$D = max(\mathbf{D}) \tag{39}$$

This option was primarily explored by determining the new consistencies with Alternative 3. The fatigue damage was calculated as explained above. Instead of using 5 km/h as the lowest speed, it was set to the minimum speed from the MDT analysis in Subsection 7.1.2 in each time period. This change was done to make the fatigue damages more comparable, as the minimum speed in the MDT analysis was set to 25 % of maximum speed. The maximum speed was determined according to Table 7.6. The ratios between damage from this adjusted load model and MDT was then found, resulting in the consistencies presented in Table 7.10.

Table 7.10: Consistency for the Consistent Load Model with adjusted speeds.

| Train | Svånå, $\zeta$ [%] | Sokna, $\zeta$ [%] |
|---|---|---|
| T1 | 53.6 | 49.0 |
| T2 | 41.0 | 43.2 |
| T3 | 45.2 | 52.3 |
| T4 | 31.9 | 26.8 |
| T5 | 30.9 | 24.0 |
| T6 | 11.8 | 13.1 |
| T7 | 30.1 | 36.8 |
| T8 | 20.1 | 33.9 |

Compared to the results in Table 7.1, the consistencies are remarkably better when the elements have adjusted speeds instead of the one initially presented in the reference trains. When the speed is adjusted to the most damaging speed, the damage from the load model becomes closer to the damage from MDT. For example, the lowest ratio for T1 is found as 0.001 in the original load model while it is 1.318 with adjusted speeds. The same tendency is found for all other reference trains, and with the small ratios avoided, a much better consistency is found. All ratios are plotted in Figure 7.12, where a huge improvement is seen for Alternative 3.

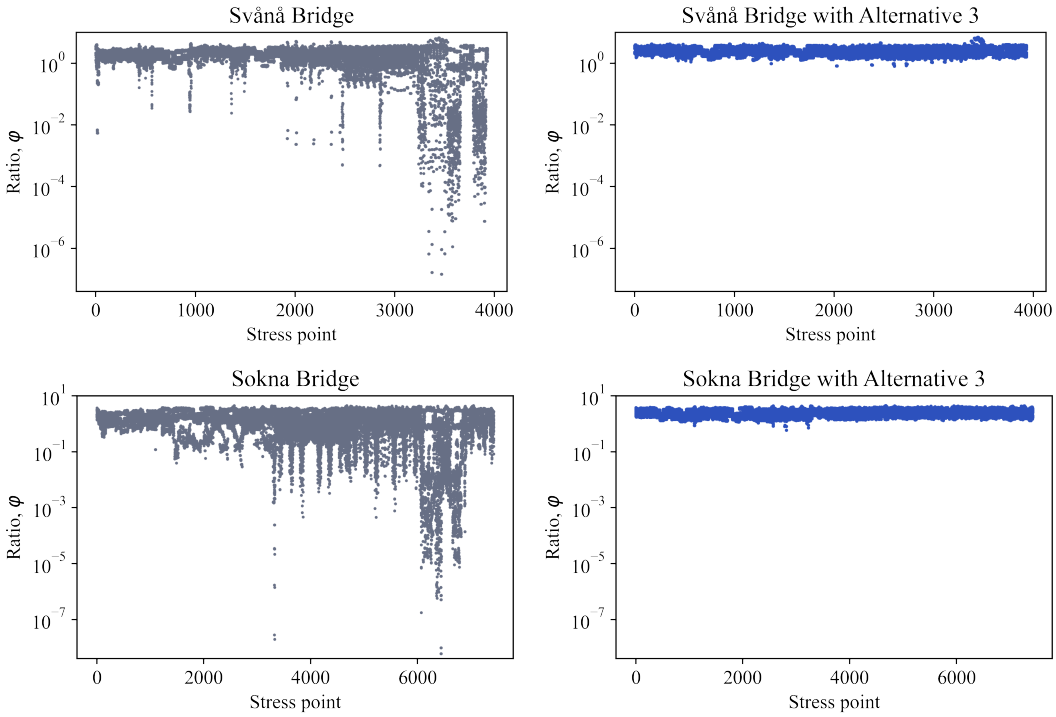


Figure 7.12: Change in ratios for Svånå and Sokna Bridge with Alternative 3.

The average consistency is 42.8 % for passenger trains and 25.1 % for freight trains. The fact that the passenger trains provide the highest consistency agrees well with the consistency measures for the calibration set. The desired consistencies were 50 % for passenger trains and 40 % for freight trains, but these are only valid for the influence lines and lengths in the calibration set. As the consistencies in Table 7.10 are valid for all influence lines of the elements in Svånå and Sokna Bridge, the new consistency levels must be assumed good.

The consistency is a bit lower for T6. This train has a smaller minimum ratio than the other trains. For Svånå Bridge, T6 also provides the highest maximum ratio. The minimum and maximum values are here linked to those elements with very low fatigue damages. As previously discussed, these are sensitive to changes, contributing to relatively high or low ratios. On the other hand, low damage values are also present in the other periods without giving particularly low or high ratios. Therefore, a lower consistency in T6 might simply indicate that T6 does not match the MDT analysis as well as the other reference trains.

### Applying Alternative 3

Alternative 3 is tested for Svånå and Sokna Bridge to examine how the most damaging speed affects the fatigue results. All other factors than the speed were kept the same as in the initial analyses with the Consistent Load Model. Table 7.11 presents the five most critical cross-sections for the Consistent Load Model with original speeds and with the most damaging speeds found with Alternative 3. Results from Bane NOR's assessments with the Conventional Load Model are also included for comparisons.

Table 7.11: Most damaged cross-section types for the different load models.

| | Svånå | | Sokna | |
|---|---|---|---|---|
| Load Model | Section | $D_h$ | Section | $D_h$ |
| Conventional | Ve3 | 1.3646 | Di2 | 0.5617 |
| | St1 | 0.9470 | LC2 | 0.5223 |
| | Di2 | 0.8468 | Ve1 | 0.3313 |
| | LC2 | 0.6373 | St | 0.3385 |
| | CG4 | 0.5485 | StCon | 0.3540 |
| Consistent | Di2 | 11.4196 | St | 14.6949 |
| | Ve3 | 10.5817 | StBr | 10.9867 |
| | St1 | 6.7964 | StCon | 8.1810 |
| | CG4 | 1.8779 | Di2 | 3.5119 |
| | Di1 | 1.7364 | StDi | 2.3978 |
| Consistent with Alternative 3 | Ve3 | 20.9406 | St | 34.7193 |
| | Di2 | 19.7891 | StBr | 13.8264 |
| | St1 | 14.2563 | StCon | 12.8834 |
| | St2 | 3.9516 | Di2 | 8.3655 |
| | LC2 | 3.3401 | LC1 | 6.0166 |

It can be seen that the fatigue damage increases with a factor of approximately 2 for most cross-section types, comparing the original Consistent Load Model and Alternative 3. The change in speed has a more significant effect on some components, resulting in a slight change in the components' priority. As the consistency for this alternative was remarkably better than in the original analysis with the Consistent Load Model, the ranking of components found with Alternative 3 should theoretically be more correct. Since Alternative 3 is an adjustment of the Consistent Load Model, the results are more comparable with this load model than the conventional one. However, it is interesting to see that both Alternative 3 and the Conventional Load Model find Ve3 as most critical for Svånå Bridge. Compared to the Conventional Load Model, it is also clear that Alternative 3 provides significantly more conservative damage results.

For all cross-section groups, including those with lower damage not presented in the table, the maximum speed is found as most damaging when applying Alternative 3. However, this does not mean that all stress points within each group necessarily have maximum speed as most damaging, only those points with the most severe damage in each cross-section group.

As presented, the adjusted load model provides even more conservative fatigue damages than the original Consistent Load Model. The consistency is also definitely better with the speed adjustments. The requirement of a conservative and consistent load model is thus fulfilled. As it comes to simplicity, the adjusted load model is a bit more complex than the original one. Since each influence line's most damaging speed has to be found, the method is somewhat more time-consuming than using the same speed for all elements. However, without the use of an MDT algorithm, it is much simpler than Alternatives 1 & 2. Therefore, it is assumed that the simplicity requirement still is accepted, especially since the speed adjustments provide such improvements in the overall consistency.

The weakness of this alternative is that the fatigue damage in each element is calculated for different speeds. In reality, when one train passes, all components are stressed at the same speed. This means that even though one element is ranked most critical to fatigue damage, others may have more severe damage if the true speeds of the passing trains have been far off from the most damaging speed in the element ranged most critical. At the same time, if the true speed is close to other elements' most damaging speed, it is possible that this element has greater damage than the theoretical most critical cross-section. This issue shows that even though the consistency is high, it is essential to acknowledge that it is a theoretical result. The ranking may be different if the real speed differs much from the most damaging one.

### Damage By Train

In the original analysis with the Consistent Load Model for Sokna Bridge, it was found abnormal that passenger trains were the biggest contributor to the fatigue damage, as presented in Table 5.8 & Figure 5.3. Reasons were further discussed, where the difference in speed was one possible reason. For Alternative 3, where critical speeds are used instead of constant speeds, this distribution has changed. The same stress points plotted in Figure 5.3 are now plotted again, shown in Figure 7.13. Freight trains are now found to be most damaging for all points, confirming that the speed was the issue also here.

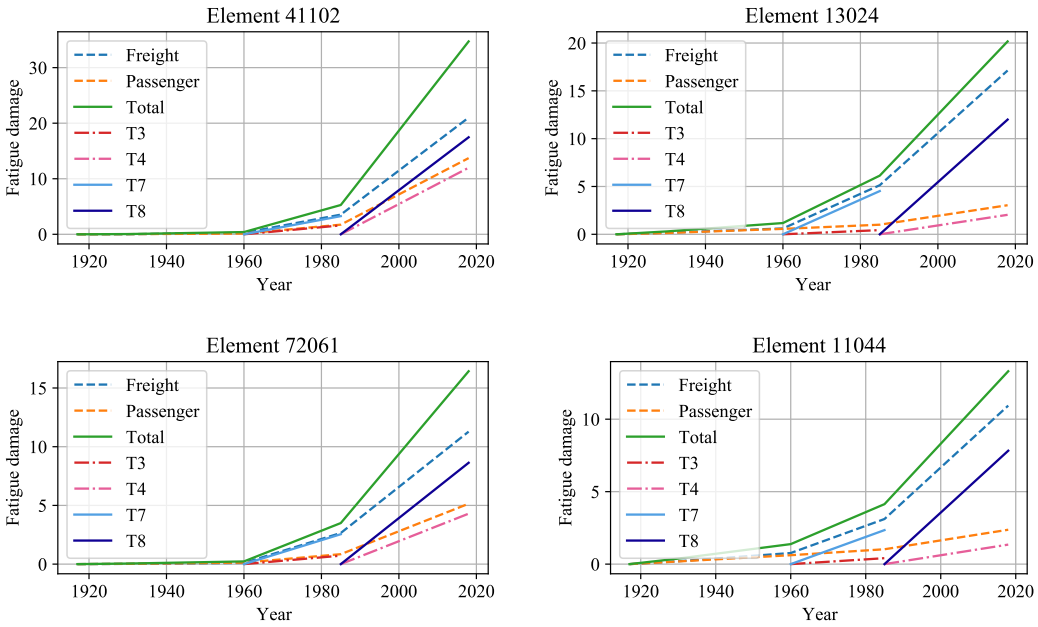


Figure 7.13: Sokna Bridge - Damage by train for most critical elements in most critical cross-section types with Alternative 3.

To investigate the differences between damage from passenger trains versus freight trains, the average damage ratios between the load model and most damaging train have been studied. Figure 7.14 presents the average ratios for Svånå, Sokna, Møstadbekken and Driva Bridge. Depending on whether the bridges have a curvature or not, different load models have been used. For the bridges with horizontal curvature, Svånå and Sokna, Alternativ 3 is used. The original Consistent Load Model is used for Møstadbekken and Driva, as it provided satisfactory consistency values for bridges without curvature.

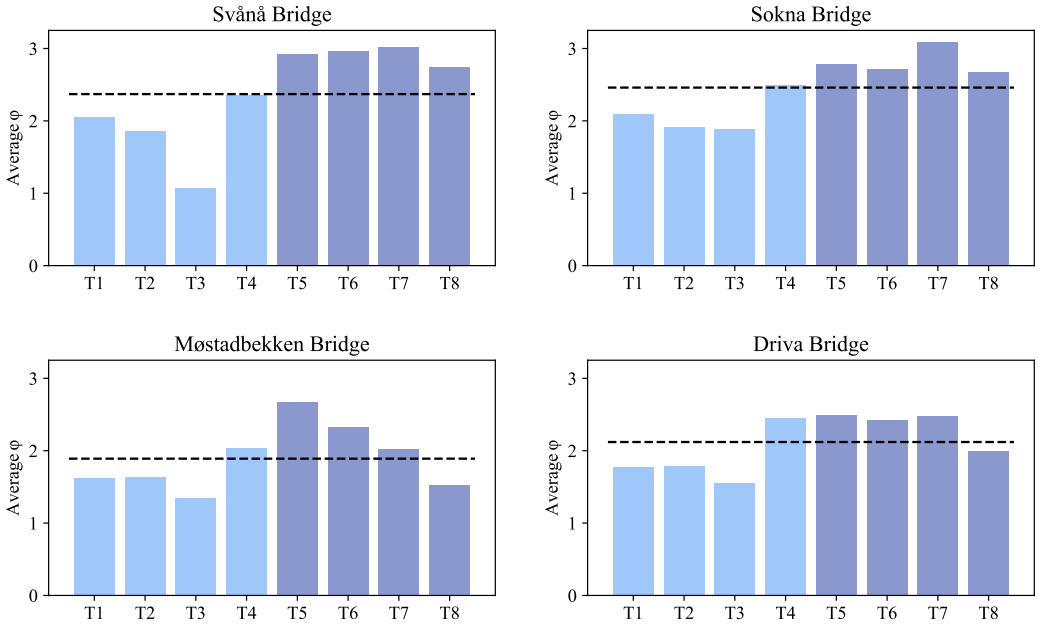


Figure 7.14: Average damage ratios. Dashed line marks mean value for T1-T8.

As seen, the average damage ratio is generally smaller for passenger trains than freight trains. Thus, the load model introduces less damage from passenger trains than freight trains relative to the most damaging train. This tendency is clear for Alternative 3, with both Svånå and Sokna Bridge having all freight averages above the mean level. The tendency is not as clear for the original Consistent Load Model, with T8 below the mean value for both Møstadbekken and Driva Bridge. T8 has a much lower speed with the original Consistent Load Model than what is found as the most damaging speed and speed of MDT. Even though the influence lines of bridges without horizontal curvature do not depend on speed, there will be differences in the dynamic amplification factor. Lower speeds provide lower DAF, thus lower response and fatigue damage. Nevertheless, considering all freight average ratios for the bridges without horizontal curvature, they are still higher than the passenger average ratios.

The difference in relative damage is important when studying damage by train. Since the load model introduces more relative damage from freight trains, the contributions from passenger trains in these figures may be too low. It is still expected that freight trains will contribute more, as they have higher axle load and more wagons, but it is realistic with higher contributions from passenger trains than indicated in the figures. Element 41102 and 72061 from Figure 7.13 show contributions from passenger trains as approximately 30 % of the total damage. With possibly even higher contributions, it is important to acknowledge that passenger trains also provide considerable damage for some bridge components.

The traffic mix coefficients may be adjusted to make the average ratios for passenger and freight trains more alike. It will then be easier to compare the results and truly confirm the contributions from each type of train. In addition, some specific adjustments may be considered for T3 and T8. When only the higher damage values were considered for Driva Bridge, T3 and T8 were still found with minimum ratios below 1.0. This means that the damage induced by the Consistent Load Model is smaller than the most damaging train for some stress points. Since T3 also has the lowest average ratios for all bridges, it may be wise to increase the traffic mix coefficient for T3 both when using the original Consistent Load Model and Alternative 3. T8 only shows low average and minimum values for the bridges without curvature. Therefore, it could be considered to increase the traffic mix coefficient for T8 only for the original Consistent Load Model.

## 7.4 The Importance of Consistency Versus Real Speed

Several methods and alternatives to increase the consistency have been presented in the last subsections. Alternatives 1 & 2 used a combination of the original Consistent Load Model and MDT analyses. Alternative 1 was not suitable, while Alternative 2 worked better. However, Alternative 2 still requires the user to master the MDT algorithm. To maintain the simplicity requirement, Alternative 2 is therefore not suggested as a solution to the issue of low consistency. The method of finding the most damaging speed, Alternative 3, showed promising results in both conservatism, consistency and simplicity. Among the presented methods, Alternative 3 is therefore the best-suited solution to improve the consistency and keep the load model simple.

However, there is still a possible issue with the ranking of the most exposed details in Alternative 3, as mentioned in Subsection 7.3.3. The damage for each influence line is highly dependent on the speed. If the actual speeds of the passing trains differ significantly from the most damaging ones, the ranking of critical components might be wrong. This issue addresses that the actual speed of the passing trains still is important, even though other speeds provide good consistency. With this issue in mind, using a more realistic speed would ensure that the ranking of critical cross-sections are close to the true ranking. On the other hand, the consistency would then not be satisfied, as the speeds in the MDT analysis differ from the assumed realistic ones. As a possible solution, the most damaging train could be found from trains only run at realistic speeds. The consistency for this specific speed would then probably be satisfying.

The significant challenge when using realistic speeds is, as already mentioned, the fact that the realistic speeds are not known. There is no data available regarding the speeds of trains historically, and it is doubtful that all trains have passed at the same speed. There could be variations in different seasons, periods and weather conditions. The weight of the trains will affect the speeds as well. There are also considerable differences in speed for each bridge, depending on the landscape, curvature, distance to the station, etc. If only one speed is assumed, the conservatism of the load model is challenged. If trains have passed with different speeds than the assumed one, the actual speeds are likely inflicting greater damage for some influence lines. The fatigue damage will then be underestimated, resulting in a less conservative load model than desired.

Alternative 3, on the other hand, ensures that the load model is both consistent and conservative for all possible speed situations. Even though there still might be some difficulties with the ranking, Alternative 3 is the better one to use when checking the theoretical resistance against fatigue failure.

The earlier presented analyses found that the latest time periods are inflicting the most fatigue damage. Therefore, it is most important that the speeds for the immediate past and future are correct. One advantage of this is that speed data can be collected and registered for today's situation. These speeds can then be implemented for the latest period and near future by changing the minimum and maximum speeds when using Alternative 3, for instance, by choosing the 5 and 95 percentile. This would ensure that the load model truly is conservative for all the periods with unknown speeds while being realistic where the actual speeds are known.

# 8 Conclusion

The object of this thesis was to evaluate the Consistent Load Model proposed by Frøseth & Rønnquist and whether or not it fulfills the criteria of being simple, conservative and consistent. This concluding chapter presents the most important remarks, including possible improvements and recommendations. Suggestions for further work are also presented.

## 8.1 Concluding Remarks

The fatigue analysis showed that the Consistent Load Model is more conservative than the Conventional Load Model used by Bane NOR, where some section classes had an increase in damage of more than 4000 %. The most critical elements in both Svånå and Sokna Bridge were found with extremely high damage, suggesting that the bridges needed reparation several years ago. As the fatigue damages are much lower with the Conventional Load Model and the bridges still are operating today, it seems like the Consistent Load Model introduces unrealistically high damage in the structural components. However, this is expected as the model is designed to introduce fatigue damage 1-2 times higher than the damage from the possible most damaging train. SN-curves also contribute to conservative fatigue calculations, but this effect should be the same for both load models.

The ranking of the most exposed details differs between the two load models. The main purpose of the Consistent Load Model is to introduce the same relative damage in all structural components. Bane NOR found the verticals most critical for Svånå Bridge. These components are also found crucial with the Consistent Load Model, but with the diagonals ranked higher. For Sokna Bridge, none of the elements were found critical by Bane NOR. This is not the case with the Consistent Load Model, where several components have damages above the critical level. As the Consistent Load Model is more conservative, this result is expected. However, what is of most interest is that the ranking of the most critical components is also changed for this bridge. Since the Consistent Load Model is finding several critical cross-sections, as well as the ones indicated most exposed with the Conventional Load Model, the new model might be considered more consistent.

Looking into each period and its contribution to the total fatigue damage, the most recent periods provide the most significant damage. T4 and T8, respectively representing passenger and freight traffic after 1985, are the most important contributors. Possible reasons are higher axle load and more wagons in the trains, largely affecting the stress ranges introduced on the steel structures.

Due to higher axle loads and a higher number of wagons, freight trains are usually assumed more damaging than passenger trains. Svånå Bridge confirms this assumption, where the most critical stress points all have higher damage from freight trains. Initially, this was not seen for Sokna Bridge, where some elements were found with most damage from passenger trains. It turned out that the difference in speeds was the cause of this abnormal result. The shape of the influence lines, and therefore the damage, are highly dependent on the centrifugal force caused by the curvature on the bridges. The passenger trains in the Consistent Load Model have generally higher speeds, such that in the cases where high speeds are most damaging, the passenger trains will provide the greatest damage. When the most damaging speeds were used for all reference trains, the freight trains were the biggest contributor to Sokna Bridge as well. It is however important to acknowledge that also passenger trains provide considerable damage for some components. It was found

that the average damage ratios between the load model and MDT were generally higher for freight trains than passenger trains, suggesting that passenger trains might contribute somewhat more than what is found in these analyses.

It is clear that the Consistent Load Model is both conservative and simple. Although it also found other and more critical components than the Conventional Load Model, it does not prove that it fulfills the consistency criteria. The desired level of 40 % and 50 % consistency of respectively freight and passenger trains are only valid for a set of calibrated influence lines and lengths. When the true consistencies were found by performing a check of the most damaging train, they turned out extremely low. The consistency requirement can consequently not be considered fulfilled.

When investigating the reasons for low consistency, the centrifugal force was again found as the problem. How the centrifugal forces affect the influence lines varies greatly. Some stress points had close to no contribution from the centrifugal force. For these stress point, the damage ratio between the Consistent Load Model and MDT were generally between 1 and 2. For others, a higher speed tends to even out the influence line, making the fatigue damage lower. However, the most distinct were the cases where a high speed increases the peak of the influence line and thus the damage. This results in the fatigue damage introduced by the load model being several million times smaller than for MDT.

The consistencies were also calculated for two bridges with no curvature. All consistencies were then found to be at least 19 %, with mean values of 40 % and 71 %. This is close to the desired levels found with the calibration set, proving that the centrifugal force's effect is causing the poor consistencies. Therefore, the consistency requirement of the Consistent Load Model is only fulfilled for a bridge not affected by centrifugal forces.

Several alternatives have been tested to increase the consistency for bridges with horizontal curvature. As it is essential to keep the load model simple, options without an MDT analysis are preferable. Alternative 3, where the most damaging speed out of a defined minimum and maximum is found for every influence line, showed remarkably better consistency than the original Consistent Load Model. This alternative is also even more conservative and relatively simple, although some extra computational time must be expected. Among those alternatives presented in this thesis, Alternative 3 is recommended.

Even though Alternative 3 showed good consistencies, there still might be trouble concerning the ranking of the most exposed details. As the most damaging speed provides the highest possible damage, it may be far from the damage caused by the actual speed of a passing train. The ranking might be different from one speed to another. Therefore, it is important to acknowledge that the results obtained with Alternative 3 are theoretical and might not show the proper ranking of the components. Since there is limited historical data on train speed for Norwegian railway bridges, the most damaging speed should be used to ensure conservatism. It is also found that the periods closest to today are most harmful. A more realistic result for these periods could be obtained by measuring the speeds on each bridge today, and defining the speed range from these measures.

As well as using the most damaging speed, some other possible improvements for the Consistent Load Model have been suggested. The number of bridge passages may be considered intermediate between passages from timetables and counts. To obtain the correct damage, it is recommended to use the passages from schedules for historical data and the passages from counts for the available years. Some other improvements should also be considered, but require further evaluations. These are presented in Section 8.2.

## 8.2 Suggestions for Further Work

### Reduction in the calculations of $D$

As stated in this thesis, the damage value is not realistic for the most exposed details. None of the two investigated bridges have collapsed, and with damage values far above 1.0, this should theoretically be the case. It is therefore valuable to reduce $D$ to a more realistic level. One possible method is to measure the actual damages and compare them with the damages from the load model. A reduction factor for $D$ could then be found. The challenge of the varying effect of the centrifugal force must still be taken into account. With Alternative 3 being even more conservative than the Consistent Load Model, there is definitively a need to reduce the calculated damage.

### Reducing the number of reference trains and adjusting the a-factors

It was found that the most recent periods contribute the most to the total damage. Since the Consistent Load Model is also conservative, it may be possible only to consider T3, T4, T7 and T8. The damage from before 1960 could either be neglected or added as a portion of the damage from after 1960. Additionally, the investigation of average ratios showed lower ratios for passenger trains than freight trains. Thus, it seems like the passenger trains should be included with higher traffic mix coefficients. Some adjustments may also be made for T3 and T8, as they showed lower average ratios than the other trains. To evaluate the traffic mix coefficients and possible reductions in the reference trains, it is suggested to study several bridges in the Norwegian railway network.

### Case studies of current speed

As stated in this thesis, it is a challenge that the speed of the passing trains through history is not known. As the speed largely affects the damages, one can not know whether the damages introduced with Alternative 3 are realistic. Therefore, case studies on real speeds are necessary. Alternative 3 could then be tested for the measured speeds, such that the difference from using most damaging speeds can be determined. Such comparisons will tell whether or not the Consistent Load Model with Alternative 3 truly is a good approach.

### Determine most damaging speed for critical components with Alternative 3

When applying Alternative 3 to Svånå and Sokna Bridge, it was found that the most damaged stress point in each cross-section class was critical at high speeds. It is therefore interesting to study other bridges and see whether or not this always is the case. If so, it might be sufficient to change the speeds in the Consistent Load Model to the highest allowable speed instead of finding the most damaging one for each stress point.

# References


[1] Bane NOR. Historisk oversikt (In Norwegian). Accessed 23.04.21. [Online]. Available: https://www.banenor.no/Jernbanen/Historie/Historisk-oversikt-jernbanen-i-Norge/

[2] G. T. Frøseth, "Load model of historic traffic for fatigue life estimation of norwegian railway bridges," Ph.D. dissertation, Norwegian University of Science and Technology, May 2019.

[3] Jernbaneverket, "Railway statistics 2015," Oslo, Tech. Rep., 2015.

[4] G. Parke and N. Hewson, *ICE Manual of Bridge Engineering*, 2nd ed. London: ICE Manuals, 2008, ISBN 9780727738028.

[5] J. Schijve, "Fatigue of structures and materials in the 20th century and the state of the art," *International Journal of Fatigue*, vol. 25, no. 8, pp. 679–702, 2003, doi: 10.1016/S0142-1123(03)00051-3.

[6] P. K. Larsen, *Dimensjonering av stålkonstruksjoner*, 2nd ed. Bergen: Fagbokforlaget, 2010, ISBN 978-82-519-2285-2.

[7] M. S. Cheung and W. C. Li, "Probalistic fatigue and fracture analyses of steel bridges," *Structural Safety*, vol. 25, no. 3, pp. 245–262, 2003, doi: 10.1016/S0167-4730(02)00067-X.

[8] R. O. Ritchie, "Mechanisms of fatigue-crack propagation in ductile and brittle solids," *International Journal of Fracture*, vol. 100, no. 1, pp. 55–83, 1999, doi: 10.1023/A:1018655917051.

[9] G. T. Frøseth, A. Rønnquist, D. Caantero, and O. Øiseth, "Influence line extraction by deconvolution in the frequency domain," *Computers and Structures*, no. 189, pp. 21–30, 2017, doi: 10.1016/j.compstruc.2017.04.014 .

[10] G. T. Frøseth and A. Rønnquist, "Evolution of load conditions in the norwegian railway network and imprecision of historic railway load data," *Structure and infrastructure engineering*, vol. 15, no. 2, pp. 152–169, 2019, doi: 10.1080/15732479.2018.1504087.

[11] SN/K 064, *Eurocode 1: Actions on structures- Part 2: Traffic loads on bridges. NS-EN 1991-2*, 2003.

[12] Johs Holt, "Utmattingsberegninger av eldre jernbanebruer, samlerapport," Bane NOR, Tech. Rep. 30170048-01, 11 2018.

[13] G. T. Frøseth and A. Rønnquist, "Load model of historic traffic for fatigue life stimation of norwegian railway bridges," *Engineering Structures*, vol. 200, 2019, doi: 10.1016/j.engstruct.2019.109626.

[14] L. Pook, *Metal Fatigue: What it is, why it matters.* Dordrecht: Springer, 2007, ISBN 978-1-4020-5597-3.

[15] W. Fricke, "Fatigue analysis of welded joints: state of development," *Marine Structures*, vol. 16, no. 3, pp. 185–200, 2003, doi: 10.1016/S0951-8339(02)00075-8.

[16] M. Matsuishi and T. Endo, "Fatigue of metals subjected to varying stress," *Proceedings of the Kyushu Branch of Japan Society of Mechanics Engineering*, pp. 37–40, 1968.

[17] J. R. C. Amzallag, J.P. Gerey and J. Bahuaudt, "Standarization of the rainflow counting method for fatigue analysis," *International Journal of Fatigue*, vol. 16, no. 4, pp. 287–293, 1994, doi: 10.1016/0142-1123(94)90343-3 .

[18] SN/K 064, *Eurocode 3: Design of steel structures. Part 1-9: Fatigue. NS-EN 1993-1-9*, 2010.

[19] A. Taras and R. Greiner, "Development and application og a fatigue class catalogue for riveted bridge components," *Structural Engineering International*, vol. 20, no. 1, pp. 91–103, 2010, doi: 10.2749/101686610791555810.

[20] S. A. Eftekhari, "A note on mathematical treatment of the dirac-delta function in the differential quadrature bending and forced vibration analysis of beams and rectangular plates subjected to concentrated loads," *Applied Mathematical Modelling*, vol. 39, no. 20, pp. 6223–6242, 2015, doi: 10.1016/j.apm.2015.01.063.

[21] K. Liu, H. Zhou, G. Shi, Y. Shi, and G. D. Roeck, "Fatigue assessment of a composite railway bridge for high speed trains. part ii: Conditions for which a dynamic analysis is needed," *Journal of Constructional Steel Research*, vol. 82, pp. 246–254, 2013, doi: 10.1016/j.jcsr.2012.11.014.

[22] L. Mao and Y. Lu, "Critical speed and resonance criteria of railway bridge response to moving trains," *Journal of Bridge Engineering*, vol. 18, no. 2, pp. 131–141, 2013, doi: : 10.1061/(ASCE)BE.1943-5592.0000336.

[23] B. M. Imam and T. Righiniotis, "Fatigue evaluation of riveted railway bridges through global and local analysis," *Journal of Constructional Steel Research*, vol. 66, no. 11, pp. 1411–1421, 2010, doi: 10.1016/j.jcsr.2010.04.015.

[24] S. Lu, S. Hillmansen, and C. Roberts, "A power-management strategy for multiple-unit railroad vehicles," *IEEE Transactions on vehicular technology*, vol. 60, no. 2, pp. 406–420, 2011, doi: 10.1109/TVT.2010.2093911.

[25] Norges Statsbaner, "Forskrifter om togs kjørehastighet, størrelse, utstyr med bremser, sammensetting og kobling samt aksellast og lasteprofiler. trykk 402." Oslo, Tech. Rep., 1983.

[26] Norges Statsbaner, "NSB Historisk statistikk 1960-1987," Oslo, Tech. Rep., 1988.

[27] Johs Holt, "Utmattingsberegninger av eldre jernbanebruer, generelle prosjektforutsetninger," Bane NOR, Tech. Rep. 30170048-00, 03 2018.

[28] G. T. Frøseth and A. Rønnquist, "Finding the train composition causing greatest fatigue damage in railway bridges by late acceptance hill climbing," *Engineering Structures*, vol. 196, p. 109342, 2019, doi: 10.1016/j.engstruct.2019.109342.

[29] S. S. Skiena, *The Algorith Design manual*, 2nd ed. London: Springer-Verlag London, 2008, ISBN 978-1-84800-070-4.

[30] E. K. Burke and Y. Bykov, "The late acceptance hill-climbing heuristic," *European Journal of Operational Research*, vol. 258, no. 1, pp. 70–78, 2017, doi: 10.1016/j.ejor.2016.07.012.

[31] Johs Holt, "Utmattingsberegninger av eldre jernbanebruer, Bru over Svånå," Bane NOR, Tech. Rep. 30170048-08, 06 2018.

[32] Johs Holt, "Utmattingsberegninger av eldre jernbanebruer, Bru over Sokna ved Lundamo," Bane NOR, Tech. Rep. 30170048-25, 11 2018.

[33] Statens vegvesen, *Håndbok R412 Bruklassifisering*, 2014.

[34] G. Frøseth. (2019) Pacril. Accessed 13.01.21. [Online]. Available: https://github.com/Gunnstein/pacril.git

[35] B. Polyak, "Newton's method and its use in optimization," *European Journal of Operational Research*, vol. 181, no. 3, pp. 1086–1096, 2007, doi: 10.1016/j.ejor.2005.06.076.

[36] D. E. Newland, *Random Vibrations, Spectral & Wavelet Analysis*, 3rd ed. New York: Dover Publications, 1993, ISBN 978-0-486-44274-7.

[37] Johs Holt, "Utmattingsberegninger av eldre jernbanebruer, Bru over Møstadbekken," Bane NOR, Tech. Rep. 30170048-15, 11 2018.

[38] Johs Holt, "Utmattingsberegninger av eldre jernbanebruer, Bru over Driva (Hesthagen)," Bane NOR, Tech. Rep. 30170048-09, 10 2018.

# Appendix

## A Train Passages on the Norwegian Railway Network

By studying historical time tables Frøseth & Rønnquist estimated the number of passages for freight and passenger trains on the Norwegian railway network [13]. These passages are presented for each subline in Figure A.1.

| Line | Subline ID | Terminal A | Terminal B | Freight trains 1900 | 1920 | 1940 | 1960 | 1980 | 2000 | 2018 | Passenger trains 1900 | 1920 | 1940 | 1960 | 1980 | 2000 | 2018 |
|---|---|---|---|---|---|---|---|---|---|---|---|---|---|---|---|---|---|
| Nordlandsbanen | 01 | Trondheim | Hell | 730 | 3650 | 3650 | 2920 | 6570 | 5110 | 2920 | 2920 | 8395 | 12045 | 16790 | 16060 | 24455 | 16790 |
| | 02 | Hell | Steinkjer | 730 | 2190 | 1460 | 1460 | 3650 | 4745 | 2920 | 730 | 5475 | 9490 | 13140 | 15330 | 21900 | 15330 |
| | 03 | Steinkjer | Mo i Rana | 730 | 2190 | 1460 | 1460 | 3650 | 4745 | 2190 | 730 | 1460 | 2190 | 2920 | 3650 | 2190 | 2190 |
| | 04 | Mo i Rana | Bodø | 0 | 0 | 0 | 0 | 1460 | 730 | 2190 | 0 | 0 | 0 | 0 | 3285 | 3285 | 7300 |
| Sørlandsbanen | 05 | Drammen | Hokksund | 2920 | 4380 | 3650 | 7665 | 10220 | 5840 | 7300 | 5840 | 7300 | 9490 | 17885 | 12045 | 28470 | 25550 |
| | 06 | Hokksund | Nordagutu | 730 | 730 | 1460 | 4745 | 9855 | 4380 | 4745 | 730 | 2920 | 6570 | 9855 | 6570 | 16790 | 21900 |
| | 07 | Nordagutu | Nelaug | 0 | 0 | 1460 | 3285 | 6205 | 3650 | 4380 | 0 | 0 | 730 | 3650 | 6935 | 8760 | 5840 |
| | 08 | Nelaug | Kristiansand | 365 | 730 | 1460 | 2920 | 7300 | 5110 | 5110 | 730 | 2190 | 2190 | 3650 | 4015 | 7300 | 5840 |
| | 09 | Kristiansand | Egersund | 0 | 0 | 0 | 2920 | 7300 | 4380 | 4380 | 0 | 0 | 0 | 3650 | 2920 | 5840 | 6570 |
| | 10 | Egersund | Stavanger | 730 | 730 | 1460 | 2920 | 5110 | 4380 | 4380 | 2190 | 2920 | 5840 | 13870 | 10220 | 24090 | 56940 |
| Dovrebanen | 11 | Eidsvoll | Hamar | 1460 | 3650 | 3650 | 5840 | 9490 | 8030 | 6570 | 3650 | 4380 | 3650 | 8030 | 6570 | 5840 | 4380 |
| | 12 | Hamar | Dombås | 1460 | 2920 | 2920 | 3650 | 6570 | 7300 | 5840 | 2190 | 2920 | 5110 | 6570 | 8760 | 5110 | 9490 |
| | 13 | Dombås | Støren | 0 | 3650 | 2920 | 2190 | 5110 | 5840 | 5110 | 0 | 1460 | 2190 | 2920 | 2920 | 4380 | 3650 |
| | 14 | Støren | Trondheim | 730 | 5110 | 5110 | 2920 | 5840 | 6570 | 6935 | 1460 | 6935 | 7300 | 11315 | 18980 | 15695 | 22630 |
| Rørosbanen | 15 | Hamar | Elverum | 730 | 2190 | 2190 | 2190 | 1460 | 730 | 1460 | 4380 | 4380 | 3650 | 8030 | 6570 | 5840 | 4380 |
| | 16 | Elverum | Røros | 365 | 1460 | 730 | 1460 | 1460 | 730 | 1095 | 2190 | 1460 | 1460 | 2920 | 3285 | 4380 | 4380 |
| | 17 | Røros | Støren | 730 | 2190 | 1460 | 1460 | 730 | 730 | 365 | 1460 | 730 | 2190 | 1460 | 2190 | 2555 | 2190 |
| Bergensbanen | 18 | Hønefoss | Myrdal | 0 | 2190 | 2190 | 2190 | 4380 | 5110 | 6570 | 0 | 2190 | 2920 | 4380 | 3650 | 3650 | 3650 |
| | 19 | Myrdal | Bergen | 365 | 730 | 2190 | 2190 | 3650 | 5110 | 6570 | 730 | 4380 | 5110 | 6570 | 9490 | 8760 | 18980 |
| Østfoldsbanen w. | 20 | Oslo S | Ski | 730 | 2190 | 2920 | 6205 | 8760 | 8030 | 5475 | 14600 | 17520 | 45260 | 54385 | 68620 | 74460 | 81760 |
| | 21 | Ski | Sarpsborg | 730 | 730 | 1460 | 4015 | 7300 | 8030 | 5475 | 7300 | 6570 | 8030 | 13870 | 26280 | 30660 | 29930 |
| | 22 | Sarpsborg | Kornsjø | 730 | 730 | 1460 | 1460 | 4380 | 6570 | 5110 | 2920 | 4380 | 3650 | 5840 | 6205 | 19710 | 14600 |
| Vestfoldsbanen | 23 | Drammen | Eidanger | 1460 | 730 | 730 | 1460 | 2920 | 730 | 365 | 2920 | 3650 | 7300 | 8760 | 8760 | 16060 | 18250 |
| Gjøvikbanen | 24 | Oslo S | Roa | 0 | 2190 | 2190 | 3650 | 6570 | 3650 | 5110 | 0 | 9490 | 11680 | 14600 | 23725 | 17520 | 24090 |
| | 25 | Roa | Gjøvik | 0 | 730 | 2190 | 2190 | 2190 | 0 | 0 | 0 | 2190 | 2190 | 4380 | 6205 | 6935 | 14600 |
| Kongsvingerbanen | 26 | Lillestrøm | Kongsvinger | 730 | 2920 | 2920 | 4015 | 4745 | 7300 | 7665 | 3650 | 3650 | 5840 | 11315 | 8760 | 17520 | 17520 |
| | 27 | Kongsvinger | Charlottenberg | 730 | 2190 | 730 | 1460 | 2555 | 4380 | 8395 | 2920 | 2920 | 3650 | 5110 | 5110 | 3650 | 2190 |
| Raumabanen | 28 | Dombås | Åndalsnes | 0 | 0 | 730 | 730 | 2190 | 2190 | 730 | 0 | 0 | 1460 | 1460 | 2190 | 2190 | 2920 |
| Solørbanen | 29 | Kongsvinger | Elverum | 0 | 730 | 730 | 1460 | 730 | 2190 | 3285 | 1460 | 2190 | 2920 | 4745 | 3285 | 0 | 0 |
| Meråkerbanen | 30 | Hell | Storlien | 730 | 1460 | 2190 | 2190 | 2920 | 1460 | 0 | 1460 | 730 | 2555 | 3650 | 730 | 1460 | 1460 |
| Hovedbanen | 31 | Oslo S | Lillestrøm | 4380 | 6570 | 8030 | 9855 | 14235 | 16790 | 14965 | 13870 | 19710 | 29930 | 43070 | 54020 | 70080 | 146730 |
| | 32 | Lillestrøm | Eidsvoll | 1460 | 2190 | 4745 | 5840 | 8760 | 8760 | 6935 | 3650 | 4380 | 9490 | 12775 | 16060 | 33580 | 73730 |
| Østfoldsbanen e. | 33 | Ski | Sarpsborg | 0 | 730 | 730 | 730 | 1460 | 730 | 0 | 0 | 2920 | 5110 | 7300 | 9490 | 12410 | 15330 |
| Randsfjordsbanen | 34 | Hokksund | Hønefoss | 2190 | 2190 | 2190 | 2190 | 8760 | 2920 | 3285 | 2190 | 2920 | 4380 | 8030 | 6205 | 7300 | 3650 |
| Bratsbergbanen | 35 | Eidanger | Nordagutu | 0 | 2190 | 1460 | 3650 | 4015 | 365 | 365 | 0 | 2190 | 6570 | 4380 | 4380 | 6570 | 7300 |
| Drammensbanen | 36 | Oslo S | Drammen | 4380 | 2920 | 3650 | 6935 | 8760 | 8030 | 8760 | 14600 | 22630 | 23360 | 34675 | 47450 | 75190 | 173010 |
| Arendalsbanen | 37 | Nelaug | Arendal | 0 | 730 | 730 | 1460 | 0 | 0 | 0 | 0 | 1460 | 5110 | 5110 | 4380 | 5110 | 5110 |
| Roa-Hønefoss | 38 | Roa | Hønefoss | 0 | 1460 | 1460 | 2920 | 5840 | 3650 | 5110 | 0 | 5110 | 5110 | 5840 | 5840 | 730 | 0 |

Figure A.1: Yearly number of freight and passenger train passages on sublines in the Norwegian railway network [2][1].

## B Definition of Train Sets for MDT Analyses

The train sets used in the MDT analyses are defined in Figure B.2 for passenger trains and Figure B.3 for freight trains. The train sets are differentiated into four different time periods, corresponding to the periods of the Consistent Load Model. Each train type and period has a set of locomotives, $\mathscr{L}$, and a set of wagons, $\mathscr{W}$.

The wagon set might contain both two axle-wagons, $\mathscr{W}_T$, and bogie wagons, $\mathscr{W}_B$ which has geometry and axle weights as shown in Figure B.1. Two-axle wagons are defined by the parameters $a$ and $b$, while the bogie wagons have an additional parameter, $c$. The axle loads, $p$, are taken from the load set $\mathscr{P}$.

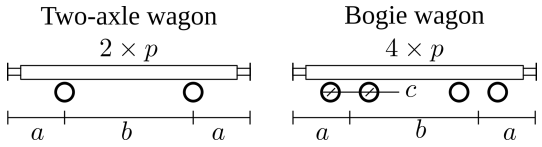


Figure B.1: Design of wagons and parameters for geometry and load [2][1].

From the locomotive and wagon set a total train set, $\Upsilon$, can be defined:

$$\Upsilon = \bigcup_{N=N\downarrow}^{N\uparrow} \mathscr{L} \times \mathscr{W}^N$$

where $N\downarrow$ and $N\uparrow$ are the minimum and maximum number of wagons in a train, such that each train has one locomotive and $N$ number of wagons.

| 1900-1930 |
|---|
| $\mathbf{N} \in [1, 20]$, $v^{\uparrow} = 90.0$ km/h |
| $\mathscr{L}$ = {2'C-2'2'[b], 2'D-2'2'[a]}, $\mathscr{P}$ = {5.0, 6.5, 8.0, 9.5, 11.0} |
| $\mathcal{W}_B$ = {(2.4, 13.4, 2.1), (2.9, 11.6, 1.9), (2.9, 13.8, 2.3)} |
| 1930-1960 |
| $\mathbf{N} \in [2, 20]$, $v^{\uparrow} = 90.0$ km/h |
| $\mathscr{L}$ = {2'D-2'2'[a]}, $\mathscr{P}$ = {6.0, 7.5, 9.0, 10.5, 12.0} |
| $\mathcal{W}_B$ = {(2.0, 16.0, 2.6), (3.2, 11.8, 2.1), (3.1, 13.4, 2.3)} |
| 1960-1985 |
| $\mathbf{N} \in [3, 20]$, $v^{\uparrow} = 120.0$ km/h |
| $\mathscr{L}$ = {B'B'[a, b], Bo'Bo'[a, b], Co'Co'[a, b]}, $\mathscr{P}$ = {7.5, 8.9, 10.2, 11.6, 13.0} |
| $\mathcal{W}_B$ = {(3.1, 13.4, 2.3), (3.8, 13.4, 3.0), (3.2, 11.8, 2.1)} |
| 1985- |
| $\mathbf{N} \in [5, 20]$, $v^{\uparrow} = 160.0$ km/h |
| $\mathscr{L}$ = {Co'Co'[a, d], Bo'Bo'[a, d]}, $\mathscr{P}$ = {8.5, 9.9, 11.2, 12.6, 14.0} |
| $\mathcal{W}_B$ = {(4.0, 19.1, 2.5), (3.8, 16.0, 2.5)} |

Figure B.2: Definition of the rolling stock for passenger trains.

1900-1930

$\mathbf{N} \in [10, 50]$, $v^{\uparrow} = 65.0$ km/h

$\mathscr{L}$ = {1'D-2'2'[a, d]}, $\mathscr{P}$ = {3.0, 5.2, 7.5, 9.8, 12.0}

$\mathcal{W}_{\mathrm{T}}$ = {(1.8, 2.0), (2.6, 4.5), (2.1, 3.7)}

1930-1960

$\mathbf{N} \in [10, 50]$, $v^{\uparrow} = 65.0$ km/h

$\mathscr{L}$ = {1'D-2'2'[a], 1'E-2'2'[a]}, $\mathscr{P}$ = {3.7, 6.5, 9.4, 12.2, 15.0}

$\mathcal{W}_{\mathrm{T}}$ = {(2.1, 7.2), (1.6, 3.7), (2.7, 6.0), (1.9, 3.2)}

1960-1985

$\mathbf{N} \in [10, 50]$, $v^{\uparrow} = 80.0$ km/h

$\mathscr{L}$ = {B'B'[a, b], Bo'Bo'[a, b], Co'Co'[a, b]}, $\mathscr{P}$ = {5.0, 8.2, 11.5, 14.8, 18.0}

$\mathcal{W}_{\mathrm{B}}$ = {(2.5, 15.7, 1.8), (2.5, 9.0, 1.8)}

$\mathcal{W}_{\mathrm{T}}$ = {(1.6, 9.0), (2.6, 9.0)}

1985-

$\mathbf{N} \in [10, 50]$, $v^{\uparrow} = 90.0$ km/h

$\mathscr{L}$ = {Co'Co'[a, d], Bo'Bo'[a, d]}, $\mathscr{P}$ = {5.6, 9.8, 14.0, 18.3, 22.5}

$\mathcal{W}_{\mathrm{B}}$ = {(2.5, 15.7, 1.8), (2.5, 9.0, 1.8)}

$\mathcal{W}_{\mathrm{T}}$ = {(4.1, 9.0), (2.4, 5.7)}

Figure B.3: Definition of the rolling stock for freight trains.

The speed of each train is restricted by the maximum speed of the locomotive and the maximum allowable speed, $v \uparrow$, yielding the following:

$$v = min(v_L,\ v \uparrow)$$

The maximum speed of each locomotive, $v_L$, is presented in Table B.1. In addition, each trains is defined with three extra speeds in order to include differences caused by the centrifugal force:

$$V = \{0.25 \times v,\ 0.50 \times v,\ 0.75 \times v,\ v\}$$

Table B.1: Maximum speed of the locomotives, $v_L$.

| Class | Subclass | Max speed $v_L$ [km/h] |
|---|---|---|
| 1'D-2'2' | (a, d) | (45.0, 45.0) |
| 1'E-2'2' | (a) | (70.0) |
| 2'C-2'2' | (b) | (65.0) |
| 2'D-2'2' | (a) | (70.0) |
| B'B' | (a, b) | (70.0, 70.0) |
| Bo'Bo' | (a, b, d) | (105.0, 115.0, 120.0) |
| Co'Co | (a, b, d) | (143.0, 120.0, 120.0) |

## C Results of Consistency for Structural Components

The damage ratio, $\varphi$, and consistency, $\zeta$, for each structural component are presented in the two following tables. All time periods have been considered in the calculations. Tables C.1 & C.2 shows the results for respectively Svånå and Sokna Bridge.

Table C.1: Svånå Bridge: Damage ratio and consistency for all structural components.

| Component | Average $\varphi$ | Max $\varphi$ | Min $\varphi$ | $\zeta$ [%] |
|---|---|---|---|---|
| Di1 | 2.0521 | 3.3795 | 0.9757 | 28.9 |
| Di2 | 1.4223 | 2.7996 | 0.6400 | 22.9 |
| St1 | 1.6866 | 4.0119 | 0.0005 | 1.3e-02 |
| StDi1 | 0.6470 | 3.6799 | 0.0001 | 2.72e-03 |
| StDi2 | 1.1874 | 3.7090 | 0.0310 | 0.8 |
| StDi3 | 1.6100 | 3.9070 | 0.4150 | 10.6 |
| St2 | 1.5487 | 6.6720 | 3.5e-09 | 5.2e-08 |
| UC1 | 2.2135 | 4.1467 | 0.9650 | 23.3 |
| UC2 | 2.0769 | 3.3801 | 1.1380 | 33.7 |
| CG1 | 2.0123 | 3.9216 | 0.5780 | 14.7 |
| CG2 | 1.9330 | 3.8110 | 0.6210 | 16.3 |
| CG3 | 1.9739 | 3.8104 | 0.6220 | 16.0 |
| CG4 | 1.9932 | 3.5862 | 0.6010 | 16.8 |
| CG5 | 1.8682 | 3.6930 | 0.1500 | 4.1 |
| CG6 | 2.1702 | 5.1632 | 0.0020 | 3.9e-02 |
| CG7 | 1.8987 | 3.6876 | 0.6158 | 16.7 |
| LC1 | 1.8872 | 4.3535 | 0.0050 | 0.1 |
| LC2 | 2.1056 | 3.5862 | 0.6830 | 19.0 |
| Ve1 | 2.2314 | 3.6830 | 1.0700 | 29.1 |
| Ve2 | 1.8234 | 4.1100 | 0.0240 | 0.6 |
| Ve3 | 1.9156 | 3.1883 | 0.6610 | 20.7 |
| WB | 0.9401 | 3.8577 | 1.1e-06 | 3.0e-05 |

Table C.2: Sokna Bridge: Damage ratio and consistency for all structural components.

| Component | Average $\varphi$ | Max $\varphi$ | Min $\varphi$ | $\zeta$ [%] |
|---|---|---|---|---|
| BB1 | 1.5987 | 3.6211 | 0.0391 | 1.1 |
| BB2 | 1.8069 | 4.5476 | 0.1258 | 2.8 |
| Di1 | 2.0048 | 3.6985 | 0.0584 | 1.6 |
| Di2 | 1.8204 | 3.7072 | 0.1448 | 3.9 |
| Di3 | 1.3781 | 3.0906 | 0.0983 | 3.2 |
| Ve1 | 1.7424 | 3.5868 | 0.0971 | 2.7 |
| Ve2 | 1.7281 | 3.3524 | 0.1113 | 3.3 |
| Ve3 | 1.7032 | 3.3603 | 0.0292 | 0.9 |
| Ve4 | 1.5977 | 3.4850 | 0.6092 | 17.5 |
| Ve5 | 1.5970 | 3.5338 | 0.6583 | 18.6 |
| Ve6 | 1.6022 | 4.1451 | 0.5545 | 13.4 |
| Ve7 | 1.6854 | 4.4837 | 0.1193 | 2.7 |
| Ve8 | 1.9911 | 4.0879 | 0.2766 | 6.8 |
| Ve9 | 1.9984 | 4.0007 | 0.1635 | 4.1 |
| Ve10 | 2.0439 | 4.0304 | 0.1986 | 4.9 |
| St | 1.7882 | 4.4296 | 0.0033 | 0.1 |
| StBr | 0.7966 | 4.2595 | 5.8e-07 | 1.4e-05 |
| StDi | 0.6344 | 4.4469 | 6.0e-09 | 1.4e-07 |
| StCon | 1.2167 | 4.5100 | 2.0e-08 | 4.4e-07 |
| UC | 1.9928 | 3.7885 | 0.1366 | 3.6 |
| CG1 | 1.8033 | 4.3649 | 0.1335 | 3.1 |
| CG2 | 1.6790 | 4.3317 | 0.0001 | 2.3e-03 |
| LC1 | 1.7331 | 3.8392 | 0.0397 | 1.0 |
| LC2 | 1.8982 | 3.6036 | 0.2181 | 6.1 |
| WB1 | 1.6546 | 3.4367 | 0.1263 | 3.7 |
| WB2 | 1.5152 | 4.2572 | 0.0815 | 1.9 |
| WB3 | 1.7022 | 3.5891 | 0.2007 | 5.6 |

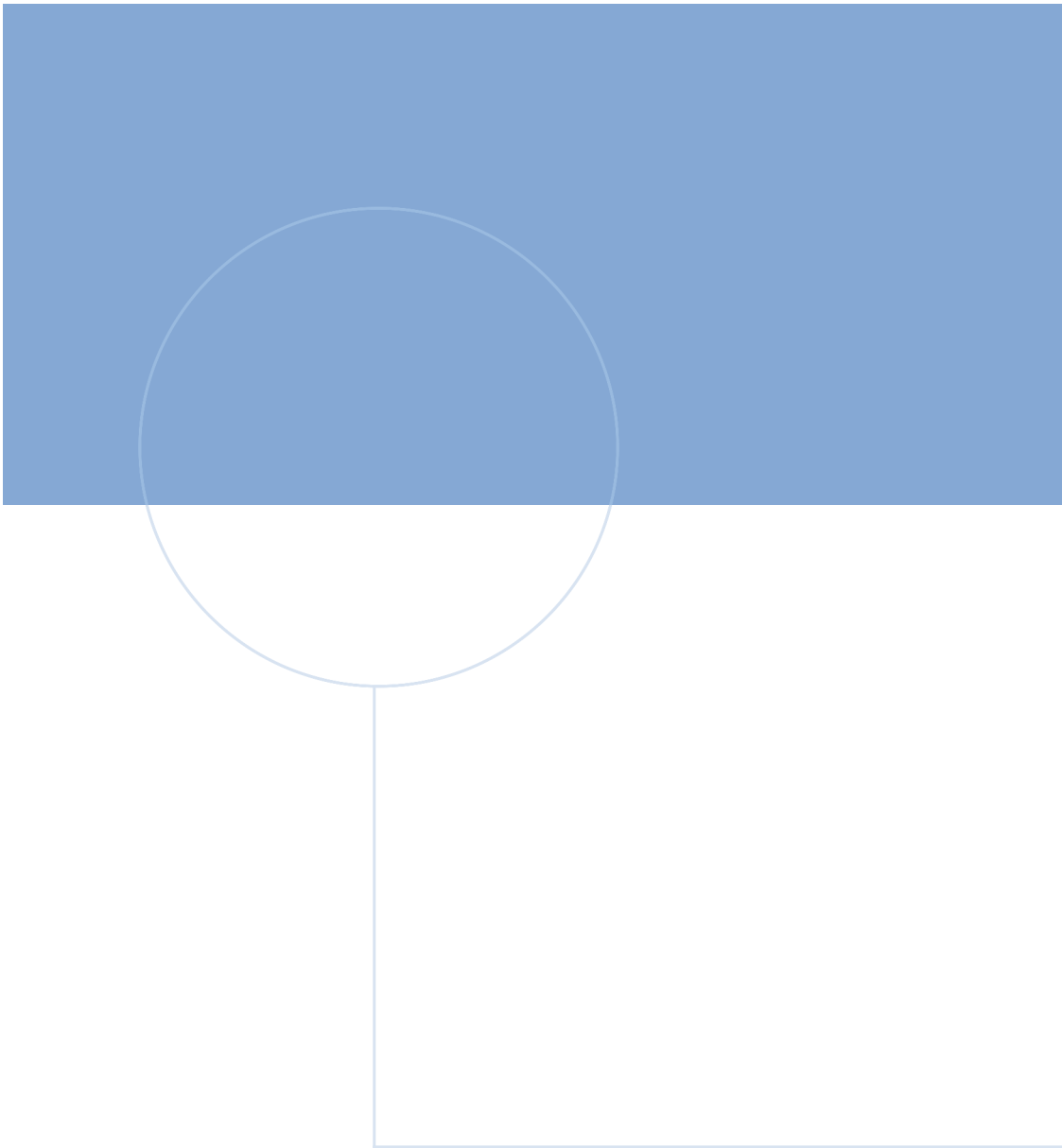

NTNU

Norwegian University of
Science and Technology